



Technical Report

Why Local Solar For All Costs Less: A New Roadmap for the Lowest Cost Grid

Prepared By:

Vibrant Clean Energy, LLC

Christopher T M Clack

Aditya Choukulkar

Brianna Coté

Sarah A McKee



Table of Contents

1. Executive Summary	- 1 -
1.1 Capacity Changes.....	- 5 -
1.2 Generation Changes	- 8 -
1.3 Carbon Dioxide Emission Changes	- 11 -
1.4 Electricity Price Changes	- 12 -
1.5 Changes in Employment	- 14 -
1.6 WIS:dom [®] -P Augmentation.....	- 15 -
2. Study Description	- 22 -
2.1 Modeled Scenarios.....	- 24 -
2.2 Model Setup.....	- 25 -
2.3 Distribution System Representation.....	- 29 -
3. Modeling Results	- 32 -
3.1 System Costs, Energy Prices, Retail Rates, and Jobs.....	- 32 -
3.2 Capacity Buildout.....	- 39 -
3.3 Electricity Generation.....	- 43 -
3.4 Emissions and Pollutants	- 50 -
3.5 Transmission Buildout.....	- 53 -
3.6 Reliability and Resource Adequacy.....	- 56 -
3.7 Siting of Generators	- 61 -
4. VCE[®] Datasets & WIS:dom[®]-P Inputs	- 64 -
4.1 Generator Input Dataset.....	- 64 -
4.2 Renewable Siting Potential Dataset	- 68 -
4.3 Standard Inputs	- 71 -
4.4 Weather Analysis.....	- 87 -



1. Executive Summary

The electricity system in the United States (US) is considered to be one the largest machines ever created.¹ With the advent of clean and renewable technologies, a widespread evolution is occurring. The renewable technologies are lower cost than fossil thermal generation on a levelized cost basis,² but their variability creates new and unique constraints and opportunities for the electricity system of the next several decades. Superimposed on the changing structure of the electricity system is a damaged climate that will continue to worsen as mankind continues to emit greenhouse gas (GHG) pollution into the atmosphere.³

The US electricity system is the second largest in the world (China has the largest). In 2018 it served approximately 150 million customers with over 3,859 terawatt-hours (TWh) of electricity from over 1,190 gigawatts (GW) of generating capacity, routed through 476,000 miles of transmission lines (over 69 kV), 55,000 substations and 6.3 million miles of distribution lines (under 69 kV).^{4,5,6} By the end of 2019, there was 86,000 MW of renewable capacity awaiting construction across the US and each year that number continues to grow.⁷ The carbon dioxide (CO₂) emissions from electricity generation across the US reached an estimated 1,659 million metric tons (mmT) in 2019, accounting for approximately 32% of the total United States (US) energy-related CO₂ emissions (5,130 mmT).⁸

The present study demonstrates, quantifies and evaluates the potential value that distributed energy resources (DERs) could provide to the electricity system, while considering as many facets of their inclusion into a sophisticated grid modeling tool. The *Weather-Informed energy Systems: for design, operations and markets planning* (WIS:dom®-P) optimization software tool is utilized for the present study. A detailed technical document of the WIS:dom®-P software can be found online.⁹ The modeling software is a combined capacity expansion and production cost model that allows for simultaneous 3-kilometer, 5-minute dispatch and power flow along with multi-decade resource selection. It includes detailed representations of fossil generation, variable resources, storage, transmission and DERs. It also contains policies, mandates, and localized data, as well as engineering parameters and constraints of the electricity system and its components. Some novel features include highly granular weather inputs over the whole US, climate change-induced changes to energy infrastructure, land use and siting constraints, dynamic transmission line ratings, electrification and novel fuel production endogenously, and detailed storage dispatch algorithms.

The distribution grid is where the majority of customers connect with the electricity system at large. However, traditional modeling tools ignore its existence almost entirely. Many

¹ <https://www.bloomberg.com/quicktake/u-s-electrical-grid>

² <https://atb.nrel.gov/electricity/2020/index.php?t=in>

³ <https://climate.nasa.gov/>

⁴ <https://www.energy.gov/sites/prod/files/2017/01/f34/Electricity%20Distribution%20System%20Baseline%20Report.pdf>

⁵ <https://www.eia.gov/electricity/data/eia860/>

⁶ <https://www.eia.gov/electricity/data/eia923/>

⁷ <https://www.eia.gov/electricity/data/eia860/>

⁸ <https://www.eia.gov/environment/emissions/carbon/>

⁹ [https://vibrantcleanenergy.com/wp-content/uploads/2020/08/WISdomP-Model_Description\(August2020\).pdf](https://vibrantcleanenergy.com/wp-content/uploads/2020/08/WISdomP-Model_Description(August2020).pdf)



assume pre-decided buildout rates of distributed solar PV (DPV), energy efficiency (EE), demand-side management (DSM), demand response (DR), and distributed storage (DS). As the electricity system continues to evolve, customers are demanding more local resources. This creates a problem because the providers of electricity (across utility service territories and RTOs) do not possess integrated modeling tools that reveal the opportunities and costs of changing distributed generation and demand as a decision variable. The opportunities could include reduced utility-scale capacity and generation, high-voltage transmission, distribution infrastructure deferrals, utility-observed peak load reduction, and increased utility-observed load factors. The costs could be more distribution infrastructure, more high-voltage transmission, increased DER buildout, and utility-scale back-up capacity and generation to cover the DER buildout.

Vibrant Clean Energy, LLC (VCE®) augmented the WIS:dom-P software to improve its representation and computations of the distribution-utility interface. The augmentations enabled a modeling framework that included the distribution grid and DERs that is tractable and akin to traditional utility planning models.

During the entire study, **fifteen** nationwide simulations were performed. Numerous intermediate simulations were used to determine the sensitivity of the modeling tool to changes in the augmentation created during the study. The model was initialized and aligned with historical data from 2018 and then the simulations evolved the electricity system across the contiguous United States (CONUS) from 2020 through 2050 in 5-year investment periods. In the present report, we focus on **four** main scenarios that answer two main questions:¹⁰

1. *Can DERs lower costs across the entire electricity system compared with alternatives, while maintaining resource adequacy, reliability and resilience?*
2. *Can DERs provide support and benefits for clean electricity goals across the entire electricity system?*

The four scenarios simulated for the present report were:

Business-As-Usual, Traditional ("BAU"): Allow economics to drive the changes in the electricity system, while including existing policies, mandates, and incentives through 2050. Deploy WIS:dom-P in a manner that mimics traditional models.

Business-As-Usual, Augmented ("BAU-DER"): Allow economics to drive the changes in the electricity system, while including existing policies, mandates, and incentives through 2050. Deploy the augmented version of WIS:dom-P that includes detailed modeling of the distribution-utility (DU) interface.

Clean Electricity, Traditional ("CE"): Enforce a nationwide clean energy standard (CES) that reduces emissions by 95% from 1990 levels by 2050. Deploy WIS:dom-P in a manner that mimics traditional models.

Clean Electricity, Augmented ("CE-DER"): Enforce a nationwide clean energy standard (CES) that reduces emissions by 95% from 1990 levels by 2050. Deploy the augmented

¹⁰ Future reports will present findings from the remaining 11 simulations. One of the simulations electrified and decarbonized the entire CONUS economy. All the remaining 11 simulations enhance or provide additional support for the conclusions detailed in the present report.



version of WIS:dom-P that includes detailed modeling of the distribution-utility (DU) interface.

The augmentation of the WIS:dom-P software to include distribution planning co-optimization results in cumulative system-wide savings of \$301 billion by 2050 ("BAU" vs "BAU-DER"), which rises to \$473 billion when considering a clean energy standard ("CE" vs "CE-DER"). Interestingly, the "CE-DER" scenario pathway is lower cost than the "BAU" scenario to the tune of \$88 billion by 2050. Figure ES-1 shows the cumulative system cost savings through 2050.

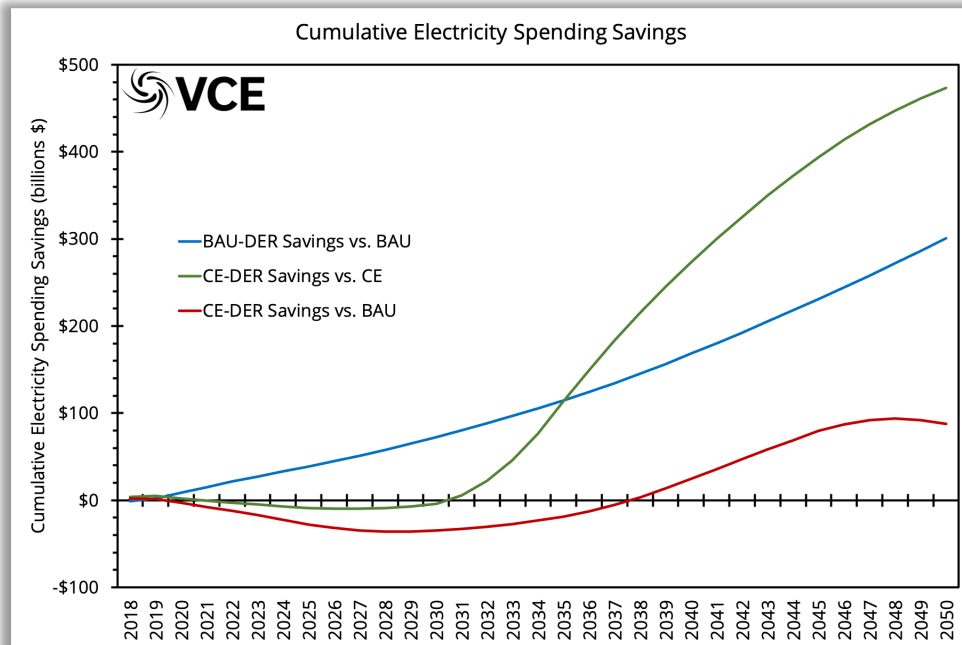


Figure ES-1: The cumulative electricity system due to the augmentation of the WIS:dom-P software to include distribution planning.

For the clean electricity system cost savings to materialize, a small amount of additional spending occurs in the first decade, however, for "BAU-DER", the savings accrue immediately. By 2035, the "BAU-DER" scenario has saved nearly \$115 billion over the "BAU" scenario, while the "CE-DER" scenario has accumulated savings of \$114 billion compared with the "CE" scenario. Over the same time period, the "CE-DER" scenario is \$19 billion more expensive than the "BAU" scenario, but has reduced cumulative emissions by 5,112 mmT (equivalent to a cost of carbon of ~\$3.70 per metric ton). By 2050, the scenario has avoided more than 10,000 mmT compared with "BAU" (as depicted in Fig. ES-2), while saving \$88 billion in costs.

If a clean electricity mandate were imposed by 2035, rather than the modeled 2050 (and the US could deploy enough generation), the DERs would bring forward the cost savings observed by 2050 to 2035, since they enable more clean utility-scale variable generation to be deployed efficiently.



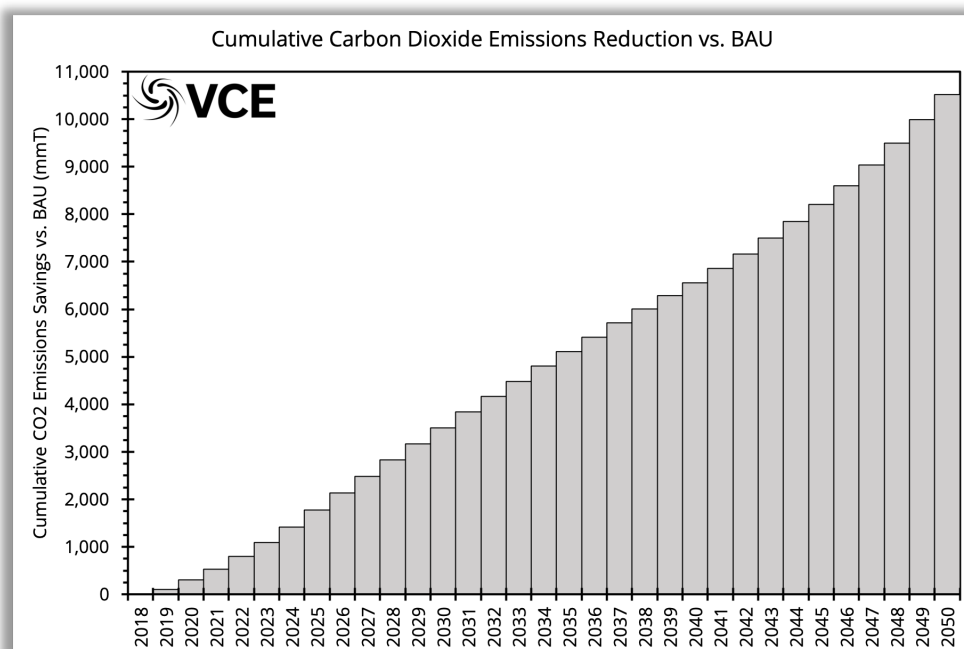


Figure ES-2: The cumulative electricity CO₂ emissions reduction from “CE-DER” compared against “BAU” .

The inclusion of distribution modeling within the WIS:dom-P software drives emergent behavior.¹¹ The distribution grid seeks to minimize exposure to the utility grid while maximizing its benefits of being connected by minimizing system costs that includes infrastructure connecting the utility and distribution grids. This manifests as increased load factors as experienced by the utility-scale grid, while reduced peak demand. Further, the more local resources can defer some distribution infrastructure costs. The sum of these is net system cost savings, increased jobs, more manageable installation rates, a more reliable and robust system, and more opportunities for private capital investments.

The striking result is that the cost savings come with relatively little change in the macro-scale view of installed capacities and generation stack. This is because a small change in the tails of production and demand can have amplified cost implications throughout the system. Additionally, the distribution cost augmentation facilitates economic tradeoff between more resources, which improves competition and reduces costs further.

¹¹ Emergent behavior is characterized by properties and behavior that is not dependent on individual components, but rather the complex interactions and relationships between those individual components. Therefore, it cannot be fully predicted by simply observing or evaluating the individual components in isolation.



1.1 Capacity Changes

In all four scenarios, the entire electricity system undergoes substantial evolution in WIS:dom-P from 2020 through 2050. The general trend is a dramatic reduction in coal and natural gas capacity in exchange for increases in wind and solar PV along with DERs and storage. The model did not include deployments of novel technologies, such as natural gas with carbon capture and sequestration (CCS), small modular reactors (SMR), or molten salt reactors (MSR). Figure ES-3 displays the installed capacity across the CONUS electricity system for each investment period and the four scenarios.

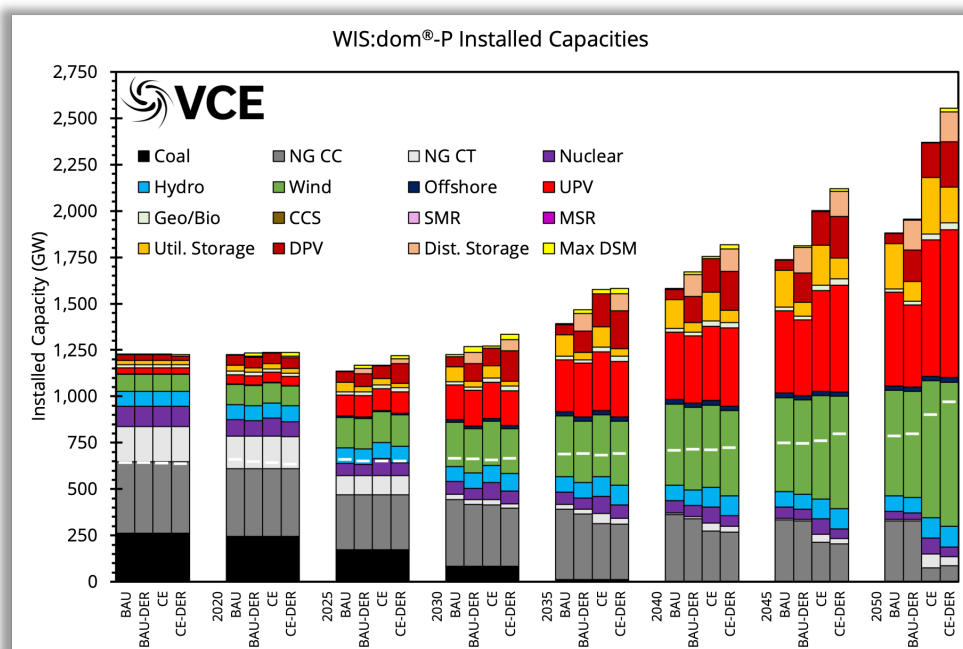


Figure ES-3: The installed capacities over the CONUS. The white bars indicate the peak coincident demand.

The highest buildout of capacity is in the "CE-DER" scenario because it is relying more on DERs and utility-scale wind and solar than the other scenarios. By 2030, the "CE-DER" already has pronounced increases in distributed solar PV and storage (with lower utility-scale counterparts) and deploys much more demand-side management (DSM). The peak demand is similar across all scenarios by 2030. Lower installed capacities of natural gas combined cycle power plants (NGCC) are observed in the clean energy standard scenarios. These scenarios deploy more natural gas combustion turbines (NG CT) to assist with capacity requirements (with lower amounts in the "CE-DER" vs the "CE" scenarios).

All scenarios show substantial growth in electricity storage capacity, with significant additional capacity in the clean energy standard scenarios. It should be noted that a shift in storage capacity occurs in the augmented scenarios from utility-scale storage to distributed scale. This is because the model finds more value deploying the storage in the distribution grid than entirely in the utility-scale grid. However, Fig. ES-3 only shows part of the capacity (power). Figure ES-4 shows the electricity storage capacity in terms of energy. The figure shows that under "CE" 8,200 GWh of storage is deployed between 2020 and 2050 (with only 200 GWh being deployed in the next decade), while in "CE-DER" a



further 1,000 GWh is installed (with 400 GWh additional by 2030). For comparison, the Tesla Gigafactory in Nevada produced, at its peak in 2018, an annualized rate of 20 GWh of batteries.¹² Thus, the “CE” would require almost the entire output of the Gigafactory through 2030 and a sharp increase over the following two decades. The “BAU-DER” and “CE-DER” scenarios require much smoother increases in the deployment requirements of energy storage through 2045 and a steep increase in the final five years of the modeling. Approximately half of the energy storage is deployed in the distribution grid between 2020 and 2050. This shift in deployments facilitates distribution demand profile shaping and shifting that supports the distributed generation and reduces utility-scale system peak demand requirements.

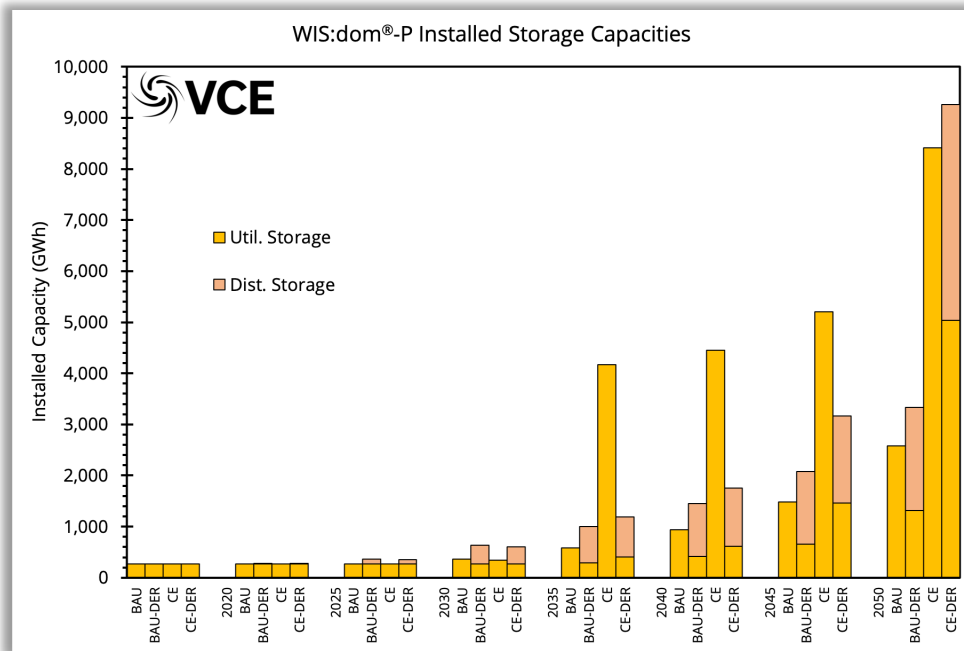


Figure ES-4: The installed capacities over the CONUS for energy storage.

The installed capacity across the CONUS rises by 50% to 100% from 2020 through 2050 in all scenarios. The substantial shift in capacity requires enormous additions and retirements over the next three decades. Figure ES-5 displays the rate of installation and retirement required for each scenario for each investment period. The peak installation rate over all the scenarios was 110 GW per year. For the entire US, the historical peak installation rate is around 55 GW and the typical rate is 10 – 25 GW per year. The rapid increase in installation rate is required to replace higher capacity factor thermal generation with lower-cost, but lower capacity factor variable generation.

More rapid deployments are observed for the “BAU-DER” and “CE-DER” scenarios compared with their traditional counterparts. This is because more utility-scale and distribution-scale variable generation is being constructed. This indicates a more equitable transition of resources because there are more opportunities for competition and siting throughout the whole electricity system, rather than just on the utility-scale.

¹² <https://www.tesla.com/gigafactory>



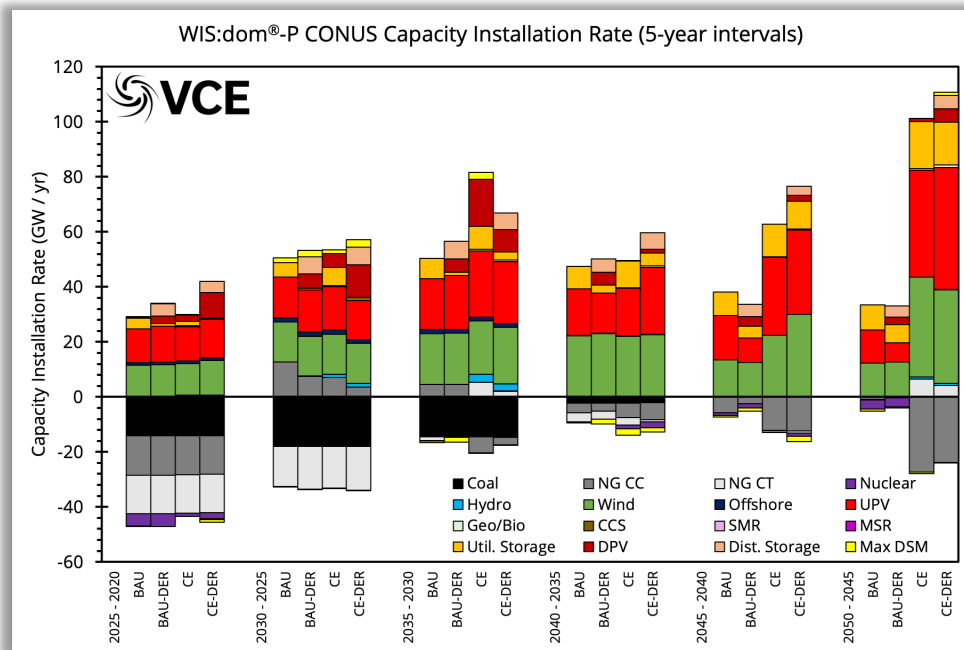


Figure ES-5: The installation and retirement rate over the CONUS.



1.2 Generation Changes

Due to the changing capacity mix generation shifts to lower-emission sources. For the “CE-DER” scenario, the shift is more rapid than the other scenarios, and generally just extends the underlying trend of moving towards VRE and storage. Figure ES-6 displays the generation for each scenario and investment period. It shows that in all scenarios the generation from coal falls to almost zero by 2035. Without the clean energy standard, more natural gas generation replaces the coal retirements. With the clean energy standard, natural gas generation stays about the same as 2018 through 2030 and then rapidly decreases through 2050.

Overall, the addition of distribution modeling results in a shift of generation siting and demand profiles that allows for a more robust system without significant macro-level adjustments to the generation mix. The cost savings come from greater efficiency and more intelligent overall system design.

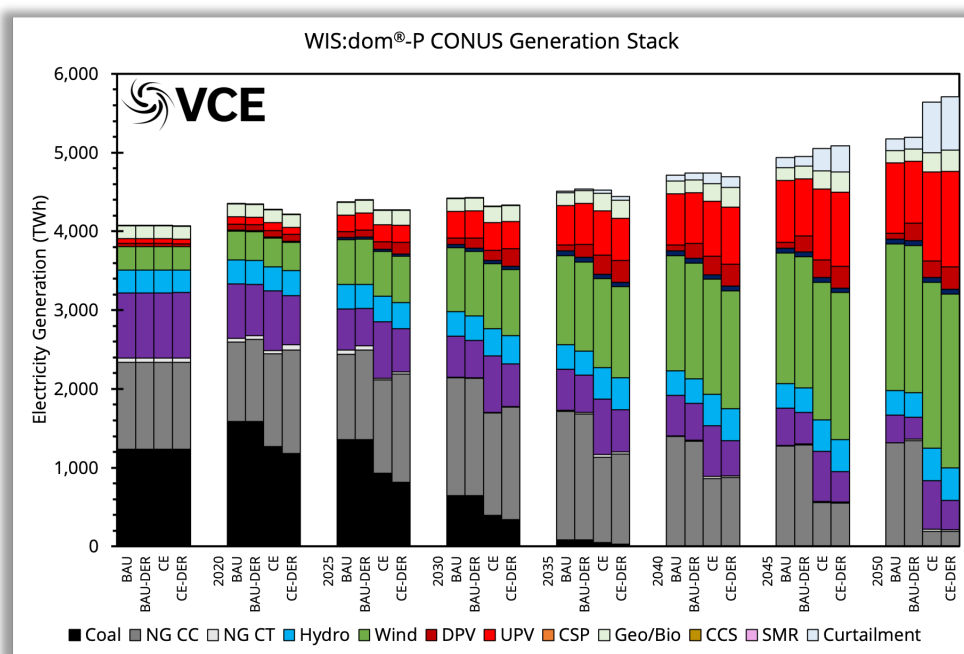


Figure ES-6: The generation breakdown for the CONUS.

By 2050, the change to the generation mix is even more stark when comparing “BAU” and “CE-DER” scenarios daily totals, as plotted in Fig ES-7. It shows the significant growth of utility-scale wind and solar PV as well as distributed PV. There is a much more fluid use of storage as well. The “CE-DER” electricity system is lower-cost than the “BAU” system in 2050; and has accumulated \$88 billion in savings since 2018. Thus, the “CE-DER” can be considered to be containing a negative carbon price. This is due to the distribution modeling augmentation. As seen in Fig. ES-6, there is much more curtailment in the “CE-DER” scenario than in the “BAU” scenario, which is an opportunity for new industries to capture low-cost electricity to help support the system further. The \$88 billion in cumulative cost savings take into account the increase in curtailment, so the savings could end up higher if novel technologies such as hydrogen electrolysis are utilized.



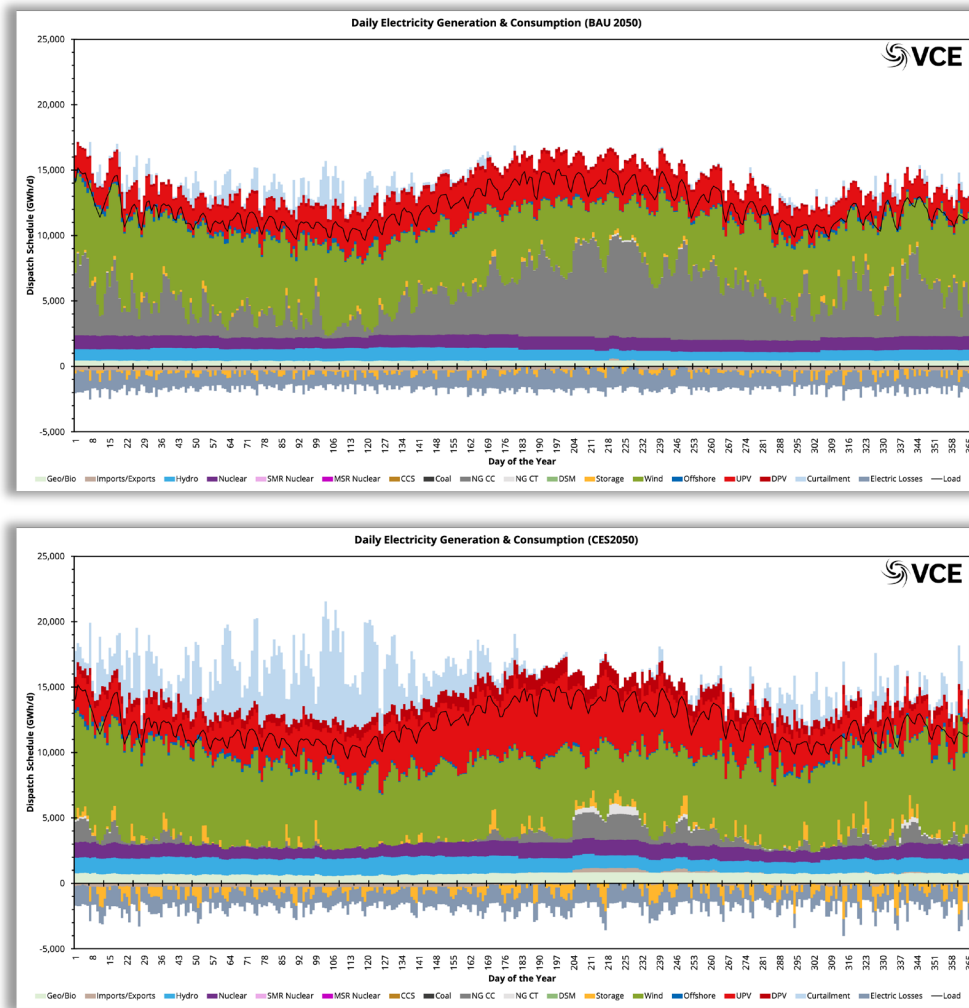


Figure ES-7: The daily generation mix of the CONUS for “BAU” (top) and “CE-DER” (bottom) in 2050.

To deal with the new additional variability of the VRE generation, the WIS:dom-P software must compute reserves and maintain supply and demand for every single time period. The important way this is achieved is that the most difficult times to meet demand are shifted to the lower demand periods where dispatchable generation, transmission, and storage (with residual VREs) can cover the demand much more easily. Figure ES-8 plots the most difficult period for 2050 for the “BAU” and “CE-DER” scenarios. The time period is easily covered by the “CE-DER” scenario with much less natural gas than the “BAU” scenario. In the “CE-DER” scenario, distributed storage, DSM and DR are called upon during these difficult times. This, in combination with both utility- and distributed- scale VRE generation, can reliably cover the coincident peak demands.



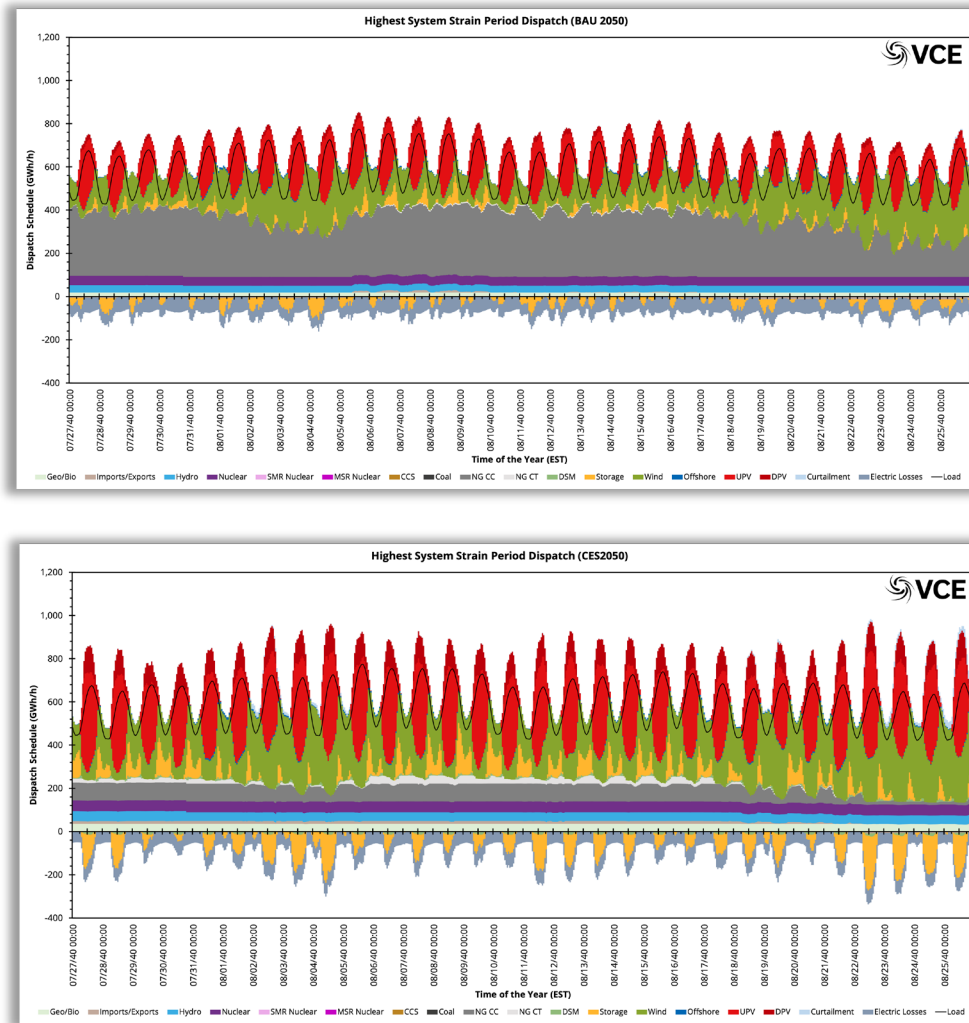


Figure ES-8: The most difficult period to supply demand for the CONUS for in 2050 for the “BAU” (top) and “CE-
DER” (bottom) scenario.



1.3 Carbon Dioxide Emission Changes

The clean electricity scenarios both reduce emissions equally through the modeling because they are constrained to do so. The “CE-DER” scenario does so through large amounts of utility-scale wind and solar generation coupled with DERs. The “CE” does it almost entirely with utility-scale generation and as such costs much more to achieve. Figure ES-9 displays the annual electricity sector CO₂ emissions.

The “BAU” and “BAU-DER” scenarios increase emissions in the early years as deployment of wind and solar are not fast enough to keep up with natural gas; however, and the model reaches 2030 CO₂ emissions fall rapidly.

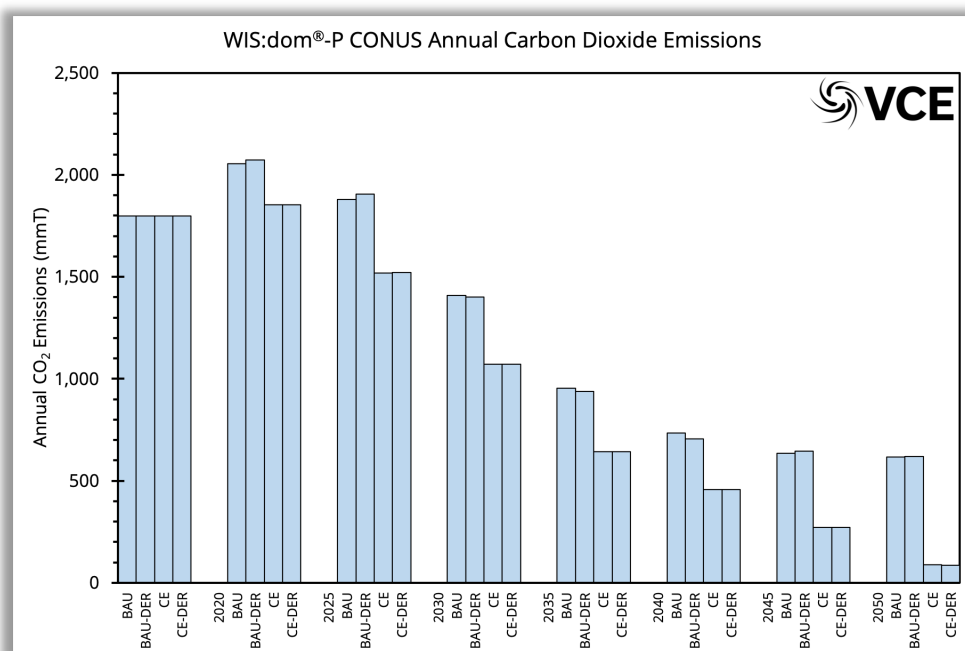


Figure ES-9: The annual CO₂ emissions from electricity production.

Cumulatively, the “CE-DER” scenario reduces emissions by 10 Gt by 2050 compared with the “BAU” scenario and costs \$88 billion less in total system costs. In contrast, the “CE” scenario reduces emissions by the same 10 Gt, but costs an additional \$385 billion over the “BAU” scenario. The “BAU-DER” scenario emits almost exactly the same amount of carbon dioxide as the “BAU” scenario through 2050 (cumulatively avoids 12 mmT), but costs \$301 billion less in total system costs.

The reduction in fossil fuel combustion within the electricity sector for all scenarios dramatically reduces the local pollutants that are damaging to the environment and health; with SO_x, N₂O, PM_{2.5}, PM₁₀, VOCs almost entirely eradicated.



1.4 Electricity Price Changes

Even though the electricity system is undergoing substantial change in the modeling scenarios, the total system costs are subdued and fall across all scenarios through 2050. This is because low-cost renewables and natural gas help reduce wholesale electricity costs. There are costs to upgrade the distribution infrastructure, but there are also cost savings from deferment of upgrades to the transmission-distribution interface (or connection points) as well as removing unnecessary utility-scale capacity reserved for peaking needs. Since the modeling reduces utility-observed system peaks by around 16% by 2050 (due to the DER coordination) compared with “BAU”, a significant fraction of utility-scale peaking and capacity is avoided.

Figure ES-10 shows that both the system costs and the average retail rates drop in each scenario from 2018. Note that the lowest rates by 2050 are for the “BAU-DER” scenario and the highest is for the “CE” scenario. In the earlier years, some additional spending does take place to upgrade the distribution system to accommodate more DERs, but these costs are repaid rapidly and harden the system for other potential changes to demand from either climate change or electrification (or likely both).

It is important to note that in the modeling we used the NREL ATB 2019¹³ cost assumptions for generation technologies. The downward trends in all of the output system costs provide reassurance that the costs can remain at or below today’s levels given possible uncertainty in price forecasts. The reduction in cost (in general) across the modeling is approximately 30% by 2050. If the NREL price forecasts are 10% too aggressive, then there would still be a 20% reduction in future system costs. Indeed, the additional savings realized by including DER coordination indicates a no-regrets decision in choosing a path that expands their presence on the electricity system.

Finally, a reduced electricity rate could help drive indirect benefits because there will be more disposable income available to customers.

¹³ <https://atb.nrel.gov/electricity/archives.html>



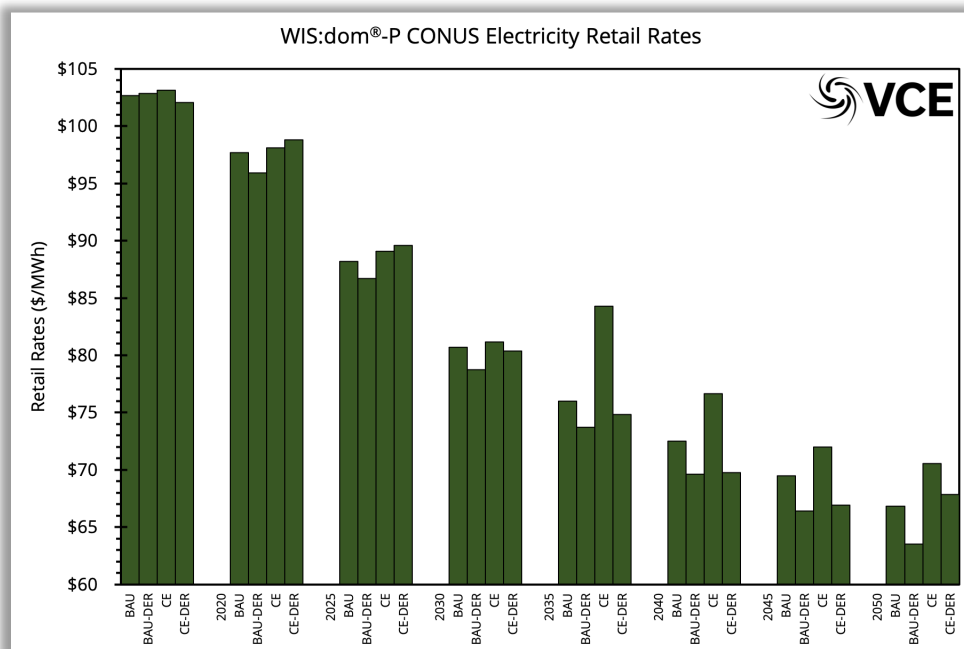
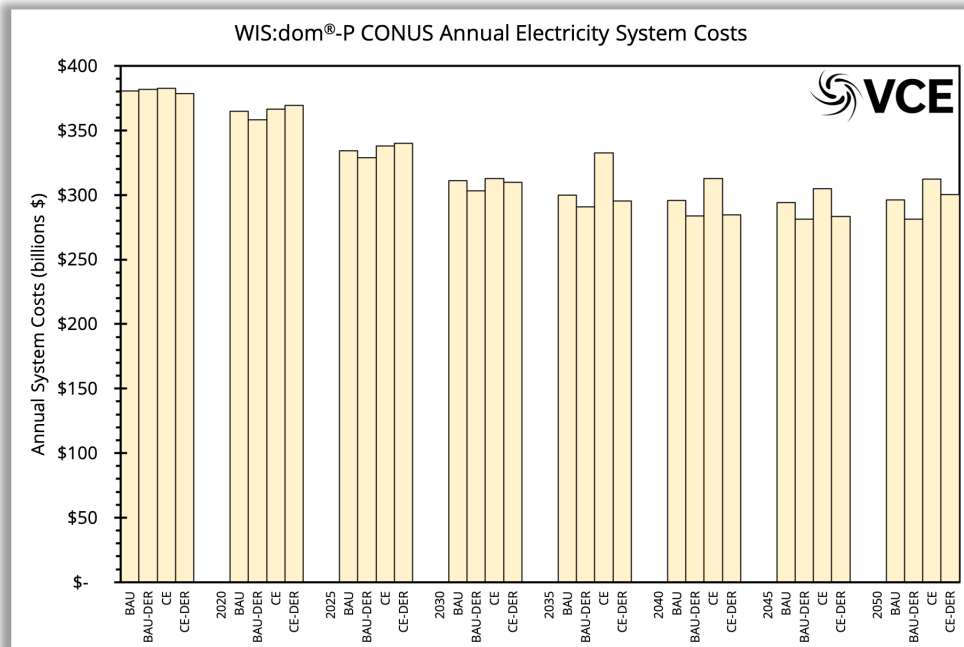


Figure ES-10: The total system costs (left) and average electricity retail rates (right).



1.5 Changes in Employment

The modeled evolution of the US electricity increases jobs. This modeled trend corresponds with historically observed trends as wind and solar generation have been deployed. When DERs are coordinated with the rest of the utility-scale grid, the job numbers accelerate. This is because DERs typically employ more workers than the utility-scale alternative. The coordination with DERs enhances the job growth in wind and solar PV on the utility-scale.

The increase in jobs will provide other benefits that are not modeled or analyzed, such as tax revenues, economic stimulus through higher employment numbers, and supporting jobs (known as induced jobs).

Different states and regions have varying degrees of job creation and reduction. These differences can be homogenized through careful policies and redistribution of savings to help facilitate the transition to a clean energy economy.

The job growth is net of losses that occur due to retirements of legacy generation. The job increases outstrip losses in every state in the for all scenarios, with higher increases in the "DER" scenarios.

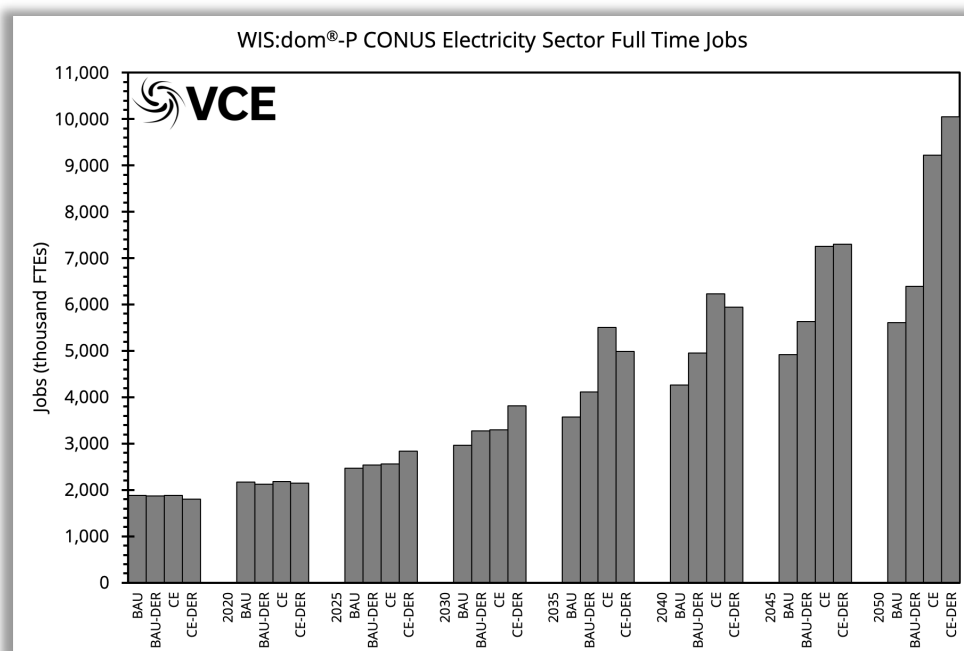


Figure ES-11: The full-time jobs from the electricity sector.



1.6 WIS:dom[®] -P Augmentation

The WIS:dom-P software was enhanced and augmented during the course of the project. The purpose of the augmentation was to better represent the interface between the utility- and distribution-scale grids. At current computing power, it is not possible to represent every distribution line, home, generator, and feeder across the entire contiguous United States. However, it is possible to parameterize and represent the infrastructure through an interface. This interface can accumulate the costs and associated infrastructure for the distribution grid as new resources are added and the flows change. The modeling sets boundary conditions for full distribution modeling at much higher resolution over much smaller geographic areas.

The interface concept translates to having two different components to the electricity system: a central core that houses the transmission system and utility-scale generation and many satellite bubbles connected to the central core that represent the distribution grids. The WIS:dom-P software is representing the topology at 3-km for generation and transmission (as well as DPV and storage), but the distribution loads are assumed to be singularities at the 69-kV substations, where the costs of the distribution infrastructure is represented with an event horizon. To cross that event horizon in either direction has a cost. For example, if power flows from the distribution grid to the transmission grid (known as back flow), the model assigns a cost for peak power and per unit of energy. The WIS:dom-P software is also simultaneously computing transmission requirements and utility-scale generation. These are all competing with each other as the model seeks a minimum system cost solution to tradeoff all the different costs and values provided by each resource and asset.

A schematic of the process is shown in Fig. ES-12. A detailed technical documentation of WIS:dom-P is available to download on the VCE website.¹⁴ The section of the technical document dedicated to the DU interface is 1.9.2.

The main purpose of introducing a DU interface into WIS:dom-P is to provide information to the optimization to account for: the cost of connecting customers in the distribution grid with the utility grid; the integration costs of distributed resources; the cost of pushing distributed generation to the utility grid; and the value of reducing the power and energy draw from the utility grid into the distribution grid. This new information fundamentally changes the structure of the optimization because it can now recognize that deployments within the distribution grid can reshape the demand observed by the utility grid.

The reshaping of the utility-observed distribution demand provides the following highest value benefits:

1. Ability to remove peaking generation on the utility grid;
2. Increase the utilization of utility grid generation that remains and reduce ramping stress;
3. Reduce burden on transmission system to move electricity at peak demand time periods;

¹⁴ [https://vibrantcleanenergy.com/wp-content/uploads/2020/08/WISdomP-Model_Description\(August2020\).pdf](https://vibrantcleanenergy.com/wp-content/uploads/2020/08/WISdomP-Model_Description(August2020).pdf)



4. Adjust demand to meet supply variability (rather than supply always adjusting to demand).

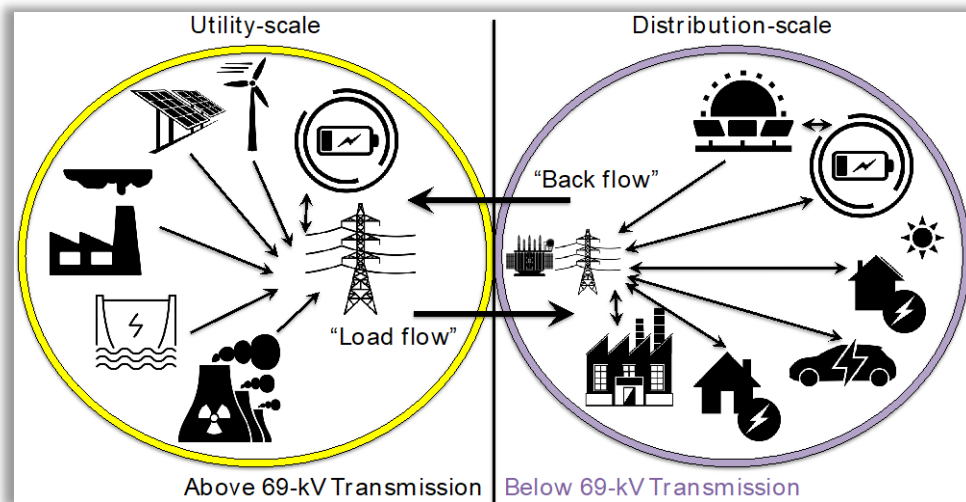


Figure ES-12: A schematic picture of the DU interface within the WIS:dom-P modeling platform.

The generation stack changes due to the DU interface can be seen for an example region in Figs ES-13 through ES-16. Figures ES-13 and ES-15 display traditional optimization framework dispatch, while Figs ES-14 and ES-16 show augmented optimization framework dispatch. The solid black lines denote the demand. These plots demonstrate how the DERs are reshaping the demand observed by the utility grid to dampen the volatile oscillatory behavior (peaks and troughs), while simultaneously capitalizing on low-cost utility-scale wind and solar when supply is high. It can also be seen that the DERs are *charging* at times of lower demand, which increases the utilization of the distribution infrastructure, increases the efficiency of utility-scale generation and transmission, and enables demand peak reduction at a later time.

Figure ES-17 displays the same data as in Figs ES-14 through ES-16, but for an entire calendar year. It is organized as a demand duration curve. The blue and red denote the change to the demand due to the DU interface augmented framework. The blue shows utility-observed demand reduction, while the red shows the increase. The grey denotes the unchanged portion of the demand duration curve. For the example region, the peak demand is reduced by over 30%, while the lowest period is increased by just under 10%. This illustrates the smoothing of utility-observed demand. The demand is reduced for approximately 80% of a calendar year, so the augmentation is more than merely a peak-shaving exercise.

Figure ES-17 captures the most important consequence of the DU interface: demand can be reshaped to meet supply in a manner that provides value for the entire electricity system.



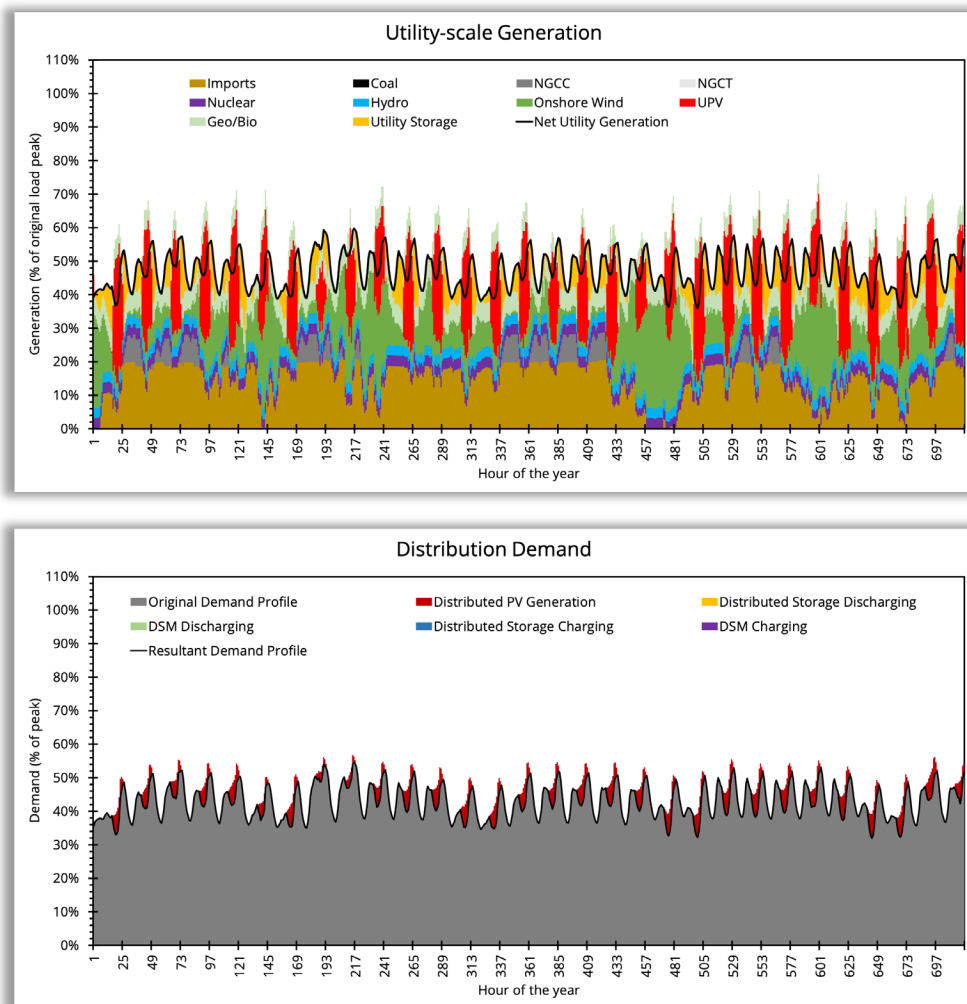


Figure ES-13: A winter example region dispatch of utility- (top) and distribution- (bottom) grid generation under a traditional optimization framework.



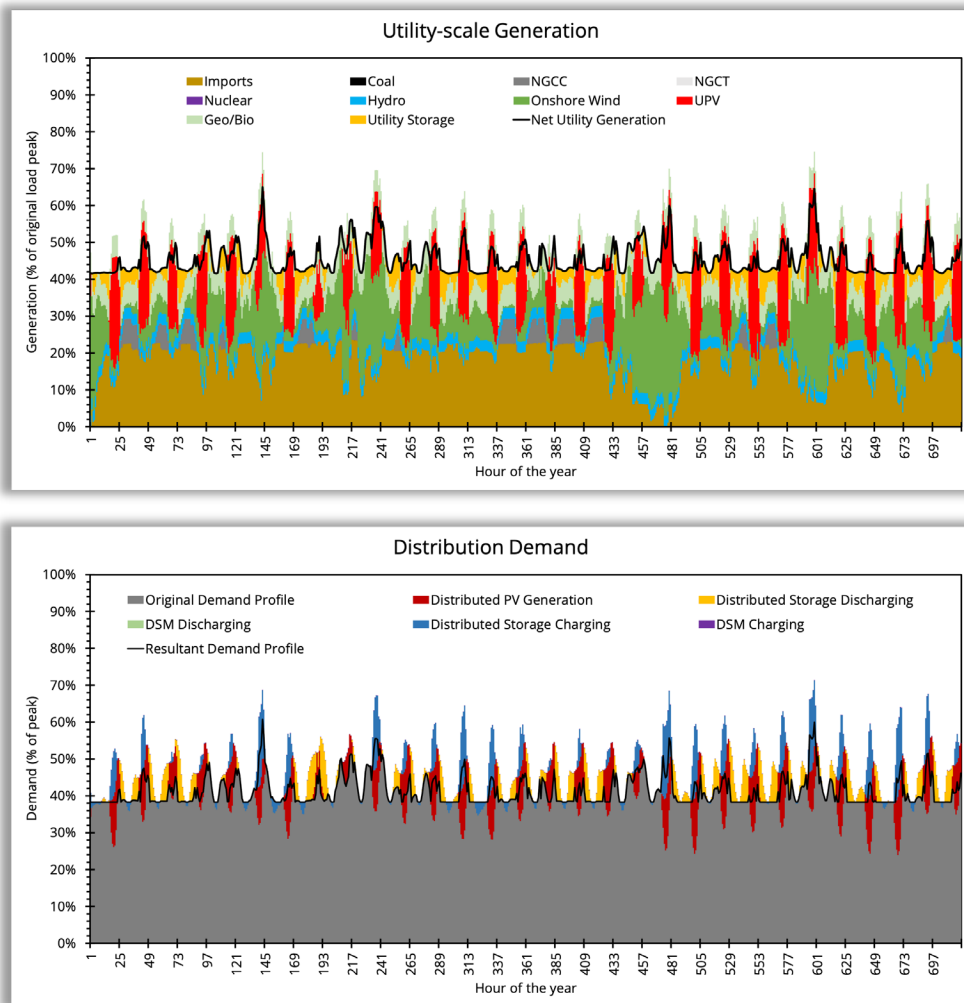


Figure ES-14: A winter example region dispatch of utility- (top) and distribution- (bottom) grid generation under an augmented optimization framework.



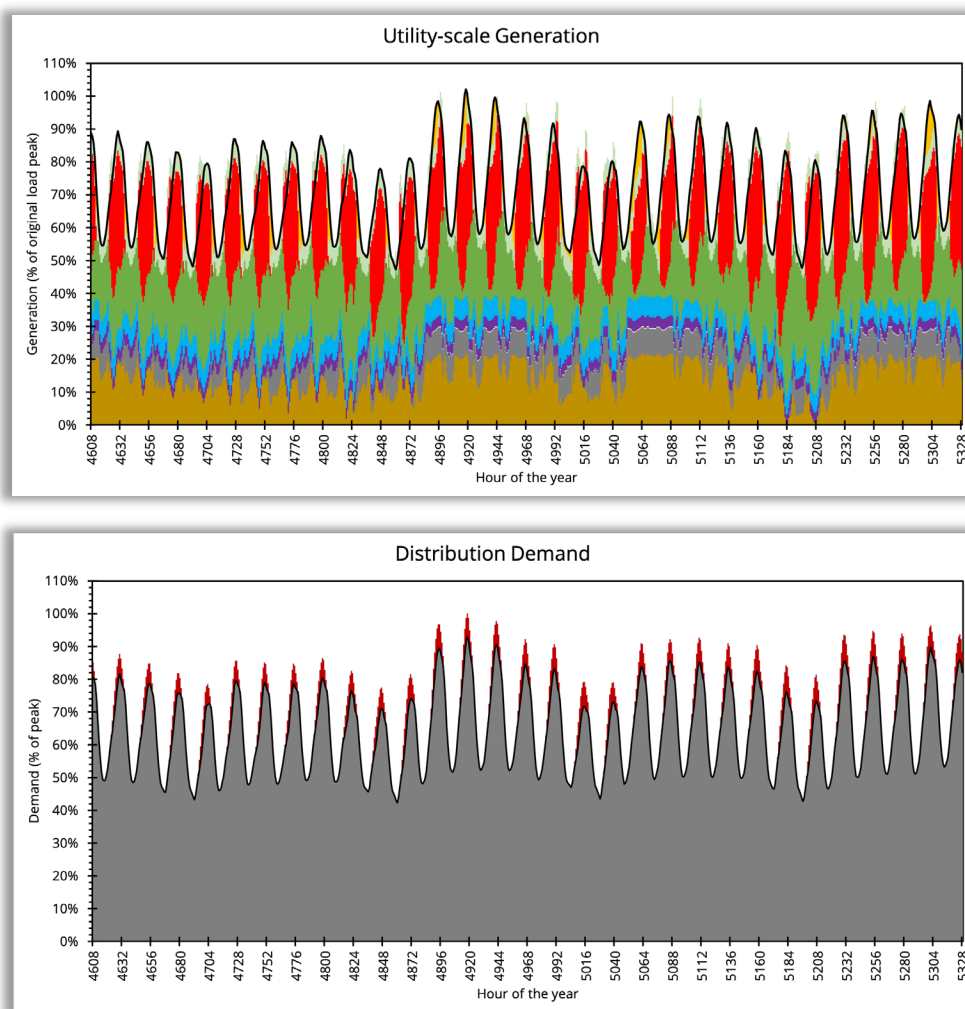


Figure ES-15: A summer example region dispatch of utility- (top) and distribution- (bottom) grid generation under a traditional optimization framework.



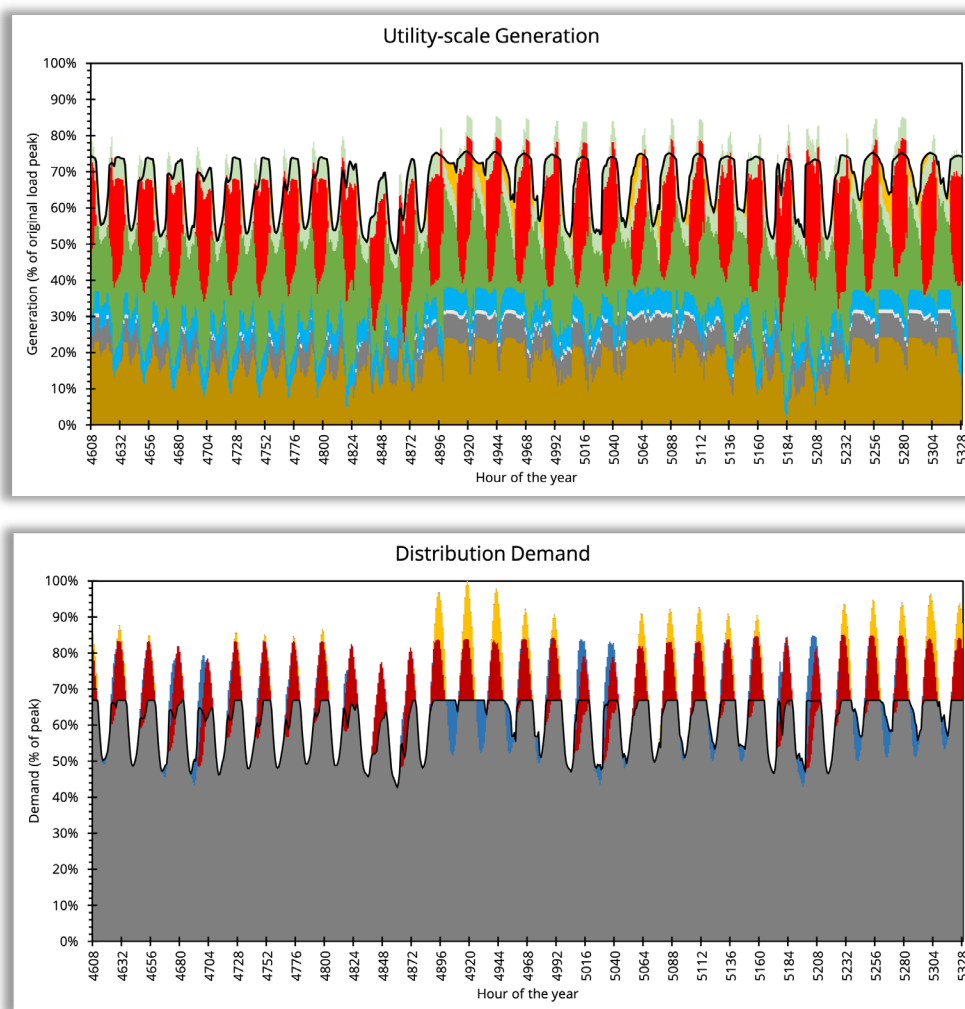


Figure ES-16: A summer example region dispatch of utility- (top) and distribution- (bottom) grid generation under an augmented optimization framework.



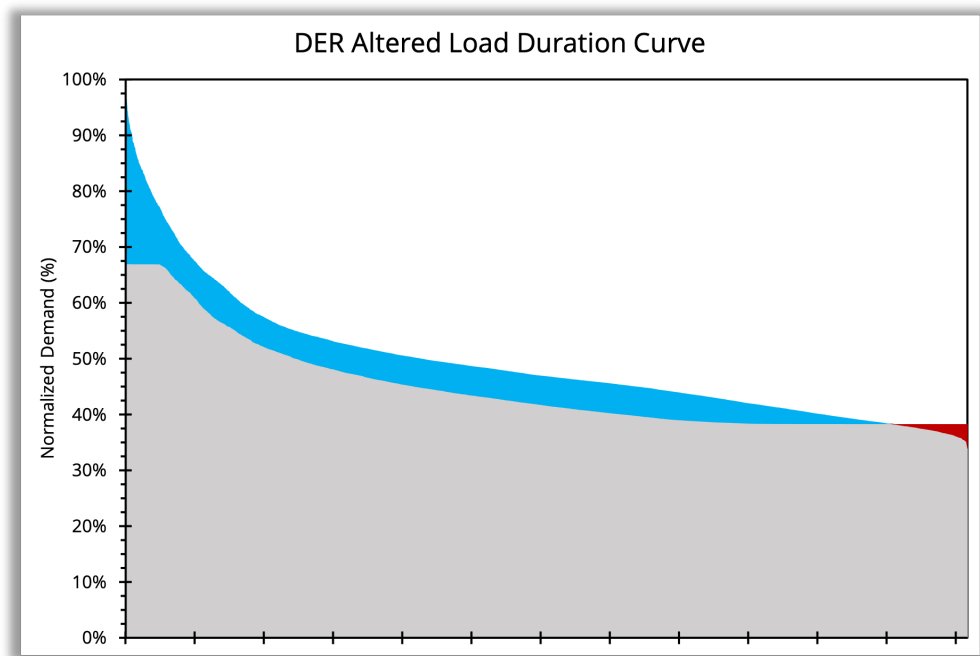


Figure ES-17: A demand duration curve for an example region that shows the reduction in demand (blue) for the majority of the year. The red shows an increase in demand.



2. Study Description

The electricity system in the United States (US) is considered to be one the largest machines ever created.¹⁵ With the advent of clean and renewable technologies, a widespread evolution is occurring. The renewable technologies are lower cost than fossil thermal generation on a levelized cost basis,¹⁶ but their variability creates new and unique constraints and opportunities for the electricity system of the next several decades. Superimposed on the changing structure of the electricity system is a damaged climate that will continue to worsen as mankind continues to emit greenhouse gas (GHG) pollution into the atmosphere.¹⁷

The US electricity system is the second largest in the world (China has the largest). In 2018 it served approximately 150 million customers with over 3,859 terawatt-hours (TWh) of electricity from over 1,190 gigawatts (GW) of generating capacity, routed through 476,000 miles of transmission lines (over 69 kV), 55,000 substations and 6.3 million miles of distribution lines (under 69 kV).^{18,19,20} By the end of 2019, there was 86,000 MW of renewable capacity awaiting construction across the US and each year that number continues to grow.²¹ The carbon dioxide (CO₂) emissions from electricity generation across the US reached an estimated 1,659 million metric tons (mmT) in 2019, accounting for approximately 32% of the total United States (US) energy-related CO₂ emissions (5,130 mmT).²²

The present study demonstrates, quantifies and evaluates the potential value that distributed energy resources (DERs) could provide to the electricity system, while considering as many facets of their inclusion into a sophisticated grid modeling tool. The *Weather-Informed energy Systems: for design, operations and markets planning* (WIS:dom®-P) optimization software tool is utilized for the present study. A detailed technical document of the WIS:dom-P software can be found online.²³ The modeling software is a combined capacity expansion and production cost model that allows for simultaneous 3-kilometer, 5-minute dispatch and power flow along with multi-decade resource selection. It includes detailed representations of fossil generation, variable resources, storage, transmission and DERs. It also contains policies, mandates, and localized data, as well as engineering parameters and constraints of the electricity system and its components. Some novel features include highly granular weather inputs over the whole US, climate change-induced changes to energy infrastructure, land use and siting constraints, dynamic transmission line ratings, electrification and novel fuel production endogenously, and detailed storage dispatch algorithms.

The distribution grid is where the majority of customers connect with the electricity system at large. However, traditional modeling tools ignore its existence almost entirely. Many assume pre-decided buildout rates of distributed solar PV (DPV), energy efficiency (EE),

¹⁵ <https://www.bloomberg.com/quicktake/u-s-electrical-grid>

¹⁶ <https://atb.nrel.gov/electricity/2020/index.php?t=in>

¹⁷ <https://climate.nasa.gov/>

¹⁸ <https://www.energy.gov/sites/prod/files/2017/01/f34/Electricity%20Distribution%20System%20Baseline%20Report.pdf>

¹⁹ <https://www.eia.gov/electricity/data/eia860/>

²⁰ <https://www.eia.gov/electricity/data/eia923/>

²¹ <https://www.eia.gov/electricity/data/eia860/>

²² <https://www.eia.gov/environment/emissions/carbon/>

²³ [https://vibrantcleanenergy.com/wp-content/uploads/2020/08/WISdomP-Model_Description\(August2020\).pdf](https://vibrantcleanenergy.com/wp-content/uploads/2020/08/WISdomP-Model_Description(August2020).pdf)



demand-side management (DSM), demand response (DR), and distributed storage (DS). As the electricity system continues to evolve, customers are demanding more local resources. This creates a problem because the providers of electricity (across utility service territories and RTOs) do not possess integrated modeling tools that reveal the opportunities and costs of changing distributed generation and demand as a decision variable. The opportunities could include reduced utility-scale capacity and generation, high-voltage transmission, distribution infrastructure deferrals, utility-observed peak load reduction, and increased utility-observed load factors. The costs could be more distribution infrastructure, more high-voltage transmission, increased DER buildout, and utility-scale back-up capacity and generation to cover the DER buildout.

Vibrant Clean Energy, LLC (VCE®) augmented the WIS:dom-P software to improve its representation and computations of the distribution-utility (DU) interface. The augmentations enabled a modeling framework that included the distribution grid and DERs that is tractable and akin to traditional utility planning models.



2.1 Modeled Scenarios

During the entire study, **fifteen** nationwide simulations were performed. Numerous intermediate simulations were used to determine the sensitivity of the modeling tool to changes in the augmentation created during the study. The model was initialized and aligned with historical data from 2018 and then the simulations evolved the electricity system across the contiguous United States (CONUS) from 2020 through 2050 in 5-year investment periods. In the present report, we focus on **four** main scenarios that answer two main questions:²⁴

1. *Can DERs lower costs across the entire electricity system compared with alternatives, while maintaining resource adequacy, reliability and resilience?*
2. *Can DERs provide support and benefits for clean electricity goals across the entire electricity system?*

The four scenarios simulated for the present report were:

Business-As-Usual, Traditional ("BAU"): Allow economics to drive the changes in the electricity system, while including existing policies, mandates, and incentives through 2050. Deploy WIS:dom-P in a manner that mimics traditional models.

Business-As-Usual, Augmented ("BAU-DER"): Allow economics to drive the changes in the electricity system, while including existing policies, mandates, and incentives through 2050. Deploy the augmented version of WIS:dom-P that includes detailed modeling of the distribution-utility (DU) interface.

Clean Electricity, Traditional ("CE"): Enforce a nationwide clean energy standard (CES) that reduces emissions by 95% from 1990 levels by 2050. Deploy WIS:dom-P in a manner that mimics traditional models.

Clean Electricity, Augmented ("CE-DER"): Enforce a nationwide clean energy standard (CES) that reduces emissions by 95% from 1990 levels by 2050. Deploy the augmented version of WIS:dom-P that includes detailed modeling of the distribution-utility (DU) interface.

The model setup (including load and transmission topology) to simulate the study scenarios is described in Section 2.2. Section 3 presents and discusses the modeling results, and Section 4 describes the input datasets for WIS:dom-P, along with a discussion of the important trends in weather that impact model results.

²⁴ Future reports will present findings from the remaining 11 simulations. One of the simulations electrified and decarbonized the entire CONUS economy. All the remaining 11 simulations enhance or provide additional support for the conclusions detailed in the present report.



2.2 Model Setup

To determine the impact of DERs on electricity system, WIS:dom-P modeled the whole contiguous United States (CONUS) in two stages: First, at state- and county- level resolution (outer); secondly at a nodal (69-kV) and 3-km granularity (inner). The purpose of the *outer-inner modeling framework* is to incorporate as much data as possible, while maintaining a tractable solution time. The solution from the outer simulation is used as boundary conditions for the inner simulation. The outer simulation is then sacrificed when the inner simulation completes.

The variable renewable energy (VRE) resources, electric storage, thermal generation, demand, and distribution infrastructure are modeled at county-level resolution in the outer simulation (taking into account transmission losses from potential 3-km sites) and then at 3-km resolution in the inner simulation. The bulk transmission is modeled at state-level granularity in the outer simulations (along with spur lines for the interconnection of resources and demand) and at nodal granularity in the inner simulations.

Figure 2.1 shows the location of generators that were in service in 2018, which is developed by aligning the Energy Information Administration Form 860 (EIA-860) dataset²⁵ with the National Oceanic and Atmospheric Administration (NOAA) High Resolution Rapid Refresh (HRRR)²⁶ model grid. More details on the existing generator topology can be found in Section 4.1.

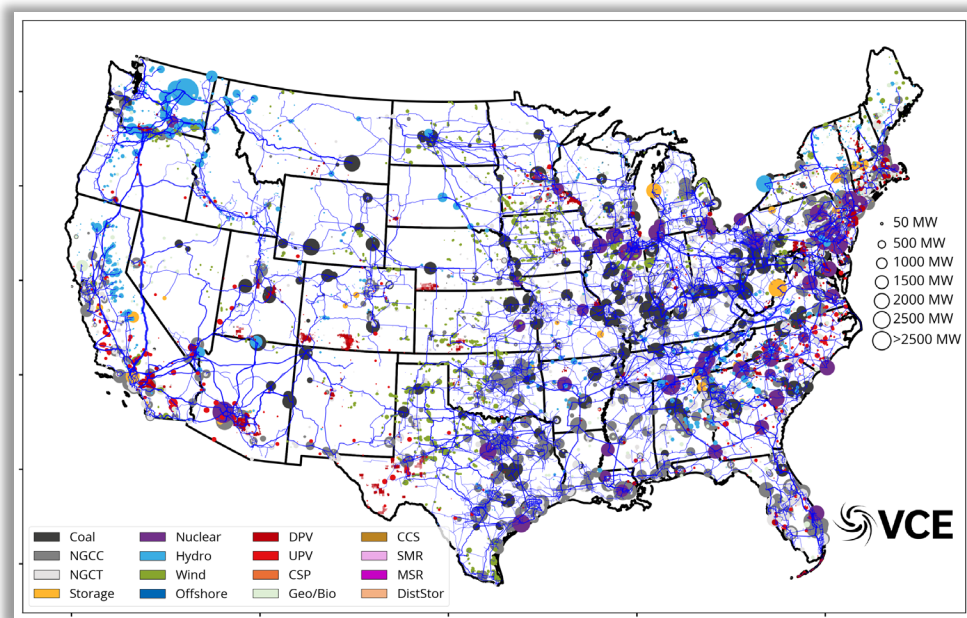


Figure 2.1: Electricity generators and high-voltage transmission in service in 2018.

The demand dataset is created by using a combination of weather data and Federal Energy Regulatory Commission form 714 (FERC-714) data.²⁷ The FERC-714 data provides total

²⁵ <https://www.eia.gov/electricity/data/eia860/>

²⁶ <https://rapidrefresh.noaa.gov/hrrr/>

²⁷ <https://www.ferc.gov/industries-data/electric/general-information/electric-industry-forms/form-no-714-annual-electric/data>



demand by reporting agency over the CONUS at hourly time resolution. This dataset is split into four components: (1) Space heating demand, (2) water heating demand, (3) transportation demand, and (4) conventional demand (including industrial demands, residential cooling demands, lighting demands, and so on). Using the weather data, profiles for space heating, water heating, and transportation are created for the required temporal and spatial resolution (from 5-minute, 3-km to hourly, state-level) as illustrated in Fig. 2.2.

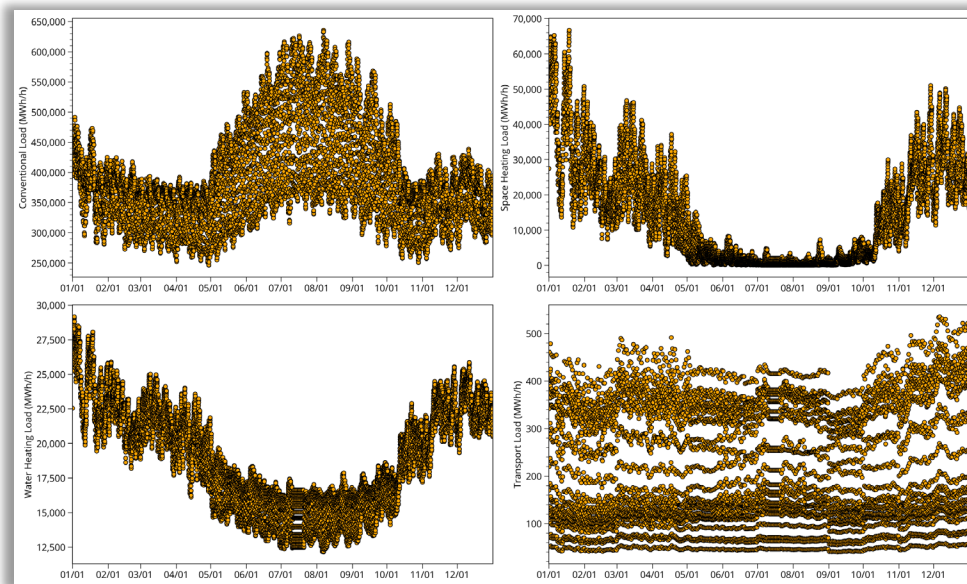


Figure 2.2: Contiguous United States demand profiles from WIS:dom-P for 2018. Conventional (top left), space heating (top right), water heating (bottom left), transportation (bottom right).

The historical demand curve created from the FERC-714 data is adjusted to remove the weather-derived profiles of space heating, water heating, and transport to produce a weather-aligned conventional demand profile. The aggregated demand profile (obtained by summation of the four components of the demand) is shown in Fig. 2.3. Further details on the procedure to create the demand dataset is discussed in Sections 2.5 and 2.6 of the WIS:dom-P technical documentation.²⁸

²⁸ [https://vibrantcleanenergy.com/wp-content/uploads/2020/08/WISdomP-Model_Description\(August2020\).pdf](https://vibrantcleanenergy.com/wp-content/uploads/2020/08/WISdomP-Model_Description(August2020).pdf)



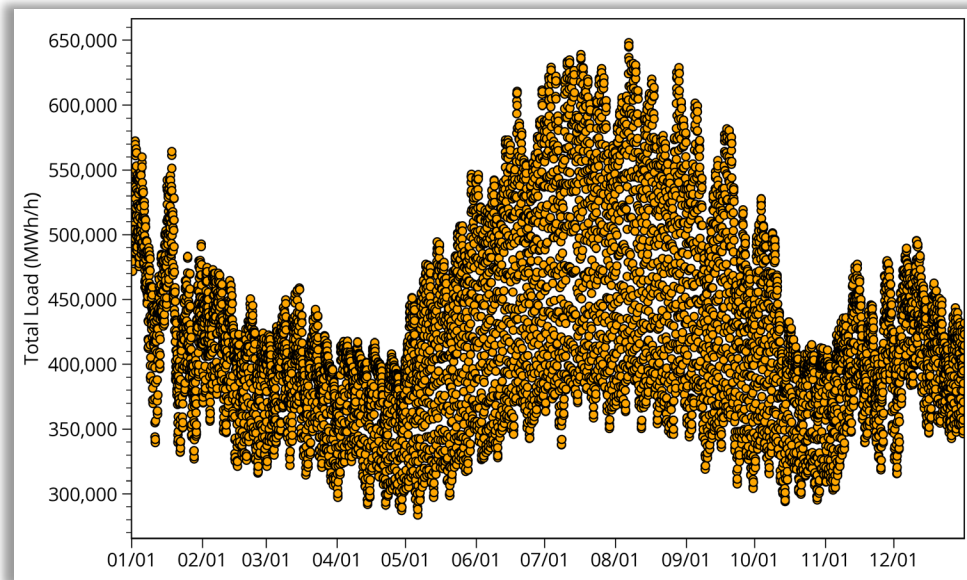


Figure 2.3: The Continental United States aggregated electric demand profile for 2018.

WIS:dom-P resolves the transmission topology of the US electricity system to a granularity down to each 69-kV substation as shown in Fig. 2.5 (top panel). The transmission topology can be aggregated to create a *reduced-form* (county- or state- level) as required for each model simulation. The transmission topology aggregated to county-level resolution is shown in Fig. 2.5 (bottom panel), while the state-level resolution is shown in Fig. 2.4. The outer simulation utilizes the state- and county- level *reduced-form* transmission systems. The county-level is for the spur lines connections, while the state-level is for the bulk transmission. The inner simulation uses the results from the outer simulation reduced-form transmission as boundary conditions upon the full 69-kV resolution transmission system.

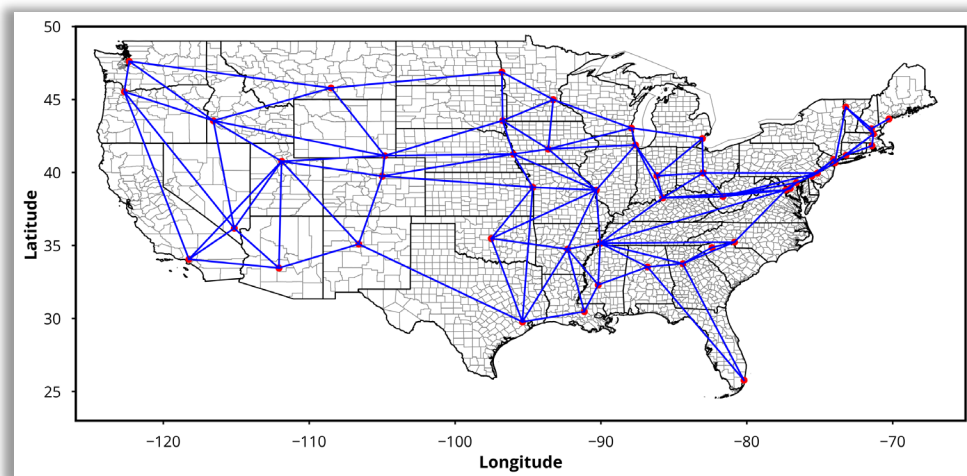


Figure 2.4: State-level, reduced-form, transmission topology of the CONUS electricity system as used in the present study outer simulations.



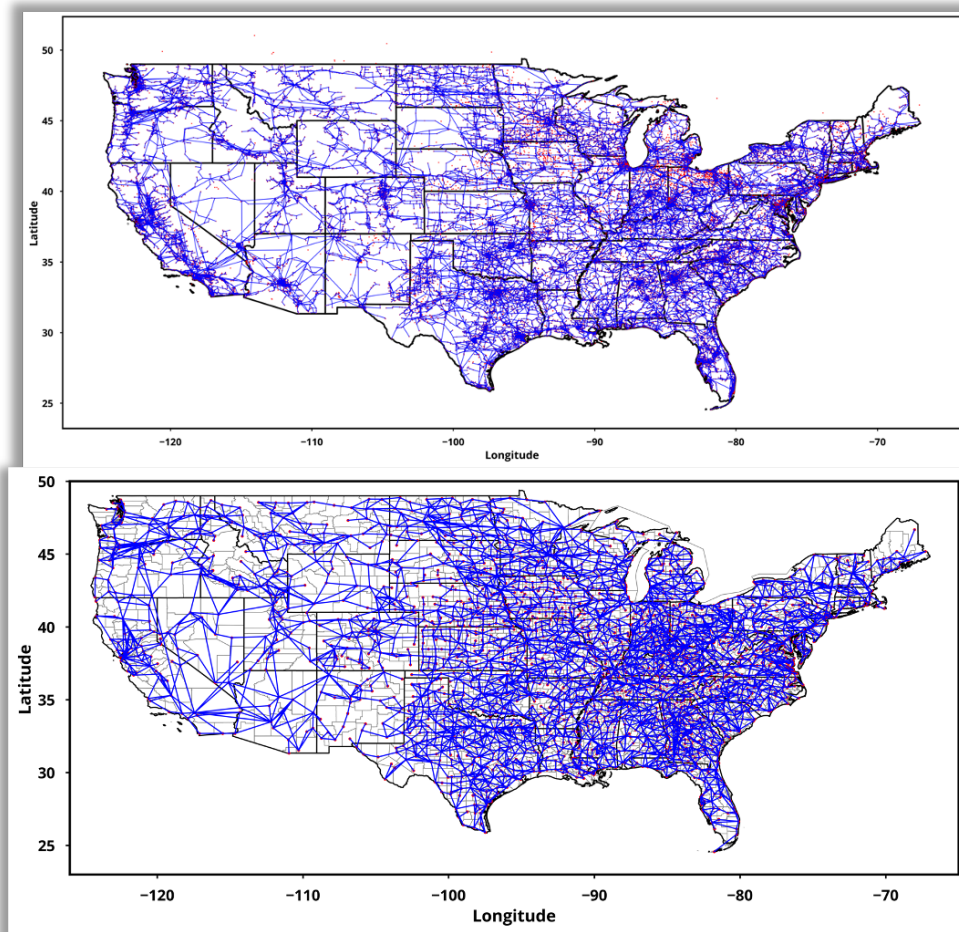


Figure 2.5: Transmission topology of the CONUS electricity system representing each 69-kV substation (top) and reduced-form to county level granularity (bottom).



2.3 Distribution System Representation

The distribution system modeling and how it interacts with the utility-scale grid is an important component of the total electricity grid. It should be modeled to more accurately determine the fundamental workings of the entire electricity system. To represent the distribution system in the WIS:dom-P software, we (necessarily)²⁹ employ a parameterization method, whereby all the demands and DERs within the distribution system are routed to the closest 69-kV substation.

The WIS:dom-P software disaggregates the DER technologies, but aggregates the distribution lines and other infrastructure at an interface (*grid edge* or *event horizon*) that electricity must cross to enter (or exit) the distribution grids (from) the utility grids. This distribution-utility (DU) interface accumulates the costs, and associated infrastructure, for the distribution grid as new resources are added and the flows change. The modeling would set boundary conditions for full distribution modeling at much higher resolution over much smaller geographic areas.

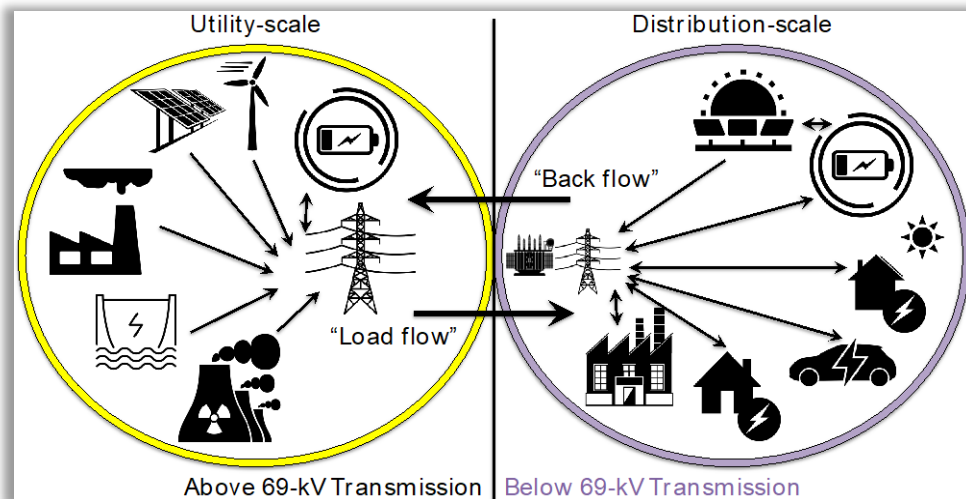


Figure 2.4: A schematic picture of the DU interface within the WIS:dom-P modeling platform.

The interface concept translates to having two different components to the electricity system: a central core that houses the transmission system and utility-scale generation and many satellite bubbles connected to the central core that represent the distribution grids. The WIS:dom-P software is representing the topology at 3-km for generation and transmission (as well as DPV and storage), but the distribution loads are assumed to be singularities at the 69-kV substations, where the costs of the distribution infrastructure is represented with an event horizon. To cross that event horizon in either direction has a cost. For example, if power flows from the distribution grid to the transmission grid (known as back flow), the model assigns a cost for peak power and per unit of energy. The WIS:dom-P software is also simultaneously computing transmission requirements and utility-scale generation. These are all competing with each other as the model seeks a

²⁹ It is necessary because there is not enough data to represent (explicitly) every distribution line and electrical feeder across the entire contiguous United States. Even if all the data existed, the modeling would become intractable due to the scale of the problem.



minimum system cost solution to tradeoff all the different costs and values provided by each resource and asset. A schematic of the process is shown in Fig. 2.6.

The parameterization of the DU interface is dependent on *three components* of the distribution system:

- a. *Utility-observed peak distribution demand;*
- b. *Utility-observed peak distribution generation;*
- c. *Utility-observed distribution electricity consumption.*

The definition of *Utility-observed* is the appearance of the metric at 69-kV transmission substation or above. Below the 69-kV, the model is implicitly solving with combinations of DERs, and what remains is exposed to the utility-scale grid at the substation. The above three components of the distribution system are made part of the optimization objective function; directly linking them to the total system costs.

The new terms for the objective function are introduced through the distribution costs function, which is written as:

$$\text{Distribution Costs} = \Lambda \cdot \left\{ \mathcal{C}_L^{dp} \cdot [\mathcal{E}_L^p + \lambda_a \cdot (\mathcal{E}_L^b + \mathcal{E}_L^m)] + \hbar \cdot \mathcal{C}_L^{de} \cdot \sum_t (\mathcal{E}_{Lt} - \lambda_b \cdot \mathcal{J}_{Lt}) \right\}.$$

where,

\mathcal{E}_{Lt} is the demand at each timestep at each 69-kV substation;

\mathcal{J}_{Lt} is the (net) generation at each time step from DERs (DPV, DSM, and distributed storage);

\mathcal{C}_L^{dp} and \mathcal{C}_L^{de} are constants that parameterize the cost of installing and operating the distribution infrastructure. These constants were obtained from "*Trends in Transmission, Distribution and Administration Costs for US Investor-Owned Electric Utilities*",³⁰

\mathcal{E}_L^p is the utility-observed peak demand;

\mathcal{E}_L^b is the utility-observed peak distribution generation or net back-flow;

\hbar is the timestep of the operational portion of the model.

The three user-defined parameters (Λ , λ_a , and λ_b) can alter the scales of different terms within the optimization. Below, we describe the possible combinations of these user-defined parameters. We highlight the two combinations (1. and 2.) used in the present study.

³⁰ https://energy.utexas.edu/sites/default/files/UTAustin_FCe_TDA_2016.pdf



1. $\Lambda = 0$, $\lambda_a = 0$, and $\lambda_b = 0$:

No co-optimization with distribution-level infrastructure. Model does still co-optimize distribution-level generation, loads, demand flexibility and storage.

2. $\Lambda = 1$, $\lambda_a > 0$, and $\lambda_b > 0$ (typically $\lambda_a = \lambda_b = 1$):

Full co-optimization with distribution-level infrastructure. Determines the benefits and costs associated with DER buildout on the distribution infrastructure. Model does still co-optimize distribution-level generation, loads, demand flexibility and storage.

3. $\Lambda = 1$, $\lambda_a = 0$, and $\lambda_b = 0$:

Co-optimization with distribution-level infrastructure, but when only accounting for load requirements and ignoring DER contribution to distribution-level infrastructure. Model does still co-optimize distribution-level generation, loads, demand flexibility and storage.

4. $\Lambda = 1$, $\lambda_a > 0$, and $\lambda_b = 0$:

Co-optimization with distribution-level infrastructure, while accounting for load requirements and peak back flow DER impacts to distribution-level infrastructure. Model does still co-optimize distribution-level generation, loads, demand flexibility and storage.

5. $\Lambda = 1$, $\lambda_a \gg 0$, and $\lambda_b \gg 0$:

The co-optimization heavily penalizes back flow onto the utility-scale grid and heavily subsidizes DER generation. This results in DER buildout that can cover the majority of distribution demands without pushing electricity to the utility-scale grid. Leads to micro-grid structures in the optimization. The distribution level can pull from the utility-scale grid for electricity, but will only do so for short periods of time due to the costs associated with it.

6. $\Lambda = 1$, $\lambda_a \gg 0$, and $\lambda_b \ll 0$:

The co-optimization heavily penalizes back flow onto the utility-scale grid and heavily penalizes DER generation. This results in almost zero DER buildout and a tendency to only use the utility-scale grid. Leads to macro-grid utility structures in the optimization. The distribution level can generate electricity, but will not do so due to cost limitations.

More details on the formulation of the DU interface in the WIS:dom-P optimization model are available in Section 1.9.2 of the technical documentation available to download.³¹

³¹ [https://vibrantcleanenergy.com/wp-content/uploads/2020/08/WISdomP-Model_Description\(August2020\).pdf](https://vibrantcleanenergy.com/wp-content/uploads/2020/08/WISdomP-Model_Description(August2020).pdf)



3. Modeling Results

3.1 System Costs, Energy Prices, Retail Rates, and Jobs

All four scenarios presented in the present report experience decreasing total system costs from 2018 through 2050 as displayed in Fig. 3.1. The “BAU-DER” scenario is seen to have the lowest system costs of all the scenarios. In particular, it is lower cost than the “BAU” scenario, which cannot access the value of the distributed resources using the co-optimization. The “CE” scenario has the highest system costs throughout as the electricity system is required to decarbonize by 95% by 2050. The “CE-DER” scenario has slightly higher total system costs compared with the “CE” scenario until 2025, but starting 2030 the “CE-DER” scenario is able to reduce costs through DER co-optimization while the “CE” scenario costs increase as it decarbonizes the electricity sector without utilizing the full benefits of DERs.

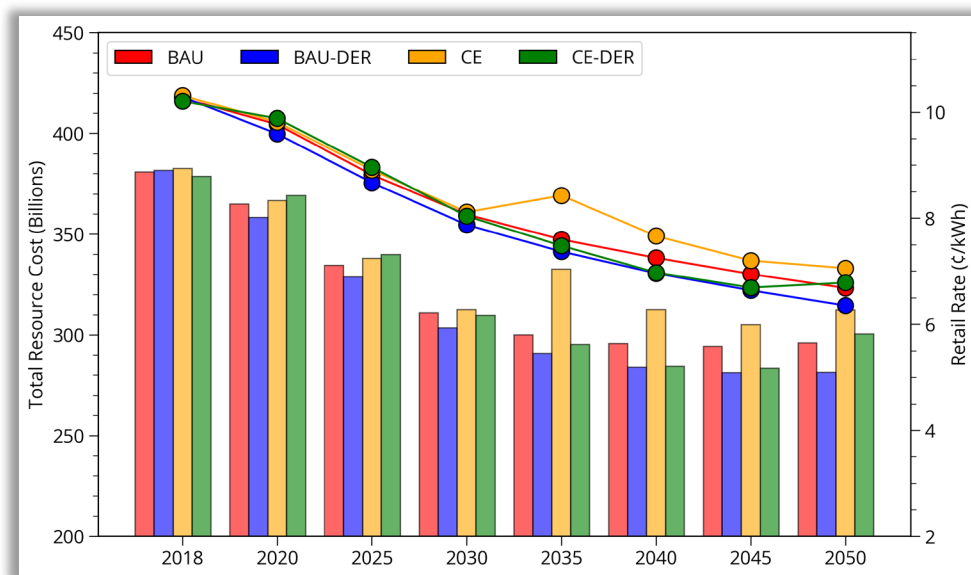


Figure 3.1: Total system costs (bars) and retail rates (lines) for the four scenarios.

In a business-as-usual environment, co-optimizing DERs (the “BAU-DER” scenario) is seen to immediately result in savings compared with the “BAU” scenario. The savings from co-optimizing DERs accumulate and by 2050 the “BAU-DER” scenario has cumulative savings of \$301 billion (see Fig. 3.2) compared with “BAU”. When decarbonizing the electricity sector, co-optimizing DERs results in a small increase in spending initially, but by 2030 savings materialize, and begin to accumulate rapidly. By 2050, the “CE-DER” scenario has saved \$473 billion compared with the “CE” scenario. The savings from co-optimizing DERs when decarbonizing the electricity sector are large enough that by 2050 the “CE-DER” scenario has cost \$88 billion less than the “BAU” scenario. Put another way, the “BAU” scenario is \$88 billion more expensive than the “CE-DER” scenario.



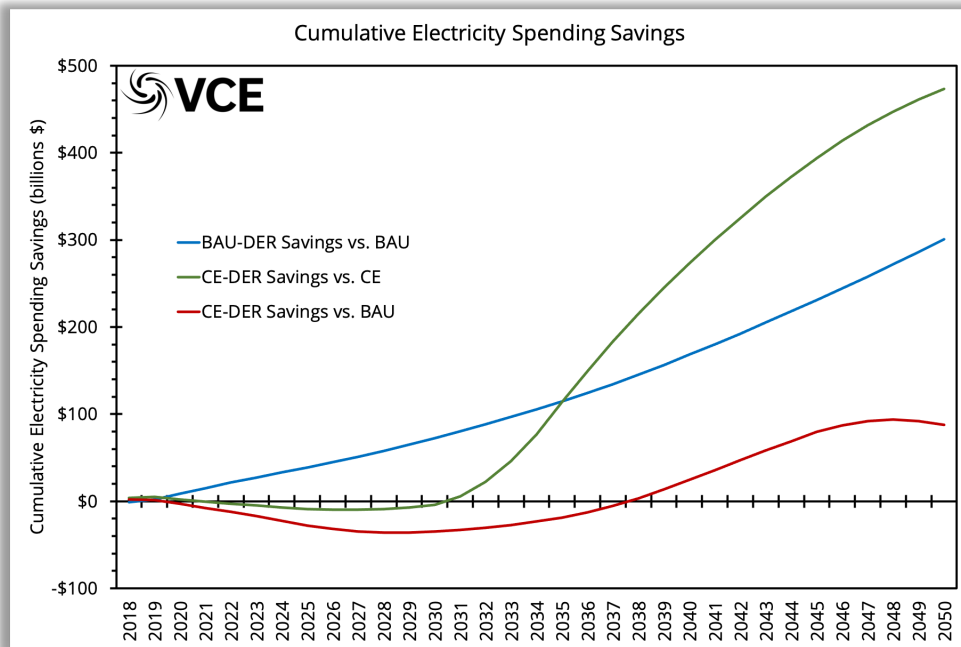


Figure 3.2: Cumulative savings in the electricity sector as a result of DER co-optimization

As shown in Fig. 3.1, the average electricity retail rates over the CONUS are seen to reduce as well from through 2050. The average retail rate for the “BAU” scenario reduces from 10.26 ¢/kWh in 2018 to 6.68 ¢/kWh. Assuming the savings in total resource cost by co-optimizing DERs (“BAU-DER” scenario) are passed on to consumers, the retail rate is expected to be lower by 0.32 ¢/kWh, a 5% savings over the “BAU” scenario. Similarly, in the “CE” scenario the average retail rate in 2050 is 7.05 ¢/kWh, and co-optimizing DERs (“CE-DER” scenario) results in saving of 0.27 ¢/kWh, a 4% savings over the “CE” scenario.

A breakdown of the retail rate by electricity system component is shown in Fig. 3.3. In 2018, approximately half the cost per kWh is due to fossil fuel generation. As the simulations progress, the expensive fossil fuel generation is retired and replaced with VRE generation. This results in lowering of total system costs, primarily due to the low marginal cost of energy from these VREs. Costs are also reduced in the “BAU” scenario by replacing aging NGCC with new NGCC generation (newer units typically have lower heat rates). In 2018, NGCC contributed to meeting 27% of the load in the “BAU” scenario and contributed 2.1 ¢/kWh to retail rate. By 2050, NGCC contributed to meeting 25% of the load and contributed only 1.6 ¢/kWh to the retail rate. The contribution of VREs to the retail rate increases from 0.36 ¢/kWh in 2018 to 1.53 ¢/kWh in 2050 in the “BAU” scenario. However, VREs contribution to meeting load goes up from 9% of the load in 2018 to meeting 55% of the load in 2050. By contrast, in the “CE-DER” scenario the contribution of VREs to the retail rate is 2.84 ¢/kWh, while meeting 67% of the load.



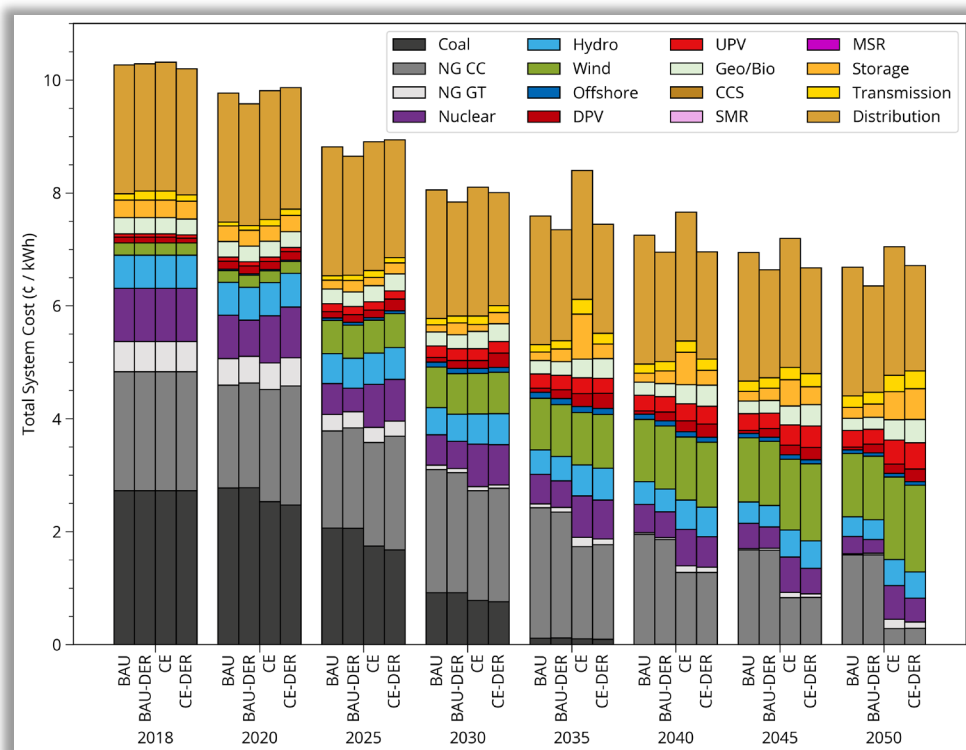


Figure 3.3: Retail rate broken down by electricity system component.

Figure 3.4 shows the percentage change in balancing region / RTO averaged retail rates by 2050 compared with 2018. Retail rates are calculated assuming that transmission costs are regionalized within each balancing region / RTO as ratio of demand from each utility in the balancing region / RTO. It is also assumed that if a balancing region / RTO makes a profit through electricity sales to other regions, only half the profits are passed on to customers as retail rate reductions, while all extra expense due to buying energy from other balancing regions / RTOs are fully passed on to customers.

Based on these assumptions, all balancing regions / RTOs in the CONUS see significant reductions in retail rates by 2050. The largest reductions in retail rates in all regions are seen in the "BAU-DER" scenario, while the lowest reductions are seen in the "CE" scenario. Figure 3.4 also shows that when including the distribution co-optimization, the retail rates reduce further for all the regions across the CONUS. Therefore, it is robust that regardless of emissions targets, the distribution co-optimization carves a lower-cost future grid than the alternative.

Figure 3.5 displays the components for the average retail rate cost changes between distribution co-optimization enabled and disabled scenarios through time. It shows that for both pairs of scenarios the additional spending in distribution resource is outweighed by the savings created in the distribution infrastructure and the utility-scale generation deployments. Interestingly, with the distribution co-optimization enabled, more utility-scale variable generation is deployed and there is an increase in spending on those resources as a result. For the "CE" comparison, in 2035 the traditional clean electricity scenario deploys enormous amounts of utility-scale storage to reach existing (and more



binding national) emission reduction targets. The deployment is directly related to the model not being able to find a lower-cost alternative. In contrast, the “CE-DER” scenario can perform the deployments more gradually because of its increased solution space. By 2050, in the “CE-DER” scenario, spending on storage actually exceeds that of the “CE” scenario.

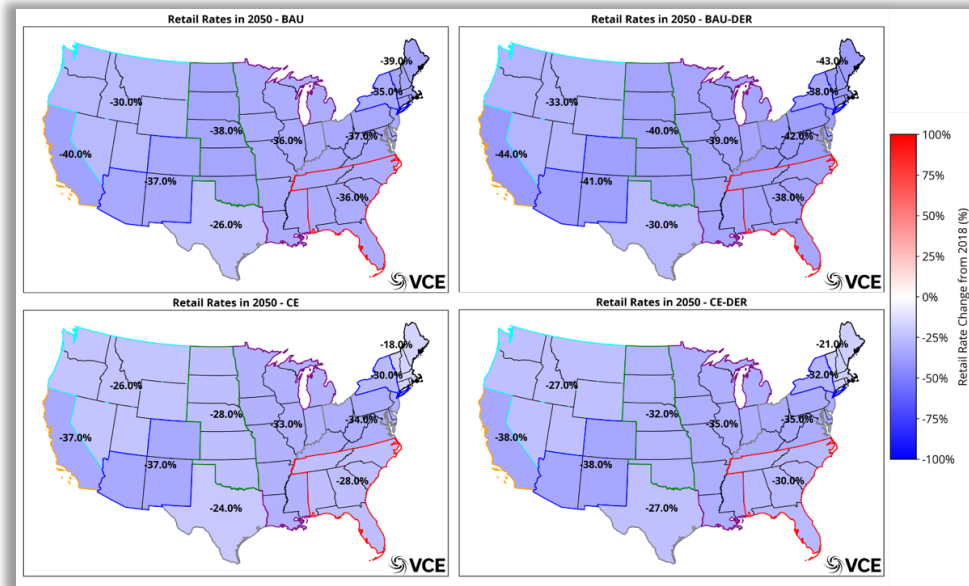


Figure 3.4: Percentage change in balancing region/RTO averaged retail rates by 2050 in the four scenarios compared to 2018 retail rates

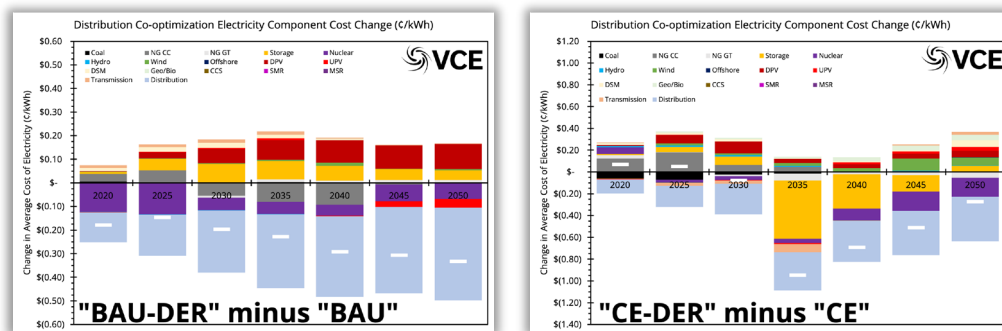


Figure 3.5: Retail rate changes due to the distribution co-optimization being enabled. Left panel is for “BAU” and right panel is for “CE”. The white bars denote the net change in retail rates due to the distribution co-optimization.

Figure 3.6 displays the retail rate change breakdown between the “CE-DER” and the “BAU” scenario. It shows that the increase in spending is in VREs and the reduction in spending is in coal, natural gas, and distribution infrastructure. The distribution co-optimization is the new addition to the modeling that enabled the solution to be found. Without the distribution co-optimization the modeling finds an increase in costs over “BAU” for a clean electricity future. It should be noted that the distribution co-optimization did not just result in deployments within the distribution grid. It fundamentally changed the entire solution vector of the electricity system – both utility and distribution scale. In fact, in totality, the



distribution co-optimization changed the utility-grid generation more than the distribution grid: trending from fossil fuel generation to renewable generation.

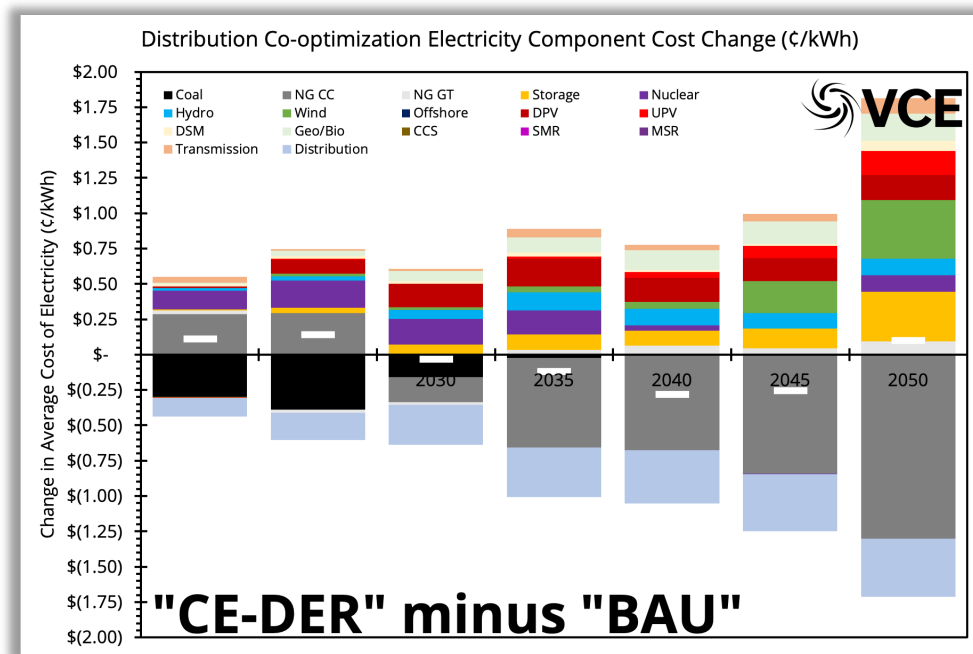


Figure 3.6: Retail rate changes due to the distribution co-optimization being enabled and clean electricity standard being enforced. The plot represents "CE-DER" minus "BAU" retail rates. The white bars denote the net change in retail rates due to the distribution co-optimization and a clean electricity standard.

To determine how the system evolves from a retail rates perspective, we analyzed the components and how they changed over time for each of the four scenarios. We display these in Fig. 3.7. The first thing that is noticeable in the panels from Fig. 3.7 is that coal reduces the electricity rates over the CONUS in an almost identical way for all the scenarios; the coal-fired power plants are retired and replaced with wind and solar primarily, which are far lower cost than the coal they are replacing. This is a consistent theme that VCE has seen in its reports and modeling.³² When clean electricity is mandated, more VREs are deployed and storage becomes a bigger component of retail rates. We also observe a consistent decline in the spending on nuclear when clean electricity is not mandated, something that is slowed when it is. However, some nuclear power plants do still retire because of their age and costs to relicense.

It appears, from Fig 3.7, that the coal-fired power plants are inflating retail rates across the country and with those retirements, capital and infrastructure is released that enables vast amounts of VREs to replace them at negative net costs.

³² See, e.g., https://vibrantcleanenergy.com/wp-content/uploads/2019/03/LCOE-Mapping/Coal-Cost-Crossover_Energy-Innovation_VCE_FINAL2.pdf, <https://www.vibrantcleanenergy.com/wp-content/uploads/2019/11/CEDS-CEI-VCE-FullReport.pdf>, https://vibrantcleanenergy.com/wp-content/uploads/2020/08/SERTO_WISdomP_VCE-EI.pdf, <https://www.vibrantcleanenergy.com/wp-content/uploads/2020/10/CO-EIM-Options-Report.pdf>, <https://www.vibrantcleanenergy.com/wp-content/uploads/2020/10/EIC-Transmission-Decarb.pdf>



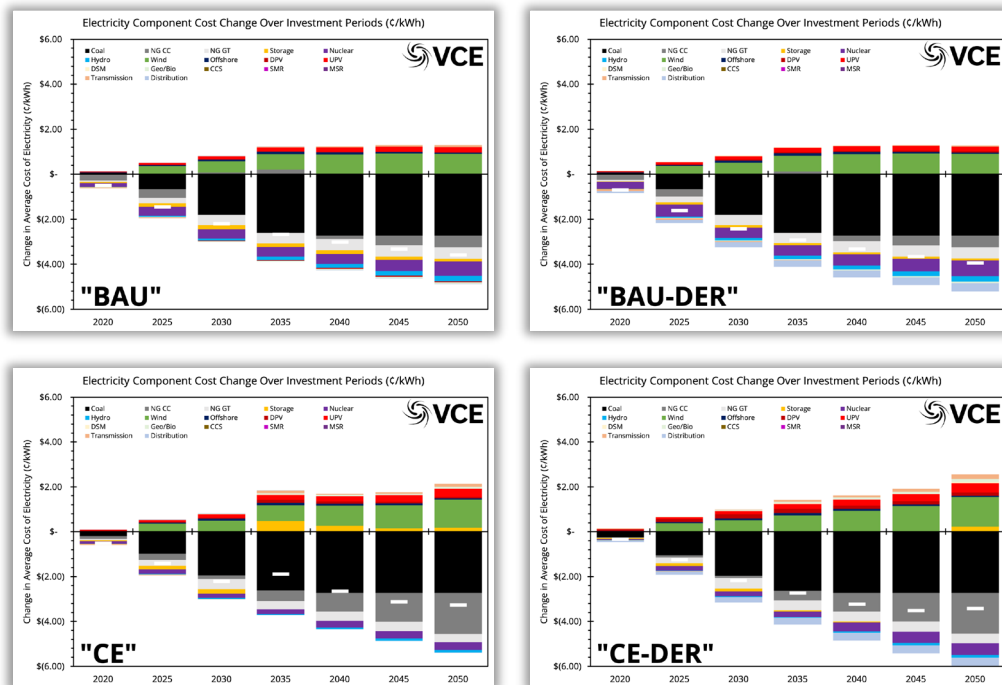


Figure 3.7: Retail rate changes over investment periods within WIS:dom-P for all four scenarios. Top left panel is for "BAU", top right for "BAU-DER", bottom left panel for "CE", and bottom right panel for "CE-DER". The white bars denote the net change in retail rates.

The full-time equivalent (FTE) direct jobs created by the electricity sector for the four scenarios are shown in Fig. 3.8. It shows that net employment increases in all scenarios as the electricity sector moves away from fossil fuel generation and towards VRE generation. The largest job gains in all scenarios are seen in the solar industry with a significant portion of the jobs in the distributed solar industry followed by the storage industry and then the wind and transmission industry. The "CE-DER" scenario shows the highest total jobs gains with almost 8 million new net jobs created after 2018. The scenarios with DER co-optimization are seen to create about one million more jobs than the corresponding scenarios without DER co-optimization.

Figure 3.9 shows the state level change in jobs created as a percentage of 2018 jobs. As seen from Fig. 3.9, all states show at least a 100% increase in jobs by 2050 compared to 2018. The biggest increase in jobs in all scenarios is seen to occur in Florida and Louisiana. In the "BAU-DER" scenario, it is seen that MS, OK, TX and NM are seen to show higher percentage growth compared to 2018 than the "BAU" scenario due to more DPV being deployed in these states owing to the better solar capacity factors. In the "CE-DER" scenario, the higher percentage job growth is seen in the SPP/MISO region apart from the southeast region as the "CE-DER" scenario installs more wind compared to the "CE" scenario most of which goes into the higher capacity SPP/MISO region.



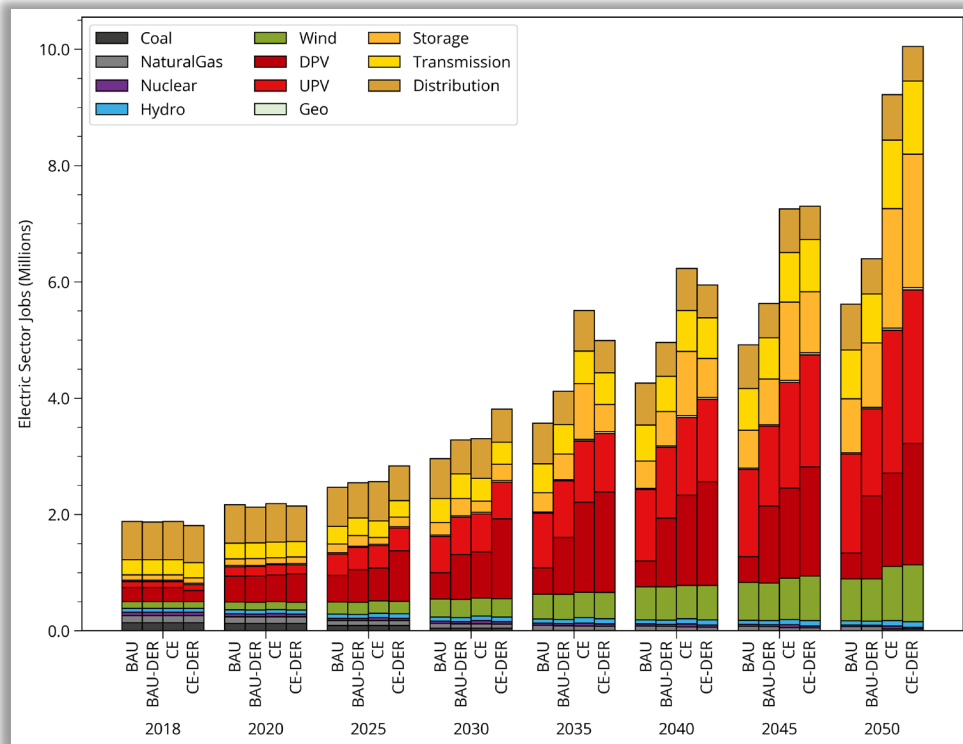


Figure 3.8: Electricity sector jobs breakdown for the four scenarios presented.

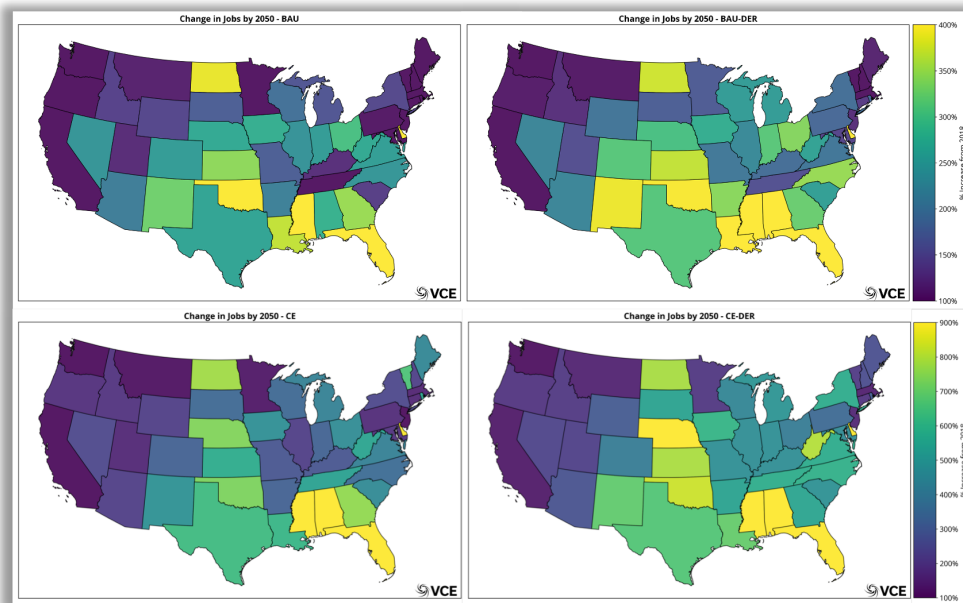


Figure 3.9: Percentage change in jobs by 2050 compared with 2018 for the scenarios presented. Note the change in color bar between the top (BAU) and bottom panels (CE).



3.2 Capacity Buildout

Figure 3.10 shows that as the WIS:dom-P model progresses from 2018 through 2050, the installed capacities in all scenarios evolves from being fossil fuel dominated to being variable renewable dominated. Coal is completely retired by 2035 at almost the same rate within all scenarios. This suggests that coal is uneconomic (whether there is a clean electricity mandate or not). Installed capacities of natural gas show significant differences between the scenarios with and without decarbonization mandate. The scenarios without a decarbonization goal ("BAU" and "BAU-DER") have approximately two and a half times more natural gas capacity compared with the scenarios with a decarbonization goal ("CE" and "CE-DER").

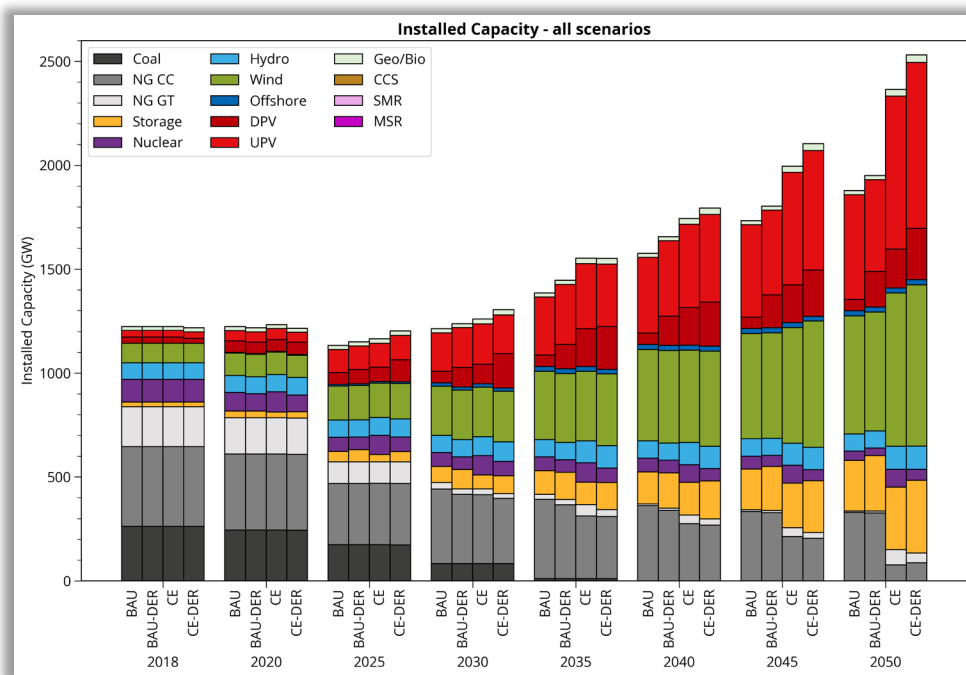


Figure 3.10: WIS:dom-P installed capacities for the four scenarios modeled for the CONUS.

The difference in installed capacities in the model simulations with and without DER co-optimization is shown in Fig. 3.11. The major difference in the "BAU" and the "BAU-DER" scenarios is substantially more DPV capacity in the "BAU-DER" scenario for each investment period compared with the "BAU" scenario. The "BAU-DER" scenario also installs slightly more storage, while installing less natural gas and UPV capacity. Comparing installed capacities between the "CE-DER" scenario and the "CE" scenario, it is seen that the "CE-DER" scenario starts to install significantly more DPV starting 2025 compared with the "CE" scenario. The "CE-DER" scenario also installs more storage and wind compared with the "CE" scenario. Additionally, the "CE-DER" scenario retires more nuclear capacity and installs less NG CTs compared with the "CE" scenario.



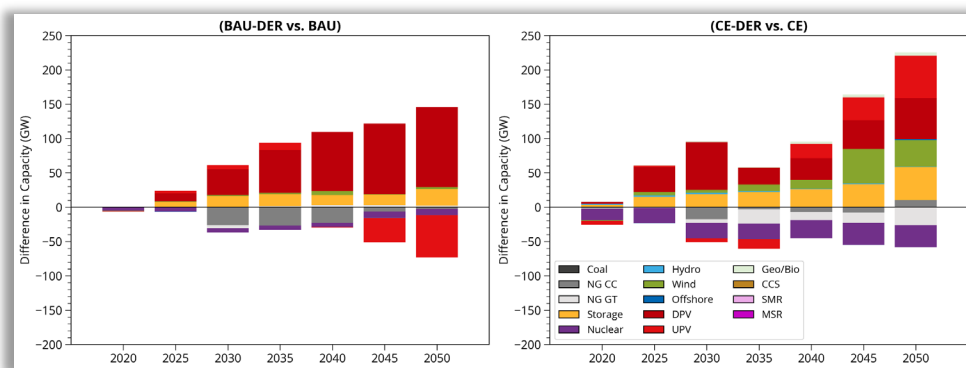


Figure 3.11: Difference in installed capacities for simulations with and without DER co-optimization. "BAU-DER" vs. "BAU" (left panel) and "CE-DER" vs. "CE" (right panel).

The installation of the utility-scale and distributed-scale solar for the four scenarios is shown in Fig. 3.12. In the scenarios that co-optimize DERs, WIS:dom-P installs more DPV compared with scenarios that do not co-optimize DERs. The higher amounts of DPV is explained by the value of construction within the distribution grid by avoiding unnecessary transmission and utility-scale generation construction. For the "BAU-DER" scenario, there is slightly less UPV than in the "BAU" scenario; however, in the "CE-DER" scenario there is more UPV than the "CE" scenario. This is because, the UPV loses out to the natural gas generation when there is no clean electricity mandate. It should be noted that the UPV capacity grows by four times in all scenarios by 2030 and over eight times by 2050.

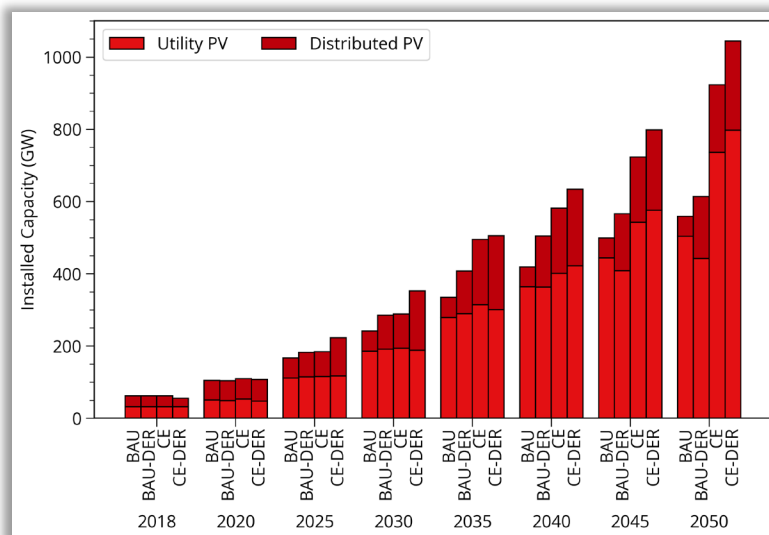


Figure 3.12: Installed capacities of UPV and DPV for the four scenarios over the investment periods.

Distributed storage provides large value when it is deployed and can be paired with DPV. The DPV along with distributed storage reduce the *utility-observed* peak (more details in Section 3.3), thus reducing the need for some utility-scale generation, but also deferring some distribution system upgrades. Figure 3.13 shows the installed storage power and energy capacities. As seen from Fig. 3.13, for the DER co-optimized scenarios ("BAU-DER"



and “CE-DER”) the installed storage capacities are split almost evenly between utility-scale and distributed-scale storage. In addition, the DER co-optimized scenarios install more storage overall.

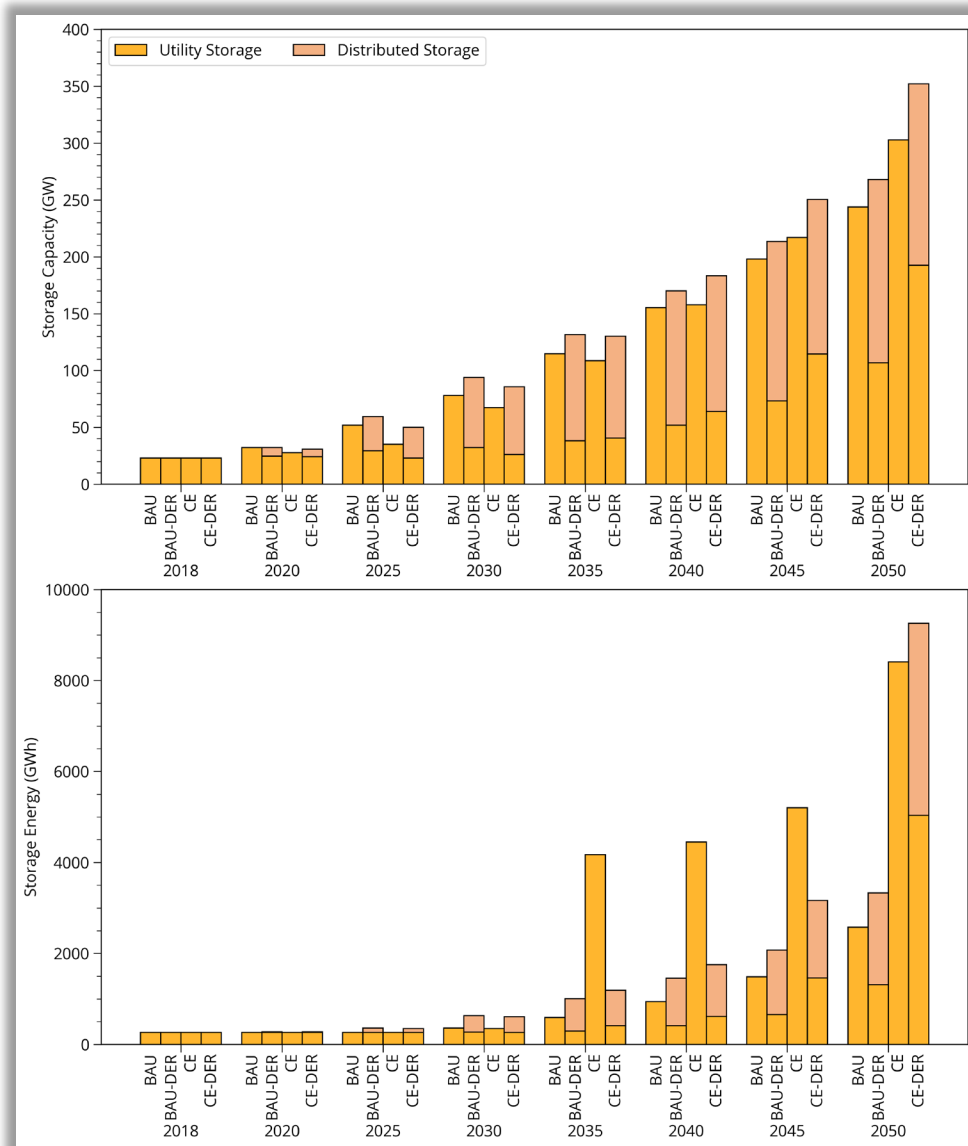


Figure 3.13: Installed storage power (top) and energy (bottom) capacities for the four scenarios.

It can also be seen from Fig. 3.13 that in the “CE” scenario, the model installs 3,826 GWh of storage energy capacity between 2030 and 2035. This large installation of storage by 2035 is required to ensure that the model can meet emission constraints to decarbonize the electricity sector by 2050 and thus needs to build storage to firm up the VRE generation. The “CE-DER” scenario on the other hand, which has the same emission constraints as the “CE” scenario, does not need to install this large amount of storage as it is able to much more efficiently use the VRE generation by shifting the demand seen by the utility scale generation to less difficult periods through effective use of DERs.



Figure 3.14 shows the average annual installation rates in the four scenarios (for five-year periods). In all scenarios, the model is seen to retire fossil generation and replace it with wind and solar (both UPV and DPV). The installation and retirement rates are seen to be fairly similar for all scenarios until 2040. After 2040, the install rates are seen to pick up for the “CE” and “CE-DER” scenarios as they accelerate to decarbonize the electricity sector. The biggest difference in install rates is seen in rate of energy storage capacity installed between 2030 and 2035 for the “CE” scenario. The model installs storage energy capacity at rate of 765 GWh / year between 2030 and 2035 in the “CE” scenario to firm up the VRE generation in order to meet the emission constraints in year 2035.

In contrast, the “CE-DER” scenario has no spike in storage as the model is able to more efficiently use utility-scale and distribution-scale storage to effectively use VRE generation without excessive curtailment. Since, there is not a short-lived spike in installation rates, it is more likely that supply chains will be able to keep up with the required storage capacity and not result in spikes in capital costs. Hence, DER co-optimization not only reduces system costs, but also ensures that supply chains are not excessively stressed allowing for a smoother transition to a decarbonized electricity sector.

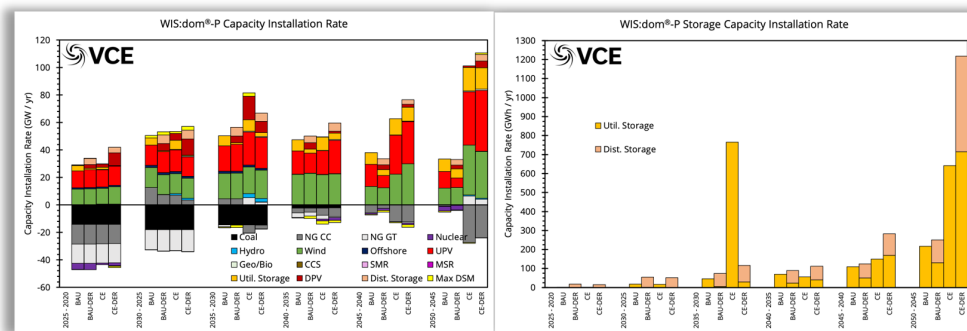


Figure 3.14: Installation and retirement rates of all technologies (left) and storage energy (right) for the four scenarios presented.



3.3 Electricity Generation

As discussed in Section 3.2, the electricity sector is seen to get cleaner in all four scenarios modeled. Figure 3.15 shows the breakdown of generation sources in the electricity sector and their evolution over the investment periods. In 2018, over 50% of the generation came from fossil fuel sources. The fossil fuel generation is seen to increase slightly over 2018 values before starting to decrease beginning 2025. Coal generation disappears by 2035 and is replaced almost completely by VREs. In the scenarios that co-optimize DERs ("BAU-DER" and "CE-DER"), the solar generation is seen to be larger than corresponding scenarios without DER co-optimizing. The additional solar generation is mostly from the additional DPV installed in the DER co-optimized scenarios. It is also seen that the "CE" and "CE-DER" scenarios have significantly more curtailment compared to the "BAU" and "BAU-DER" scenarios due to higher renewable penetration required to meet the decarbonization goals. This large curtailment opens the possibility to use the excess energy either to make hydrogen or other fuels either as storage mechanism or for industrial use, and thus further reduce the cost of energy in the "CE" and "CE-DER" scenarios. It should be noted that the curtailment is economic and is accounted for in the modeling of the electricity market bidding strategies of the generators.

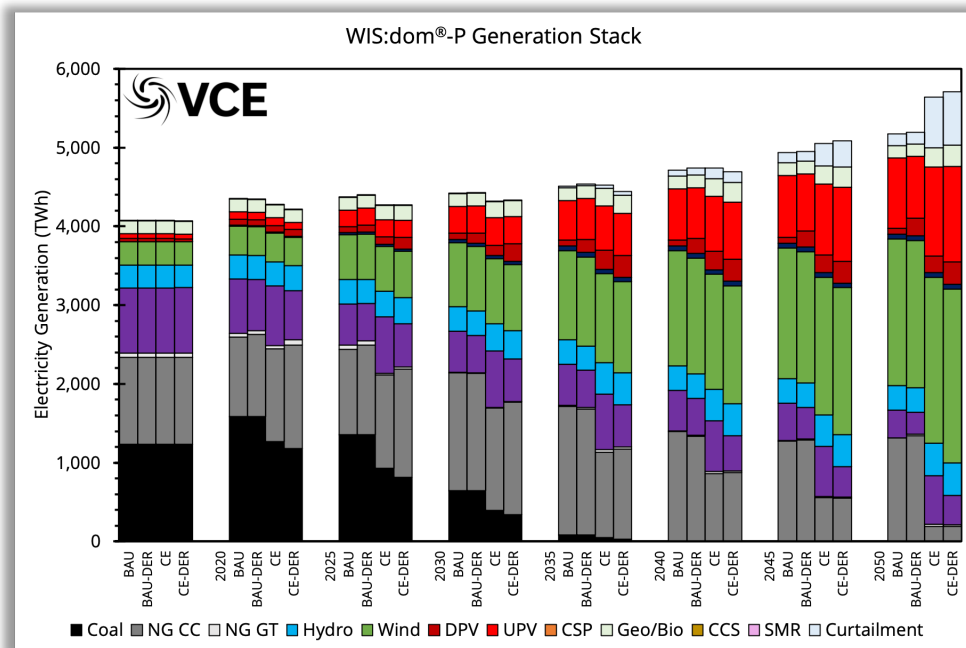


Figure 3.15: The evolution of generation sources in the four modeled scenarios.

The difference in the sources of generation between the scenarios with and without DER co-optimization is shown in Fig. 3.16. As seen from Fig. 3.16, the "BAU-DER" starts out with slightly higher natural gas generation and lower nuclear generation compared to the "BAU" scenario. As the investment periods progress, it is seen that the "BAU-DER" scenario has more generation from DPV and lower generation from nuclear, natural gas and UPV compared with the "BAU" scenario.



The change in nuclear generation is starker when comparing the “CE” and “CE-DER” scenarios. It is observed that the “CE-DER” scenario has higher natural gas generation in the earlier years and then higher wind, UPV, and DPV generation in the later years compared with the “CE” generation. It is seen that nuclear generation is lower across all investment periods for the “CE-DER” scenario compared with the “CE” scenario.

The lower nuclear generation observed in the scenarios that co-optimize DERs (and hence have more DPV installations) is expected and was also observed in the southeast RTO study conducted by VCE.³³ In the southeast RTO study, it was observed that co-optimizing DERs resulted in earlier nuclear retirements, while not allowing nuclear to retire resulted in lower DPV installations and generation. This trade-off between nuclear and DERs is probably due to the fact that the DER cop-optimization results in increasing capacity factors of all utility scale generation (discussed in detail later in this Section). As a result of increasing capacity factors other thermal generation (especially natural gas) becomes more economic to run compared with nuclear. Therefore, nuclear is less competitive and is forced to retire earlier and as seen in Fig. 3.12, more natural gas generation is observed in the DER co-optimization scenarios.

Note that these changes, while robust, are a small percentage of total generation around 5%. This demonstrates the impact of the tails of distributions for generating resources. Further, in the clean electricity mandate scenarios (“CE” and “CE-DER”) there is more nuclear generation than in the business-as-usual scenarios (“BAU” and “BAU-DER”).

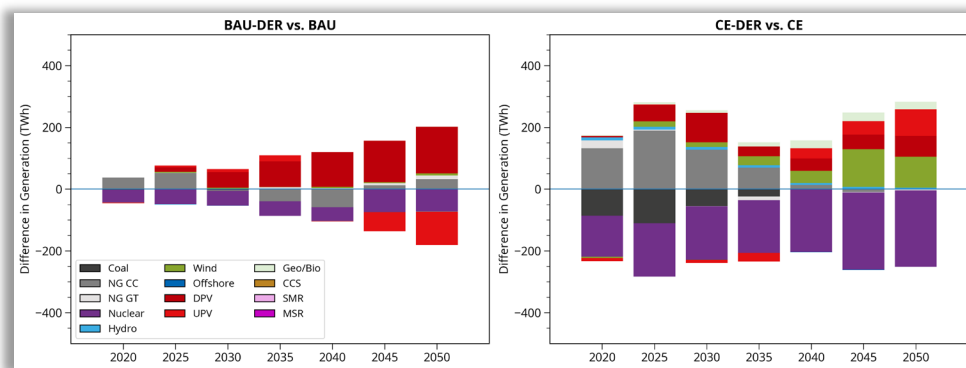


Figure 3.16: Difference in generation between scenarios with and without DER co-optimization.

The diurnal operation of VREs helps to explain how the WIS:dom-P model utilizes wind, solar, and storage to meet demand at each timestep. Figure 3.17 shows the average diurnal behavior of wind, solar, and storage in winter (top panel) and summer (bottom panel). As seen from Fig. 3.17, solar and wind generation complement each other well in winter. As the wind generation ramps down during the day, the solar generation starts to ramp up and in the evening as the solar generation ramps down, the wind generation is seen to ramp back up. Wind has higher capacity factors at nighttime in winter (of about 55%) and lower capacity factors during the day. Winter demands have dual peaks, one in early morning and the second in the evening. Therefore, storage is seen to play a role in helping

³³https://vibrantcleanenergy.com/wp-content/uploads/2020/08/SERTO_WISdomP_VCE-EI.pdf



meet demand during these hours where winter loads peak, which are also periods of transition from wind generation during the nighttime to dominantly solar generation during the day and similarly in the evening from solar generation to wind generation. In short, the storage pairs with the VREs to bridge the transition periods between wind and solar production.

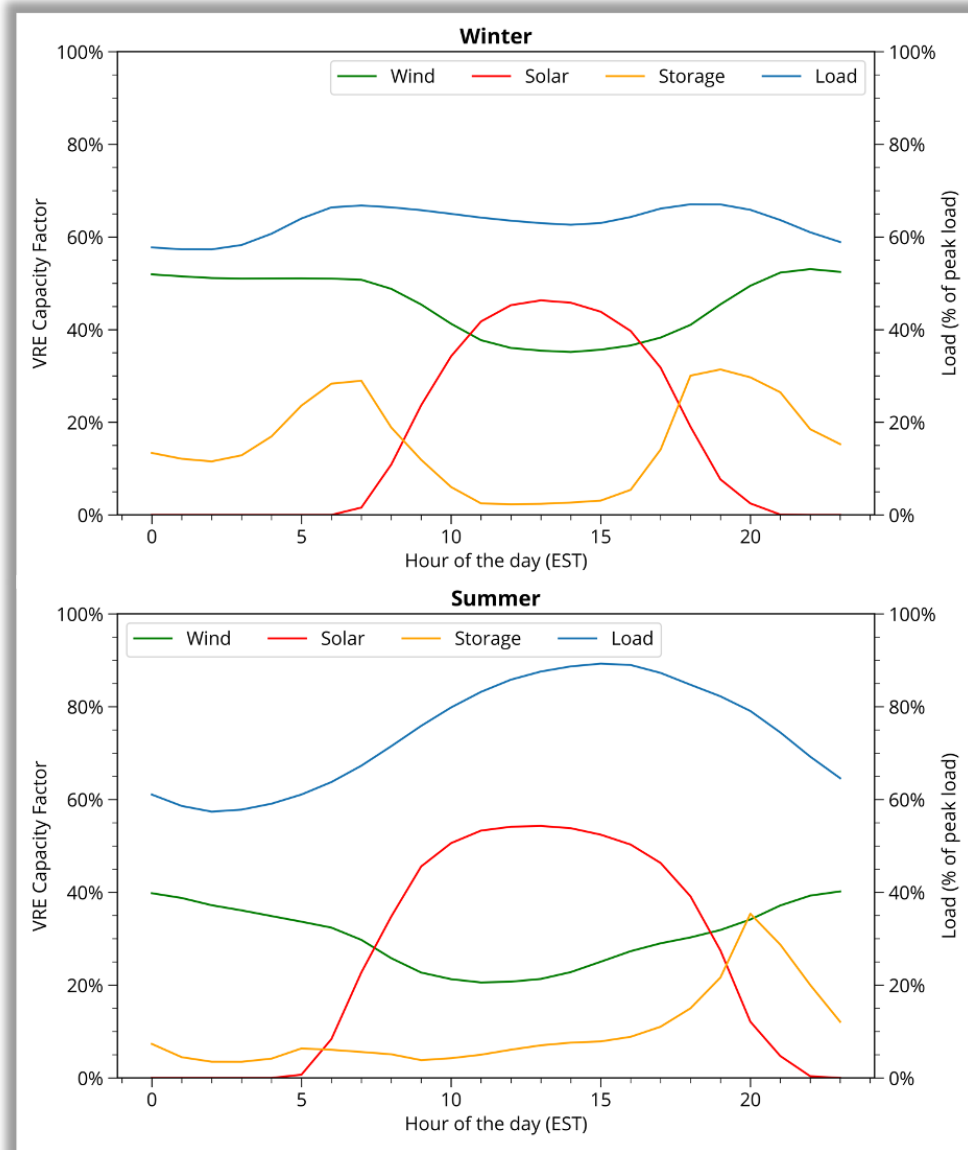


Figure 3.17: Average diurnal VRE behavior over the CONUS in winter (top) and summer (bottom) in year 2050 for the "CE-DER" scenario.

During summertime, wind capacity factors are lower peaking, around 40% during nighttime; however solar generation is higher due to the longer days and higher solar irradiance. The summer demand is seen to peak around 3:00 PM (local time) in the afternoon corresponding with air-conditioning loads that peak with the rising temperatures. The solar generation is better correlated with the summer demands;



however, the solar generation ramps down faster than the demand. Therefore, storage working alongside wind generation helps meet demand during the evening transition period. Storage is seen to play a minor role during the daytime hours in summer as net demand is low and wind is able to meet demand along with other thermal generation. The charging and discharging behavior of utility- and distribution- scale storage show interesting characteristics during winter and summer (as shown in Fig. 3.18). It is observed from Fig. 3.18 that in winter, storage charges in the middle of the day when the demand is slightly lower and there is excess generation from solar. Both utility scale and distribution scale storage are seen to have similar charging and discharging characteristics during the winter.

However, during the summer we see interesting differences between the charging and discharging characteristics of utility-scale and distribution-scale storage. Utility-scale storage charges during the day, similar to winter time, when there is excess generation from solar and continues to charge until about 5:00 PM (local time) when the solar generation starts to ramp down. However, the distribution-scale storage starts to charge right after midnight when demand is at its minimum and charges continuously until about noon. The distribution storage stops charging around noon as by this time the demand is ramping up quickly to reach its peak at 3:00PM as shown in Fig. 3.17. The distribution storage stops charging in order to ensure it does not exacerbate the peak load seen by the utility-scale generation. By shifting the charging of distributed storage to the nighttime/early morning hours, the charging demand is shifted to lower demand periods, which not only keeps peak distribution demands low, but also keeps the utility grid load factor high. Note that the WIS:dom-P model is performing this way to ensure least cost solutions. It must ensure that no asset is making a loss (all assets must breakeven), while reducing total system costs. This means that the distribution storage is not performing these charging and discharging actions solely to balance the grid, they are doing it to sell electricity at a price point higher than what they purchased it for.

In addition to using distributed storage, the model uses DPV to reduce peak load on the distribution system while ensuring minimal back-flow. The model builds DPV to help meet demand locally and pairs the DPV with distributed storage to ensure that as much excess DPV generation is taken up by the distributed storage as economically efficient. Further, the distributed storage charges off the utility-scale generation during low demand periods (nighttime and early mornings) so that it is ready to help meet demand during the evening transition in summer.

Another way to visualize the impact that DERs have on the demand observed by the utility-scale generation is shown in Figs 3.19 and 3.20. Figure 3.19 shows a utility-grid dispatch stack with the utility-observed demand (top panels) along with the distribution generation and demand stack (bottom panels) for winter (left) and summer (right) for the scenarios without DER co-optimization ("BAU" and "CE" scenarios). Comparing the top and bottom panels in Fig. 3.19, there is little difference between the utility-observed demand and the original demand within the distribution grid. Therefore, the utility-scale generation is required to almost entirely shift and reshape generation to meet demand.



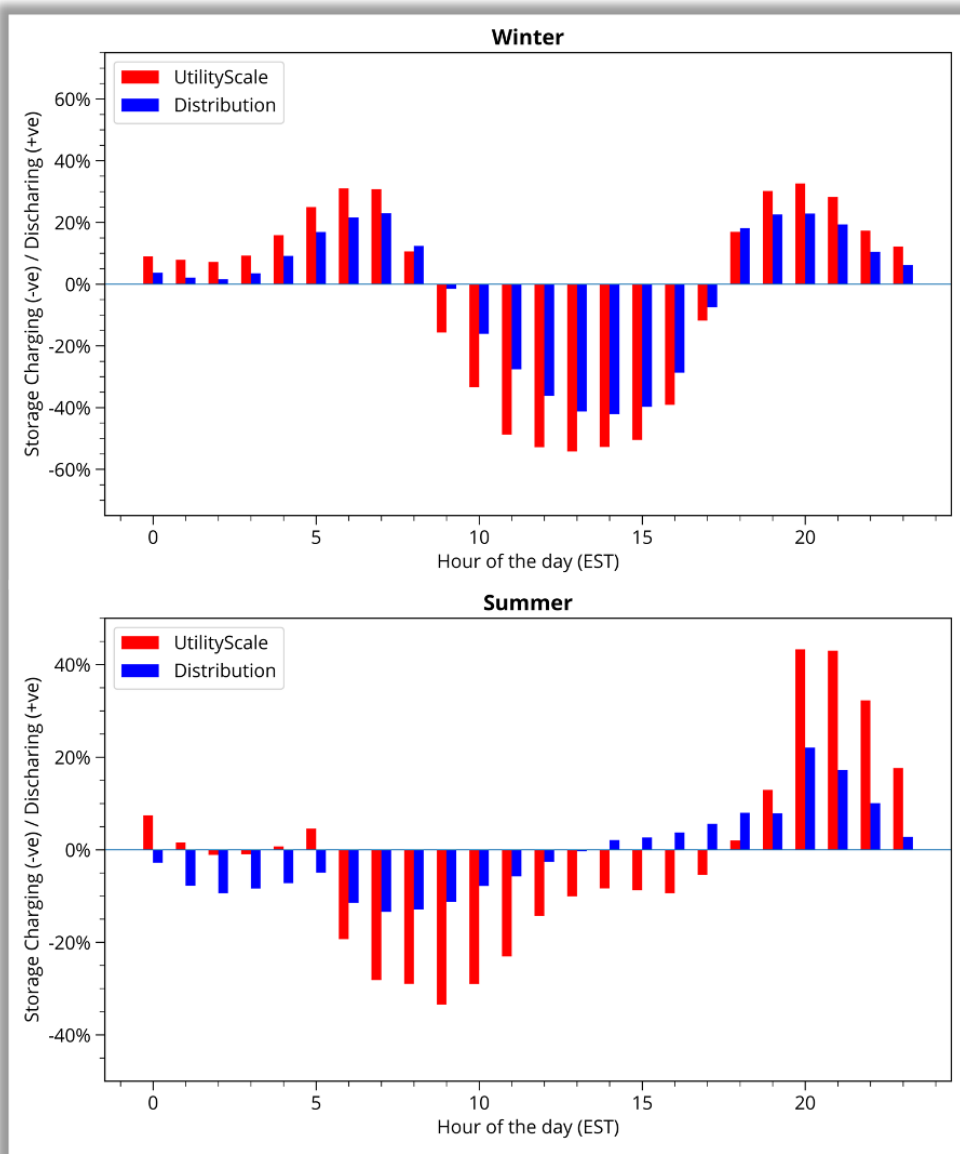


Figure 3.18: Behavior of utility-scale and distribution-scale storage in winter (top) and summer (bottom) in the year 2045 in the "CE-DER" scenario.



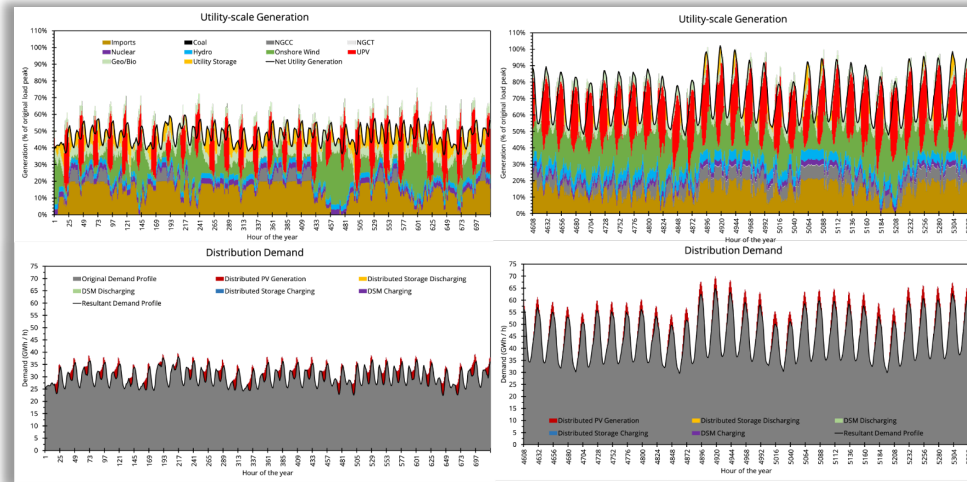


Figure 3.19: Utility grid generation and demand (top panels) and distribution generation and demand (bottom panels) when DER co-optimization is **OFF**.

Figure 3.20, similar to Fig. 3.19, shows a utility-grid dispatch stack with the utility-observed demand (top panels) along with the distribution generation and demand stack (bottom panels) for winter (left) and summer (right) for the scenarios with DER co-optimization ("BAU-DER" and "CE-DER"). When the distribution grid is co-optimized with the utility grid, it is seen that DERs reshape the *utility-observed* demand to not only reduce the diurnal variability in demand, but also the inter-day and inter-week variability. DERs reshape demand using the strategies discussed earlier of charging during periods of low demand and discharging during periods of high demand to reduce peak load.

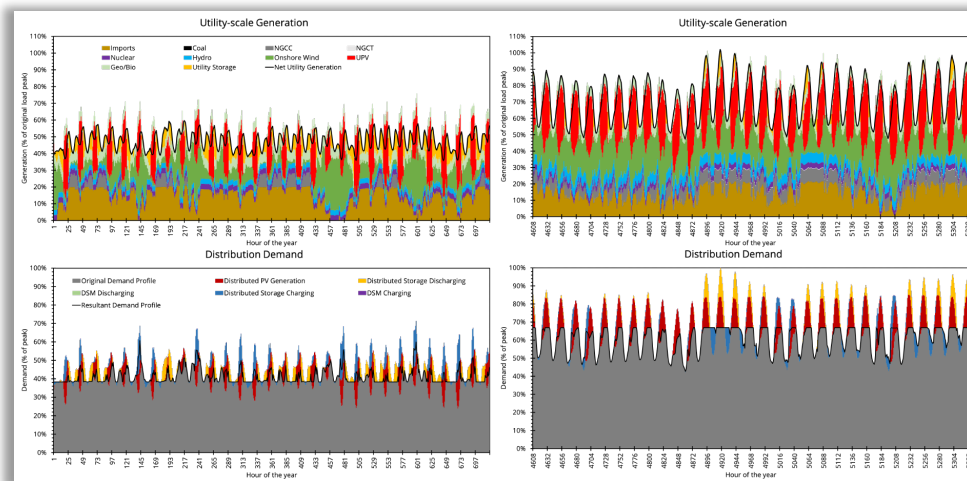


Figure 3.20: Utility grid generation and demand (top panels) and distribution generation and demand (bottom panels) when DER co-optimization is **ON**.

As a result of these strategies, the peak demand of the system is seen to reduce as shown in Fig. 3.21. Figure 3.21 shows the original load duration curve and the DER modified load duration curve. The DER modified load duration curve is flatter and reduces the peak demand from 774 GW to 647 GW, a 16.3% reduction. In addition, the minimum load is seen to increase from 344 GW to 379 GW, a 10% increase. The reduction in demand occurs for



over 85% of the year. As a result, the DER modified load has a higher load factor compared to the original load, which helps make the electricity grid more efficient, reduces need for peaking generation as well as increasing the capacity factors of the existing thermal generators: all resulting in lower cost of energy.

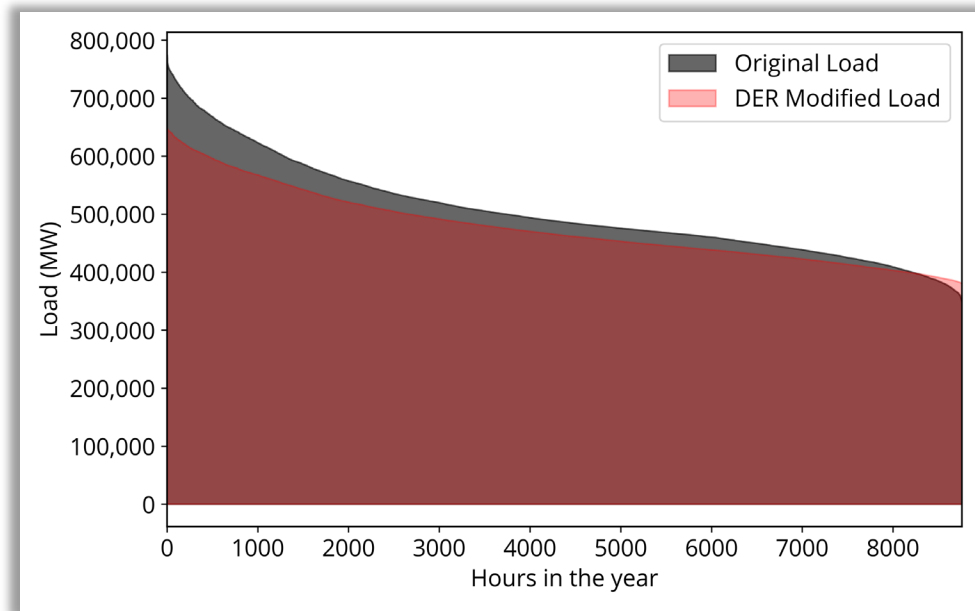


Figure 3.21: Continental United States aggregated load duration curves for the original and DER modified demands in 2050 for the "CE-DER" scenario.



3.4 Emissions and Pollutants

The evolution of carbon dioxide (CO₂) emissions for the four scenarios is shown in Fig. 3.22. In all the four scenarios, the CO₂ emissions reduce over the investment periods as older fossil generation is replaced with cheaper and cleaner VRE generation. The emissions increase slightly in 2020 as the grid transitions from being fossil dominated to VRE dominated and then steadily reduces to 2050. The emissions in the “BAU-DER” scenario are seen to be slightly higher than the “BAU” scenario until 2025 after which they are lower or about the same. Cumulatively, it is seen that the “BAU-DER” scenarios results in about 12 mmT less cumulative CO₂ emissions by 2050. The CO₂ emissions in the “CE” and “CE-DER” scenarios are seen to reduce equally as they are constrained by the decarbonization goals to reach 95% carbon-free electricity sector.

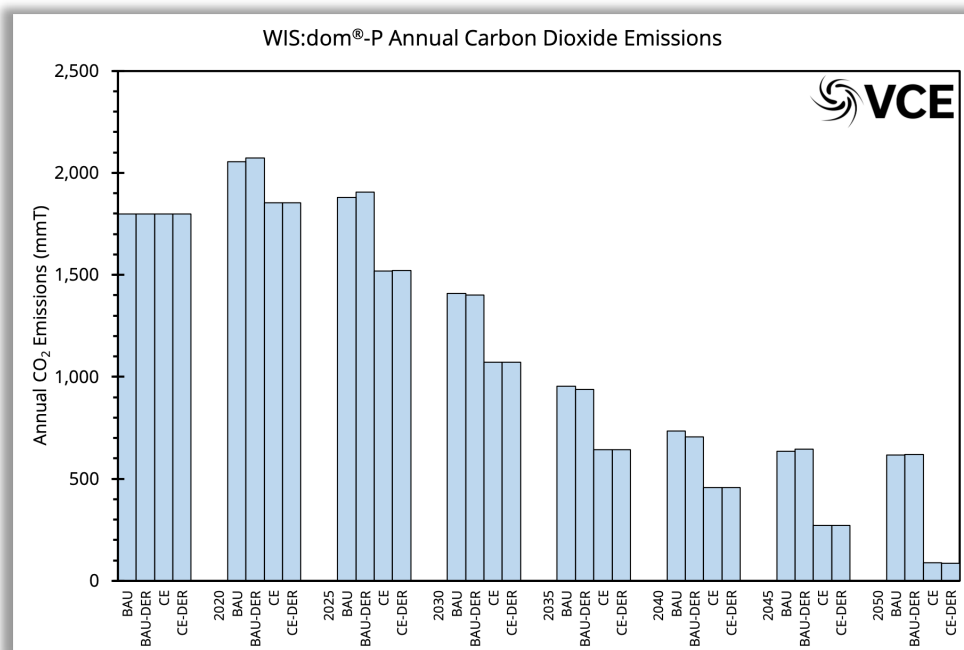


Figure 3.22: CO₂ emissions in the four scenarios discussed in this report.

The cumulative emission reduction in the “CE” and “CE-DER” scenarios compared with the “BAU” scenario is shown in Fig. 3.23. It is seen that there is an almost linear increase in emission reduction between the decarbonization scenarios and the “BAU” with savings accelerating slightly after 2045. The “CE” scenario results in cumulative CO₂ emission reduction of 5,129 mmT by 2035 at an additional cost of \$132 billion, which is equivalent to a carbon cost of \$25.82 / metric ton of CO₂. By 2050, the “CE” scenario results in cumulative emission reductions of 10,531 mmT of CO₂ at an additional cost of \$385.4 billion, which is equivalent to a carbon cost of \$36.59 / metric ton of CO₂. Both the *shadow costs of carbon* are lower than the social cost of carbon.³⁴ The “CE-DER” scenario on the other hand, results in 5,112 mmT of cumulative CO₂ emission reductions by 2035, which is equivalent to a carbon cost of \$3.64 / metric ton of CO₂. By 2050, the “CE-DER” scenario

³⁴ <https://www.pnas.org/content/114/7/1518>



achieves cumulative emission reduction of 10,521 mmT of CO₂ while saving \$88 billion cumulatively, which is equivalent to a **negative carbon cost** of $-\$8.34$ / metric ton of CO₂. This negative cost of carbon achieved by the “CE-DER” scenario shows that co-optimizing DER buildout can result in significant cost savings, while also reducing emissions (and increasing jobs created).

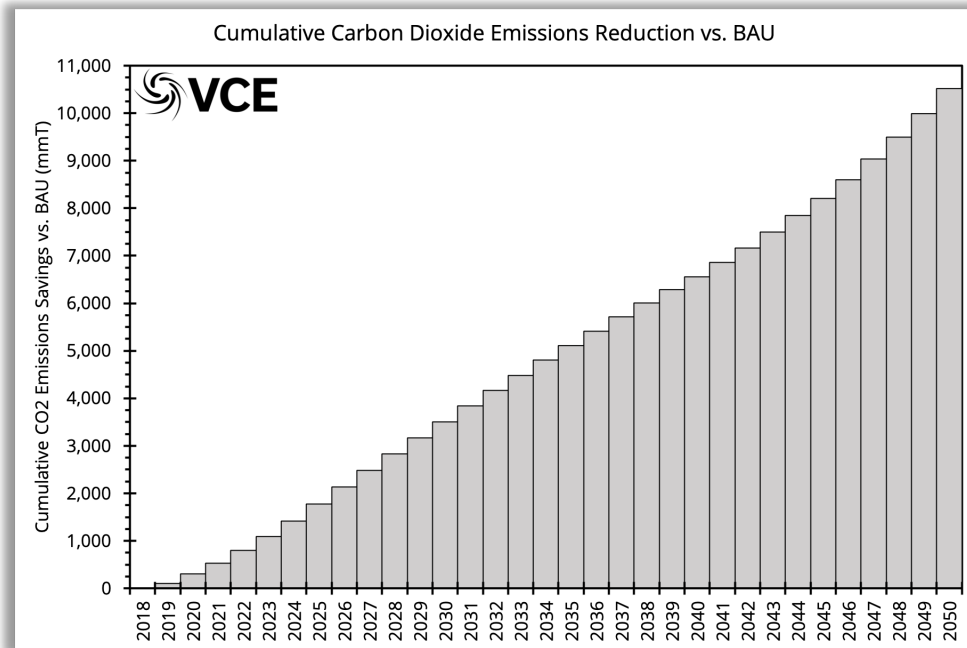


Figure 3.23: Cumulative electricity sector CO₂ emission reductions in the “CE” and “CE-DER” scenarios compared with the “BAU” scenario.

The cumulative global warming potential (GWP) in terms of equivalent CO₂ (CO₂e) emissions from the electricity sector for the “BAU-DER” scenario and the “CE-DER” scenario are shown in Fig. 3.24. It is seen that CO₂ is the major contributor to GWP, while CH₄ and N₂O make minor contributions due to their much lower emissions in the electricity sector. The cumulative CO₂e emissions in the “BAU-DER” scenario are seen to accumulate rapidly from 2020 to 2030 due to a significant portion of the generation coming from coal and natural gas. Starting in 2030, the growth in cumulative CO₂e emissions slows substantially because all of the coal generation has retired and been replaced by VREs. In the “CE-DER” scenario, the cumulative CO₂e emissions grow much slower as less coal and gas generation is used to meet demand due to the decarbonization constraints. The growth in cumulative CO₂e emissions is seen to be almost flat starting 2035 due to retirement of all coal generation and rapid reduction in use of natural gas generation to meet demand.



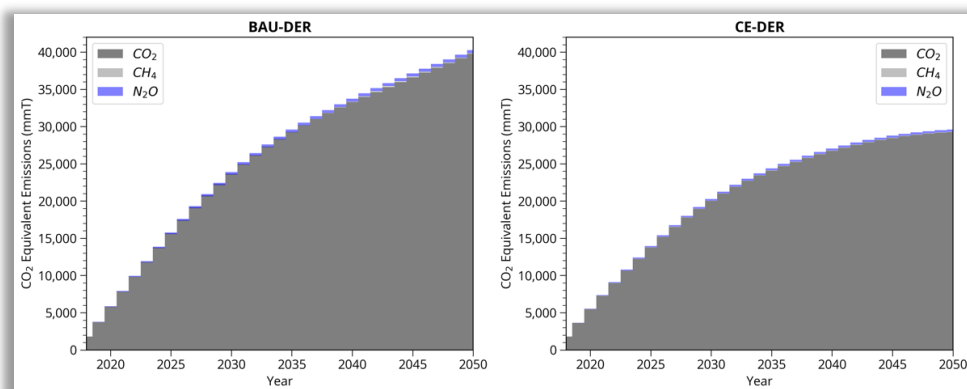


Figure 3.24: Cumulative CO₂ equivalent emissions for the "BAU-DER" scenario (left) and the "CE-DER" scenario (right).

In addition to CO₂, in all scenarios it is observed that other criteria pollutants, such as NO_x, SO₂, CH₄, PM_{2.5}, PM₁₀, and VOC, are seen to reduce substantially or go to zero as the electricity system retires all coal generation and moves to mostly VRE generation. Figure 3.25 shows all the pollutants (except CO₂) for the "BAU-DER" and "CE-DER" scenarios. As seen from Fig. 3.25, emissions from all pollutants increase in the short-term in the "BAU-DER" scenario from the increased coal and gas dispatched to meet demand. However, they start to fall starting 2025. Notably, SO₂, N₂O, PM_{2.5}, and PM₁₀ are almost completely eliminated from the electricity sector, while the remaining pollutants are reduced by over 50%. In the "CE-DER" scenario, emissions start to drop immediately in order to meet decarbonization constraints and all pollutant emissions are reduced by at least 95% by 2050, with the slowest reductions occurring in NO_x due to the small amount of natural gas generation that remains. Reductions in these criteria air pollutants will result in better air quality and improved health outcomes especially in lower incomes regions where most of the fossil fuel generation is located.

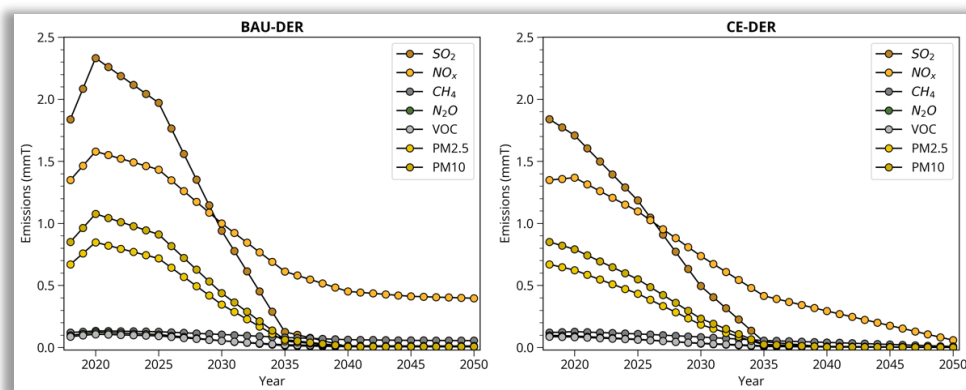


Figure 3.25: Change in emissions of criteria pollutants tracked by WIS:dom-P in the "BAU-DER" scenario (left) and the "CE-DER" (right).



3.5 Transmission Buildout

The transmission topology used for all scenarios in this study is discussed in Section 2.2. The initial transmission capacities for each of the connections over the CONUS is determined by initializing the model using 2018 EIA-860 generation data and allowing the model to solve for transmission capacities that ensure the 2018 demand is satisfied based on 2018 weather and generation existing on the grid in that year. The model then determines the optimal transmission expansion necessary to help meet demand as it moves through each investment period.

Figure 3.26 shows the additional transmission added by the model for the four scenarios discussed in this report. It is seen that transmission expansion occurs at approximately the same rate for all four scenarios until 2035. Starting 2035, it is seen that both the “CE” and “CE-DER” scenarios start building transmission at a faster rate compared with the “BAU” and “BAU-DER” scenarios. The amount of transmission built in the “BAU” and “BAU-DER” scenarios is seen to be almost exactly the same while the transmission built in the “CE” and “CE-DER” scenarios is roughly similar, but higher than the “BAU” and “BAU-DER” scenarios. It should be noted that the “CE-DER” scenario builds more transmission than the “CE” scenario (based upon the GW-miles metric) by 2050. Therefore, the WIS:dom-P model is not simply removing transmission and replacing it with distributed resources; rather it is removing transmission lines that are no longer economic and constructing new ones that are more economic and assist with the decarbonization of the grid.

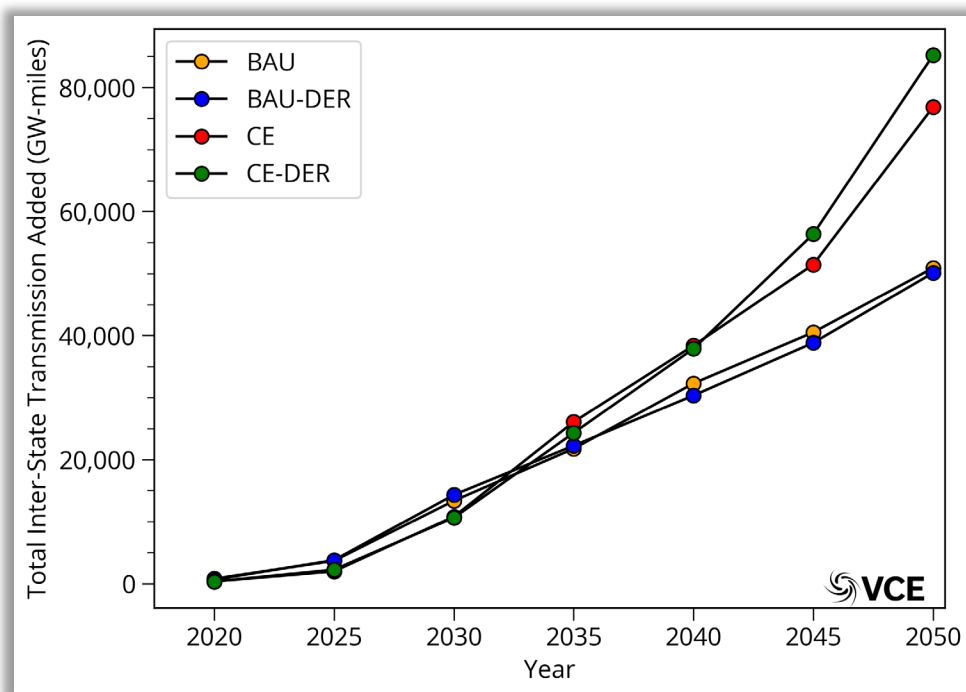


Figure 3.26: Total additional transmission installed since 2018 in the four scenarios modeled.

While Fig. 3.26 shows that the total transmission built in the scenarios with and without DER co-optimization is roughly similar, Fig. 3.27 shows that the location of transmission



buildout differs. As seen from Fig. 3.27, in some states the scenarios without DER co-optimization have more transmission buildout than the scenarios with DER co-optimization, and vice-versa in other states. While there are exceptions, it is seen that in the southeast the DER co-optimization scenarios have higher transmission buildout, while in the northeast states, scenarios without DER co-optimization have higher transmission buildout. The reason for higher transmission buildout in the southeast in the DER co-optimization scenarios is that transmission helps firm up the VRE generation, while in the northeast transmission is needed in the scenarios without DER co-optimization to help meet demand using utility scale generation. A similar trend as in the southeast is seen to a lesser extent in the southwest states, where solar generation is higher. While for the rest of the states in the WECC and Midwest, there is no discernable trend and each state optimizes transmission to use its resources efficiently.



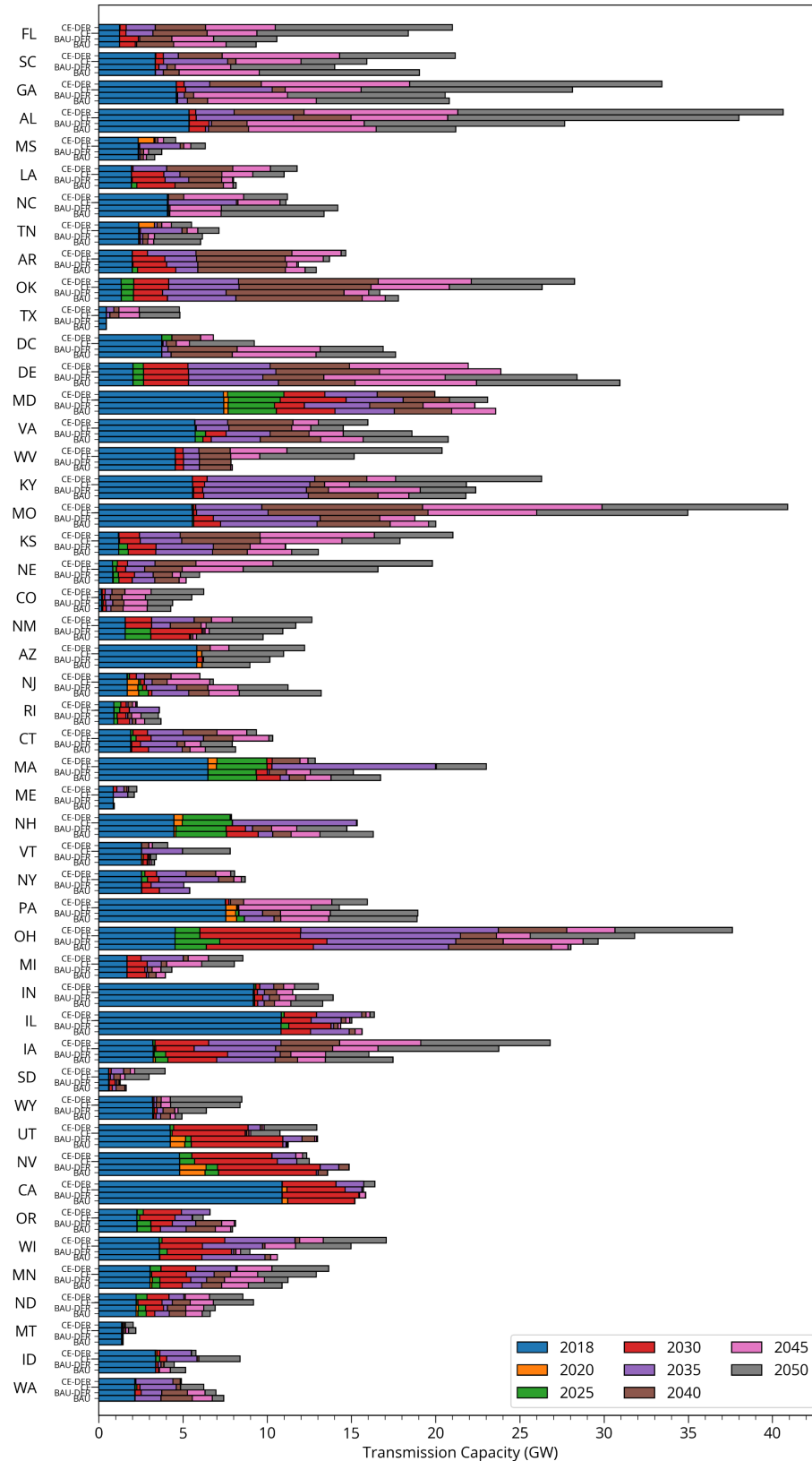


Figure 3.27: Interstate transmission capacity installed for the four scenarios modeled.



3.6 Reliability and Resource Adequacy

WIS:dom-P ensures reliability by making sure that the installed capacity in each investment period can meet demand along with a 7% load following reserve without fail at each operational time period. Resource adequacy is ensured by meeting the North American Electric Reliability Council (NERC) specified unforced capacity (UCAP) Planning Reserve Margins (PRM) for each balancing area modeled. UCAP represents the capacity available at a given time taking into account the generator's forced outage rate. The modeled forced outage rates for thermal generators are given in Table 3.1.

WIS:dom-P models the reliability and resource adequacy as part of the capacity expansion process. The way this is done is that for every capacity installation decision, WIS:dom-P ensures that at every timestep, the sum of expected generation from VREs and the unforced capacity for thermal units is greater than the load plus the PRM for the balancing region in question. Therefore, in addition to choosing sites with best capacity factors and correlation to demand, WIS:dom-P also has to consider the impact on the grid when the generation from VREs is low or non-existent. As a result, WIS:dom-P ensures that the even for periods of lowest or zero VRE generation, the PRM requirements are met for each balancing region. More details on how the model handles reliability and resource adequacy is described in WIS:dom-P technical documentation Section 3.14.³⁵

Generator	Coal	NGCC	NGCT	Nuclear	Hydro	Geo	CCS	SMR	MSR
UCAP	87.7%	86%	85.3%	90.3%	89.5%	89.1%	86%	95%	95%

Table 3.1: Unforced capacity fractions for thermal generators

Since WIS:dom-P solves for the PRM explicitly, the user can extract the common metrics for capacity value rather than ingesting them as inputs.

The most common metric to determine the capacity values of VREs is the Equivalent Load Carrying Capacity (ELCC). ELCC is determined by calculating the additional load that the system can carry due to the addition of a VRE generator, while maintaining the same loss of load probability as before the VRE generator was added. Figure 3.22 shows the ELCC calculated based on the capacities installed by WIS:dom-P over the CONUS for the "CE-DER" scenario.

As seen from Fig. 3.28, ELCC for solar is initially at 55% and then gradually decreases over the investment periods as more solar is added to the grid reaching 10% by 2050. Wind, on the other hand, starts with an ELCC of 100% in 2018 as most of the load over the CONUS peaks in the summer while wind capacity factors peak in the winter. Hence wind has a larger load carrying capacity compared against solar. As more wind is added to the grid, its ELCC reduces gradually over the years before going up slightly in 2045 and 2050. The increase in 2045 and 2050 is due to the model being forced to find more diverse wind sites (irrespective of wind capacity factors) in order to meet the decarbonization constraints in the "CE-DER" scenario. Storage is also seen to start with ELCC of 100% in 2018 and then gradually decrease over the investment periods as more storage is added to the grid. However, storage capacity factors keep reducing eventually hitting 8% by 2050.

³⁵ [https://vibrantcleanenergy.com/wp-content/uploads/2020/08/WISdomP-Model_Description\(August2020\).pdf](https://vibrantcleanenergy.com/wp-content/uploads/2020/08/WISdomP-Model_Description(August2020).pdf)



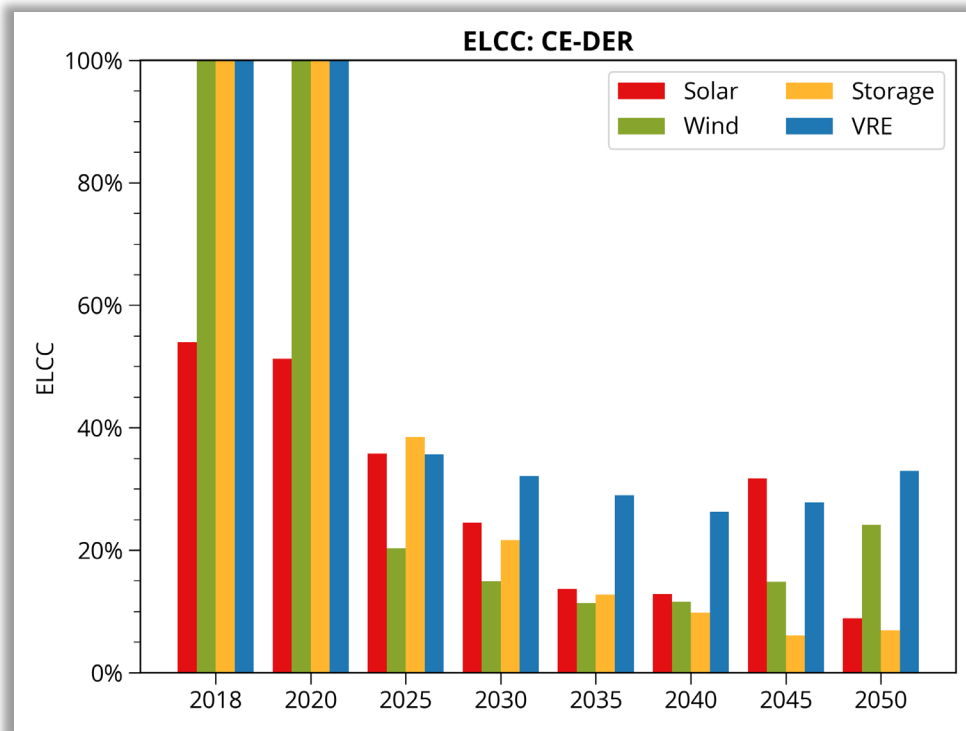


Figure 3.28: ELCC of wind, solar, storage and combined VRE system over the CONUS for the “CE-DER” scenario.

While the ELCC measures the equivalent “firm” capacity of a VRE generator, it does not take into account its role in meeting load during periods of high demand. The capacity value of VRE generators determined based on their contribution as a fraction of their installed capacity during periods of peak demand is shown in Fig. 3.29. As seen in Fig. 3.29, solar has a capacity value of 85% in 2018. This higher capacity value compared with the ELCC is due to the fact that most high demand periods in the CONUS occur in the summer when solar generation is higher. As a result, solar is able to contribute more towards meeting load in periods of high demand resulting in the higher capacity value. The capacity value of solar is seen to increase to 97% in 2020, after which it drops steadily and ends up at 18% in 2050; as the addition of significant amount of solar saturates the grid.

Figure 3.29 shows that wind has a capacity value of 30% in 2018. The lower capacity value of wind compared to the ELCC metric is due to the fact that most the difficult demand periods are in summer while wind generation is seen to be higher in winter and lower in summer. In addition, demand is seen to peak during the day, while wind generation peaks during nighttime. Hence, wind is unable to contribute as much as solar during periods of peak demand resulting in a lower capacity value. Wind capacity value is seen to increase slightly in 2020, then decreasing steadily and ending at 2% in 2050. Since there is no electrification of the economy, most of the new load increases occur during the summer further exacerbating the disconnect between the wind generation and peak loads, which results in a very low-capacity value for wind.



Storage capacity values are seen to be closer to that of solar with 70% in 2018 and increasing to 100% in 2020. Storage capacity values are then seen to drop steadily as more storage is added resulting a capacity value of 10% by 2050. The capacity value of storage is seen to decrease as the peak load periods, which occur during the daytime, are overwhelmingly being met by solar.

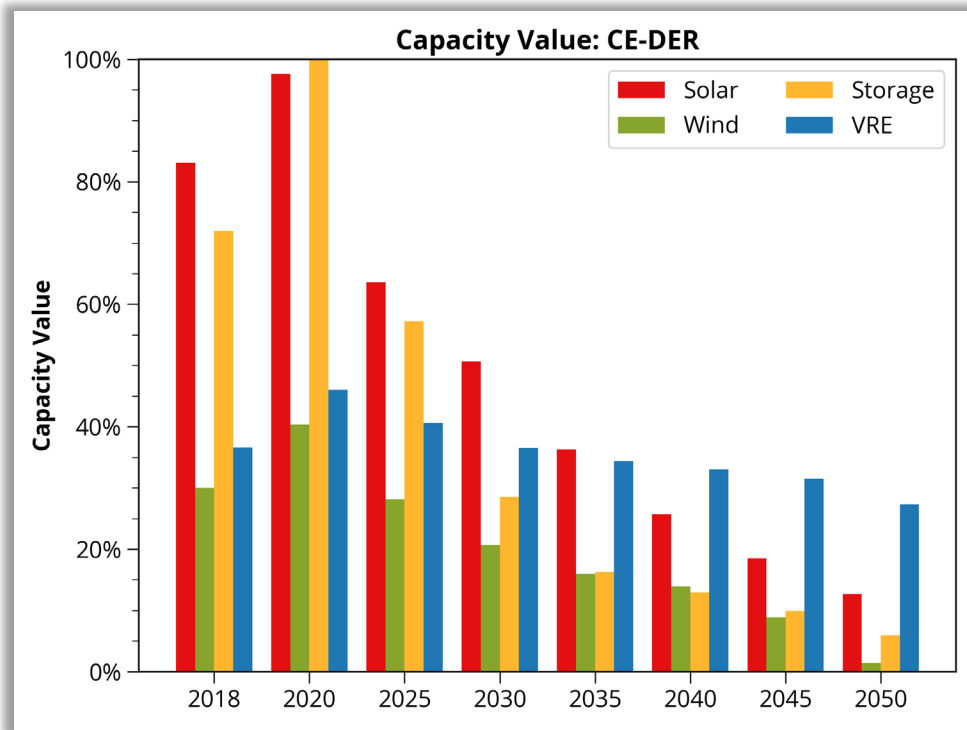


Figure 3.29: Capacity value of VREs calculated based on contribution during periods of peak demand for the "CE-DER" scenario.

Since VRE generation is dependent on weather, it is to be expected that the capacity value of VRE generators will show seasonal characteristics correlated with their seasonal generation trends. Figure 3.30 shows the monthly averaged capacity value of wind, solar and storage in scenario in the year 2050 for the "CE-DER" scenario. As seen in Fig. 3.30, solar capacity value peaks during the summer months, while wind capacity value peaks in the winter months. Storage capacity value is correlated with the wind capacity value as storage comes into play along with wind in meeting load during the winter.



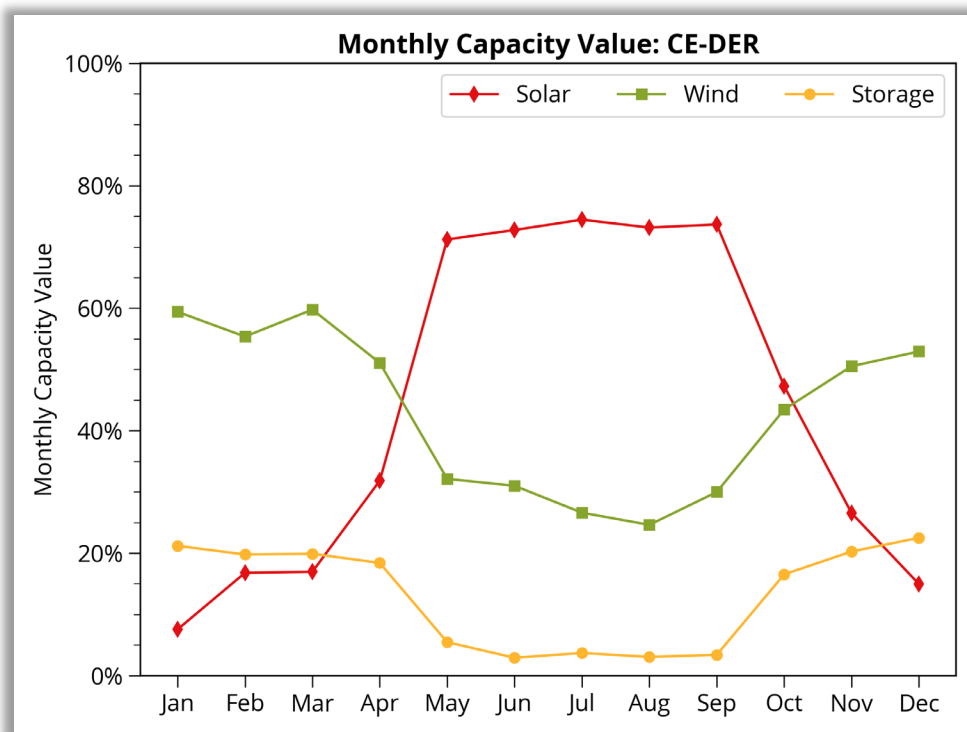


Figure 3.30: Monthly average capacity values of VRE in 2050 for the “CE-DER” scenario.

Figure 3.31 shows how the system handles periods of high system strain. The electricity system is defined to be in high strain when thermal generators are utilized to their maximum, VRE generation is at its lowest and demand is at its highest. As part of ensuring reliability and resource adequacy, WIS:dom-P deploys VRE generation such that the periods of highest system strain is moved to evening hours in August where solar generation is ramping down and wind generation does not show up to meet the ramp up in demand. As seen in Fig. 3.31, the “BAU” scenario and the “CE-DER” scenario meet this difficult period in very different ways. The “BAU” scenario deploys natural gas combined cycle units to help meet demand. In the “CE-DER” scenario, on the other hand, the grid deploys a combination of natural gas Peaker units (natural gas combustion turbines) and storage to meet demand during these periods of high system strain.

Therefore, there are several paths to ensuring system reliability during periods of high system strain and WIS:dom-P chooses the optimal path taking into account system cost, emission constraints, and available resources.



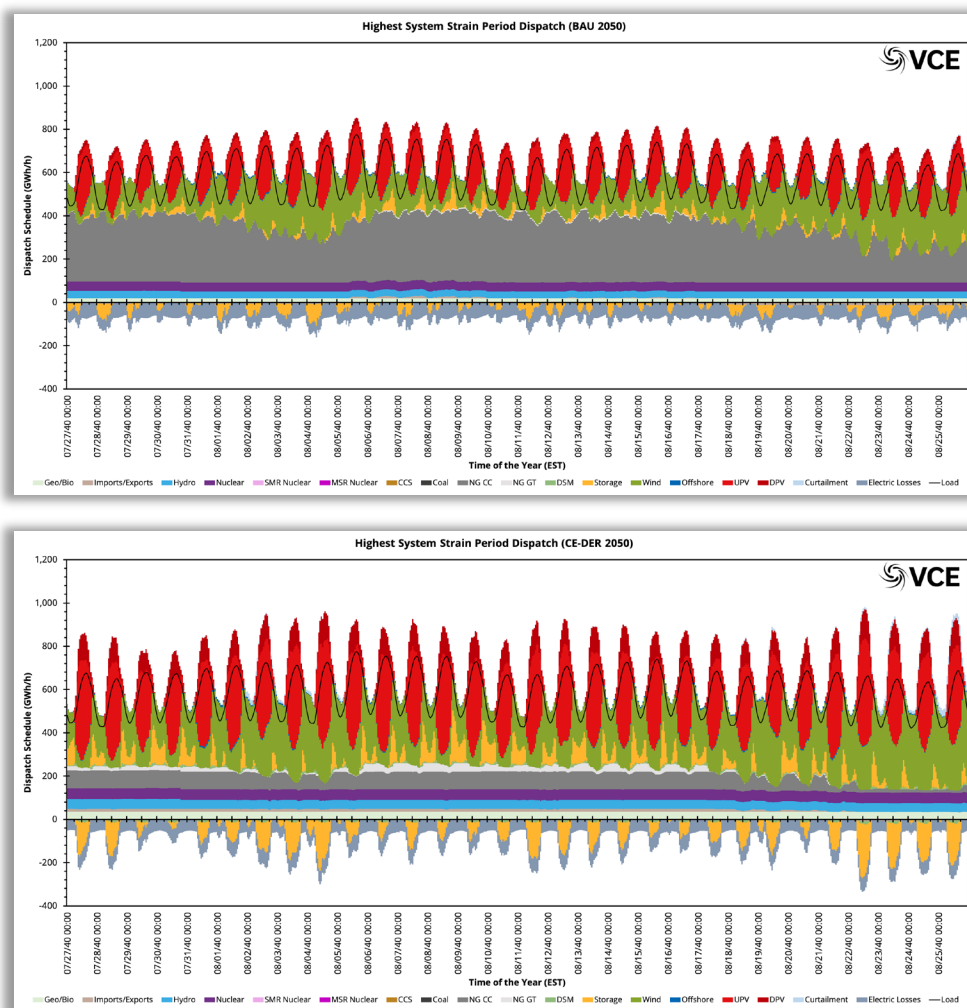


Figure 3.31: The most difficult period to supply demand for the CONUS for in 2050 for the “BAU” (top) and “CE-DER” (bottom) scenario.



3.7 Siting of Generators

Using the multi-year 3-km, 5-min weather dataset available over the contiguous United States, WIS:dom-P is able to perform optimal siting of generators. Figure 3.32 (top panel) shows the installed capacities over the CONUS in 2050 for the “BAU” scenario and Fig. 3.32 (bottom panel) shows the optimal siting of generators for the “BAU-DER” scenario in 2050. As seen from Fig. 3.32, Texas goes from deploying predominantly wind and UPV in the “BAU” scenario to having significant amount of DPV in the panhandle and western ERCOT region. A similar trend is seen in Oklahoma where the Oklahoma panhandle gets significant DPV installation along with wind in the “BAU-DER” scenario.

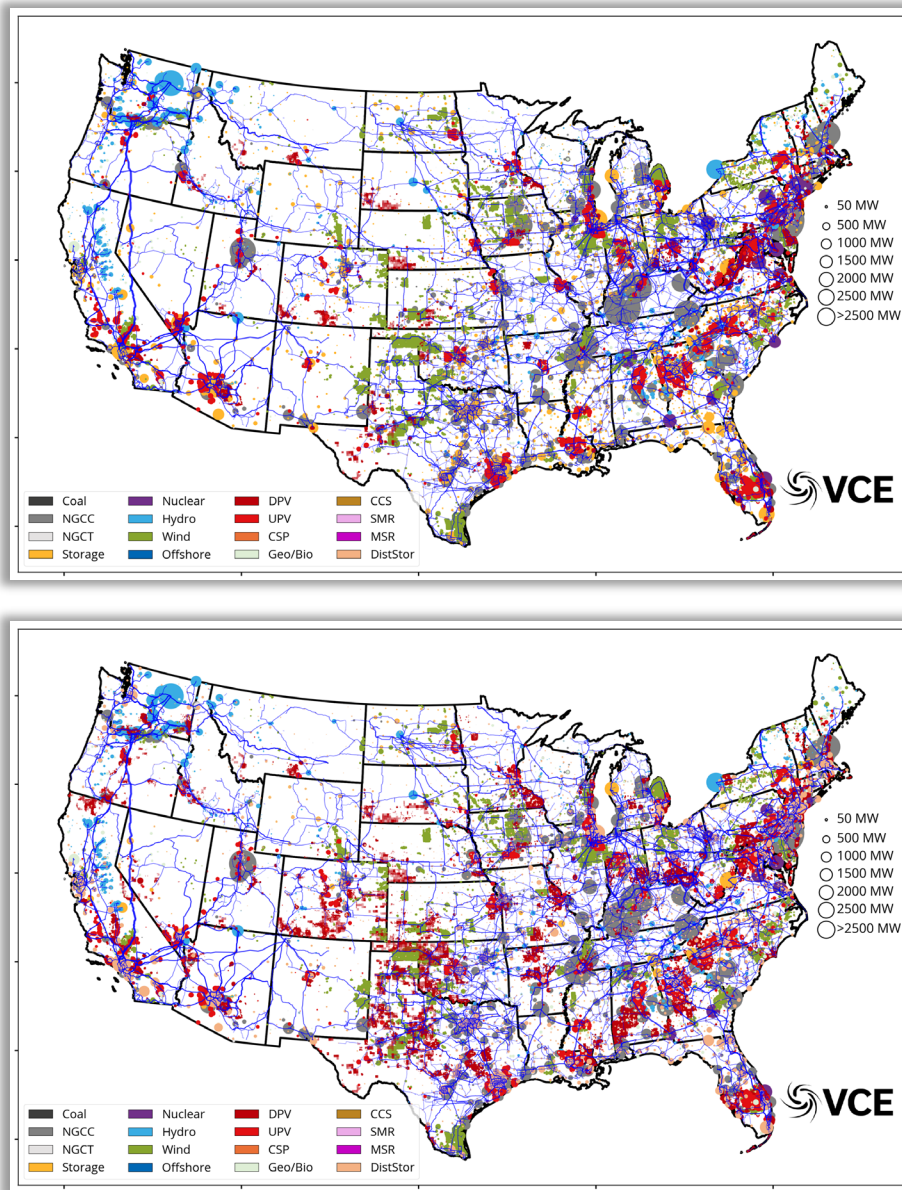


Figure 3.32: Optimal siting of the generation on the 3-km grid for the “BAU” (top panel) and “BAU-DER” (bottom panel) scenarios in year 2050.



Figure 3.33 (top panel) shows the optimal siting on the 3-km grid for the “CE” scenario and the bottom panel shows the optimal siting for the “CE-DER” scenario in 2050. Similar to the “BAU-DER” scenario, the “CE-DER” scenario installs substantially more DPV in the Texas and Oklahoma panhandle, in addition to more DPV installations in Kansas, Nebraska and South Dakota compared to the “CE” scenario. However, it is seen that in Louisiana and Mississippi there is less DPV installation in the “CE-DER” scenario compared to the “CE” scenario.

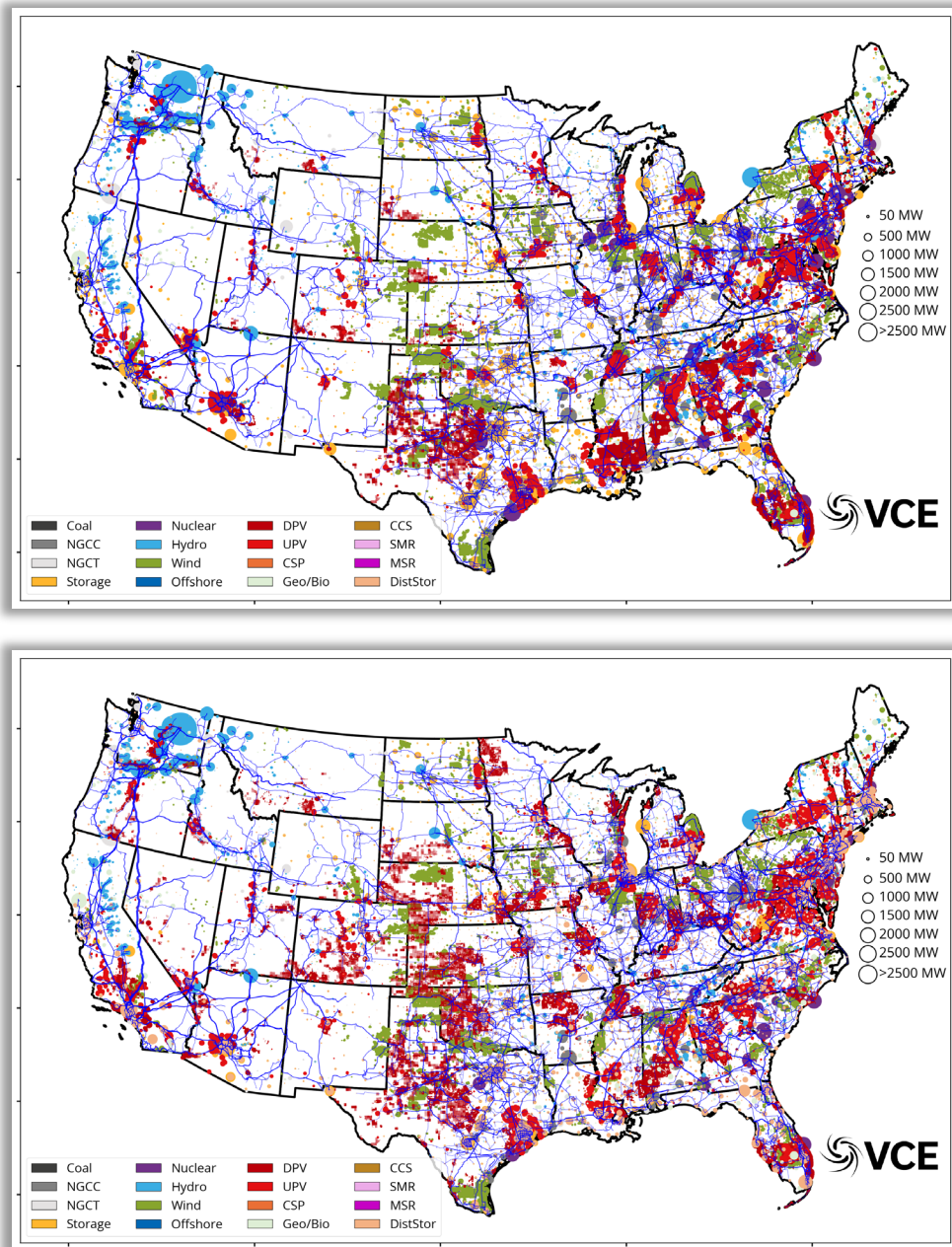


Figure 3.33: Optimal siting of the generation on the 3-km grid for the “CE” (top panel) and “CE-DER” (bottom panel) scenarios in year 2050.



When making the siting decisions the WIS:dom-P model takes into account several criteria to determine the optimal siting for the generators. In addition to taking into account expected generation and distance from the demand, the model ensures that generation is not sited in unsuitable locations. The criteria used to filter out unsuitable locations for VRE generation are discussed in Section 4.2. In addition, the model has to ensure that it does not exceed the technical potential of each grid 3-km grid cell. The technical potential for the various VRE technologies in each grid cell is determined by taking into account several factors such as population, land cover, terrain slope and so on. In addition, each technology is limited by the maximum packing density allowed to ensure that the generators do not hamper performance of other generators in the grid cell such as through wakes for wind turbines and excessive shading for solar panels. The details on these metrics and the available technical potential for the CONUS are discussed in greater detail in Section 4.2.



4. VCE[®] Datasets & WIS:dom[®]-P Inputs

4.1 Generator Input Dataset

VCE processed the Energy Information Administration (EIA) annual data from 2018 to create the baseline input generator dataset for the present study. From this dataset, information for the contiguous US was obtained. This large geographic area contains over 1,190 GW of installed generation capacity. WIS:dom has the ability to solve over such scales at 5-minute resolution for several years chronologically.

The WIS:dom-P generator input datasets are built upon the publicly available EIA 860 and EIA 923 data. The 2018 data was used for the present study. VCE carry out several steps to align and aggregate technology types to the 3-km model grid space that matches the National Oceanic and Atmospheric Administration (NOAA) High-Resolution Rapid Refresh (HRRR). In the process, year-on-year changes were analyzed. Across the United States, general trends show (for fossil fuels) coal capacities falling with natural gas combined cycle growing. Wind, solar and storage plants are on the rise as well. The trend continues in the data throughout 2019 based upon the recently released annual data for that year.

Below, we outline the VCE process to prepare the generator input datasets:

1. *Data is merged, aligned, and concatenated between the EIA 860 and EIA 923 data.*
2. *Initial quality control is applied to the data to ensure accuracy between datasets.*
3. *Align the location of the generators to the nearest 3-km HRRR cell. Care is taken to ensure the correct grid cell is chosen within state boundaries and water sites.*
4. *Aggregation of the generator types within each 3-km cell; e.g., multiple generators of the same fuel type are summed for capacity and capacity-weighted averaged are applied to operational parameters.*
5. *Further spatial verification is performed to ensure the output aligns with the original data.*
6. *Final model input format produced. A county level average of all generator types is also created.*

VCE coordinates with the Catalyst Cooperative (<https://catalyst.coop/>), a company with the goal to help the energy research community by processing major publicly available sources into a format that is organized and stream-lined to use. This assists our processes and will allow it to become more rapid and frequent for these input datasets.



1	Coal
2	Natural Gas Combined Cycle
3	Natural Gas Combustion Turbine
4	Storage
5	Nuclear
6	Hydroelectric
7	Onshore Wind
8	Offshore Wind
9	Residential Solar
10	Utility-scale Solar
11	Concentrated Solar Power
12	Geothermal
13	Biomass
14	Other Natural Gas
15	Other Generation
16	Natural Gas - CCS
17	Pumped Hydro Storage
18	Small Modular Reactors
19	Molten Salts

Figure 4.1: The VCE generator technology bins.

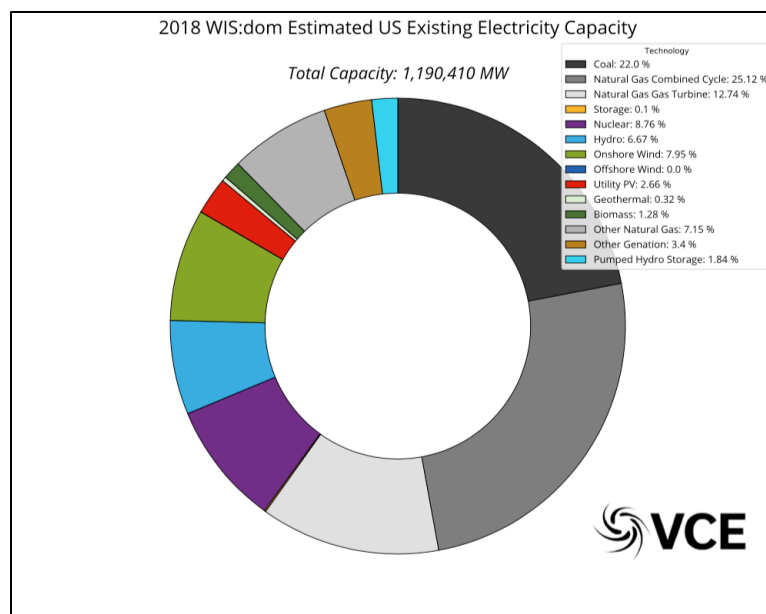


Figure 4.2: WIS:dom estimated installed capacity from 2018 the contiguous United States. The total capacity modeled is 1,190 GW.

Figure 4.1 displays the generation technology types that are standard within the WIS:dom-P modeling. Figure 4.2 shows the installed capacities over the contiguous US footprint. It is clear that the US is dominated by thermal generators (coal, natural gas and nuclear) with over two-thirds coming from fossil fuels. Variable Renewable Energy (VRE) capacities are smaller, with highest shares from hydroelectric, wind and solar. All told, the amount of installed clean generation (including VRE and nuclear) is just over a quarter all generator capacities in the US. For comparison, the same chart is shown below for all the generation produced across the contiguous US in Fig. 4.3. Coal and natural gas units produce around 64% of the generation. VRE account for 15% of the US generation. At the generation level,



hydroelectricity still produces more terawatt-hours than wind. Finally, nuclear makes up the majority of the remaining generation produced at just under 20% of the total.

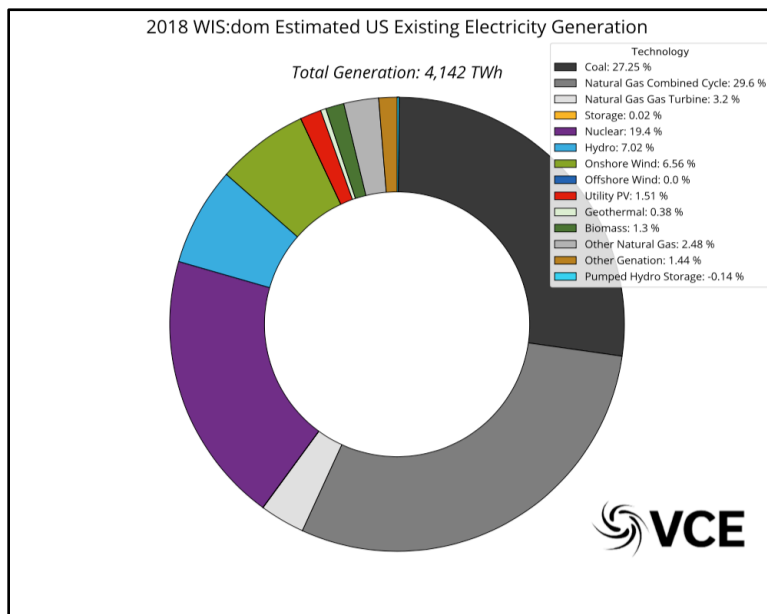


Figure 4.3: WIS:dom estimated technology generation for the contiguous United States. The total generation modeled is 4,142 TWh.

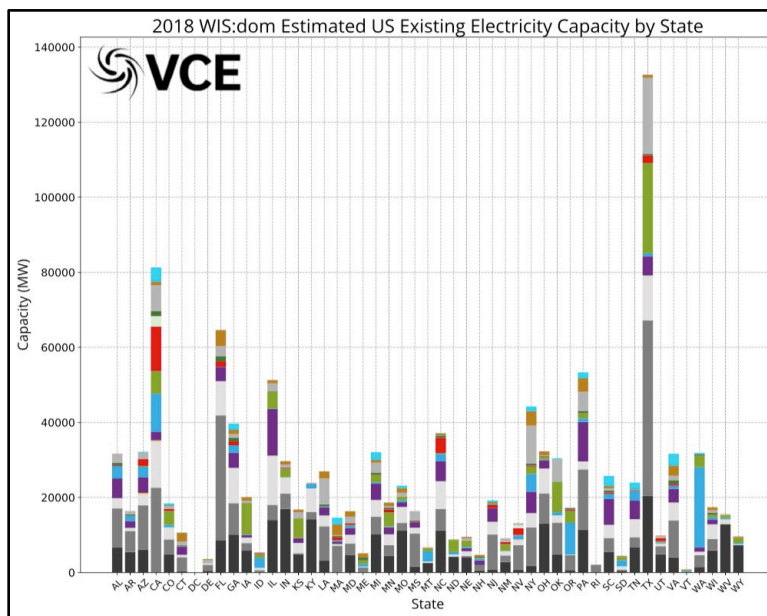


Figure 4.4: WIS:dom capacity installed broken out by states in the EI.

Figure 4.4 shows the technology capacity stacks for each state. Texas has the largest amount of installed capacity, followed by California and then Florida. Texas holds over 10% of the contiguous US installed capacity. Together, Texas, California and Florida contain almost 20% of the installed US capacity. The largest nuclear presence resides most in Illinois and Pennsylvania, though the majority of states in the eastern US have some presence of nuclear. Texas, followed by Indiana, has the highest capacity of installed coal. Coal



comprises the majority of the generator technologies in West Virginia and Wyoming, making up over 83% and 75% of the generator capacity installed within those states respectively. California, Florida, Nevada and North Carolina have the highest solar capacity. Texas has the most wind capacity, followed by Iowa, Oklahoma, and Kansas. Figure 4.5 shows the locations of installed generators across the US. It is observed that large solar clusters are along the east coast, in southern California and in southern Minnesota. Wind shows up most along the Great Plains states with high concentrations in the Texas Panhandle, western Oklahoma, southern Kansas, Iowa and southern Minnesota. Larger hydro groups are seen along the Sierra Nevada, Cascade, Rocky and Appalachian Mountain ranges. There are also noticeable hydro clusters in the northeast New England states. Coal has an evident presence up and down the Missouri and Ohio rivers. Many nuclear installations are also observed in the Great Lakes regions.

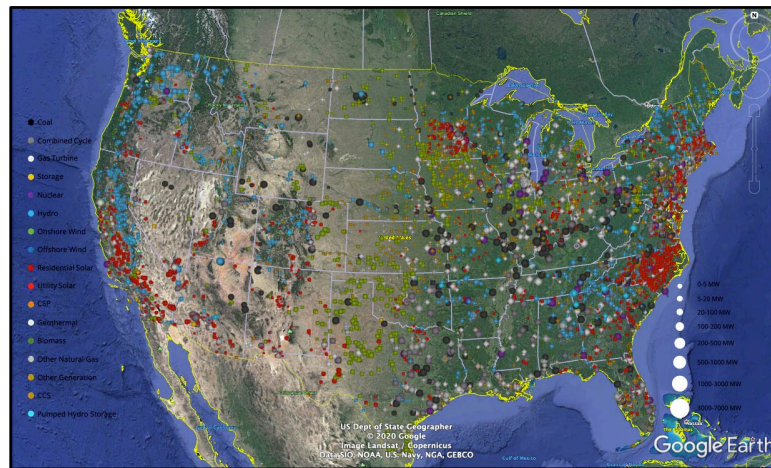


Figure 4.5: WIS:dom estimated location of various technologies for the US.



4.2 Renewable Siting Potential Dataset

VCE performs an extensive screening procedure to determine the siting potential of new generators across the contiguous US. This ensures that the WIS:dom model has constraints on where it can build new generation. First, USGS land cover information is utilized as a base within each 3 km grid cell to determine what is there (Fig. 4.6 top left panel). Figure 4.7 shows this same information with specific number scales. Onshore and offshore wind are also split out.

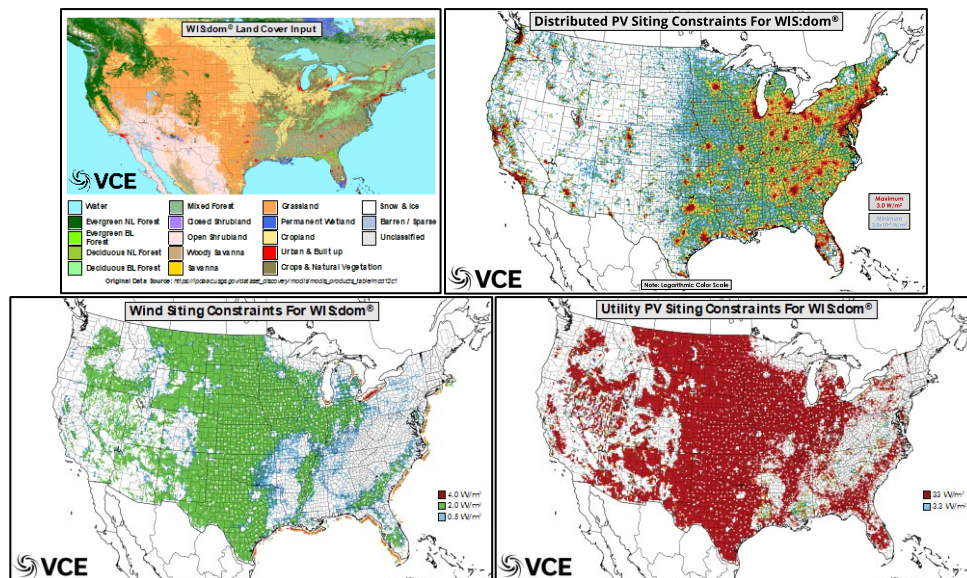


Figure 4.6: WIS:dom land cover (top left), distributed solar PV siting bounds (top right), utility-scale wind bounds (bottom right) and utility-scale solar PV (bottom right).

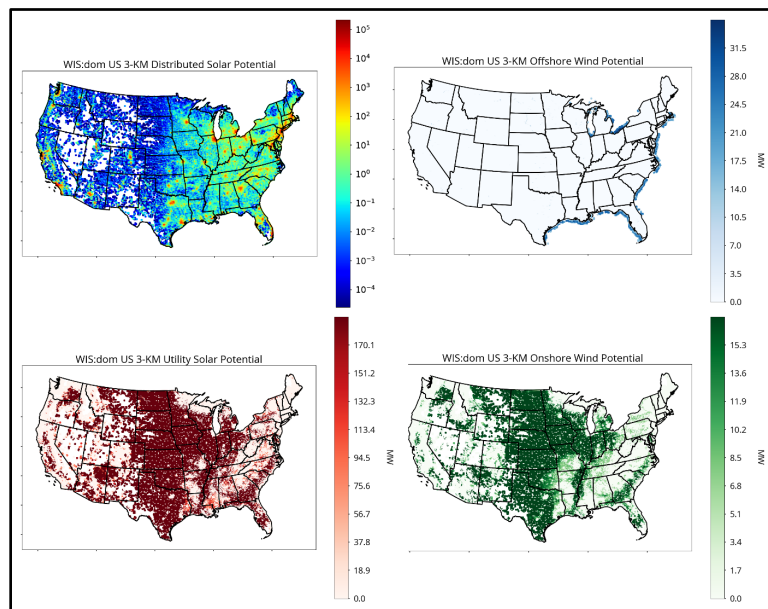


Figure 4.7: WIS:dom Rooftop Potential (top left), Offshore Wind Potential (top right), Utility-scale Solar Potential (bottom right) and Onshore Wind Potential (bottom right) in MW. The Distributed Solar Potential is converted to a Logarithmic Base 10 scale due to the ranges of value for that parameter.



The first screening algorithm follows these steps:

1. *Remove all sites that are not on appropriate land-use categories.*
2. *Remove all sites that have protected species.*
3. *Remove all protected lands; such as national parks, forests, etc.*
4. *Compute the slope, direction and soil type to determine its applicability to VRE installations.*
5. *Determine the land cost multipliers based on ownership type.*
6. *Remove military and other government regions that are prohibited.*
7. *Avoid radar zones and shipping lanes.*
8. *Avoid migration pathways of birds and other species.*

The above, along with the knowledge of what is already built within a HRRR cell from the Generator Input data provides WIS:dom with a view of where it can technically build certain generators as well as certain technologies. Figure 4.6 shows the siting constraints for wind, utility-scale solar PV and distributed solar PV.

For wind, utility-scale solar PV, distributed solar PV, and electric storage the available space use converted into capacity (MW & MWh) by assuming a density of the technologies. This is particularly important for wind and solar PV because of wake effects and shading effects, respectively. The maximum density of wind turbines within a model grid cell was restricted to no more than one per km² (< 4 MW / km²). Solar PV was restricted to a maximum installed capacity of 33 MW per km². For storage, it is assumed for a 4-hour battery the density is 250 MW / km². For all thermal generation, the density assumed for new build is 500 MW / km². Thus, for a 3-km grid cell the resulting maximum capacities (in the CONUS) are:

- **Wind – 36 MW;**
- **Utility Solar PV – 297 MW;**
- **Distributed solar PV – 68 MW;**
- **Storage (4-hr) – 2,250 MW or 9,000 MWh;**
- **Thermal generators – 4,500 MW.**

These densities and values also ensure that WIS:dom does not over build in a single grid cell because the combined space is constrained, as these numbers are maximums assuming only that technology exists.

Figure 4.8 shows that California, Texas and Florida have the highest potential for distributed solar. In general, the more populous states provide more buildings for distributed solar. Offshore wind has the highest potential in Florida. Louisiana comes in following Florida. Of note is also Ohio which has high offshore potential with Lake Erie. Utility solar potential is highest in Texas. Many of the Great Plains states also have high utility scale solar potential. This potential generally decreases from the central states to the coasts. This same pattern is also apparent with onshore wind.



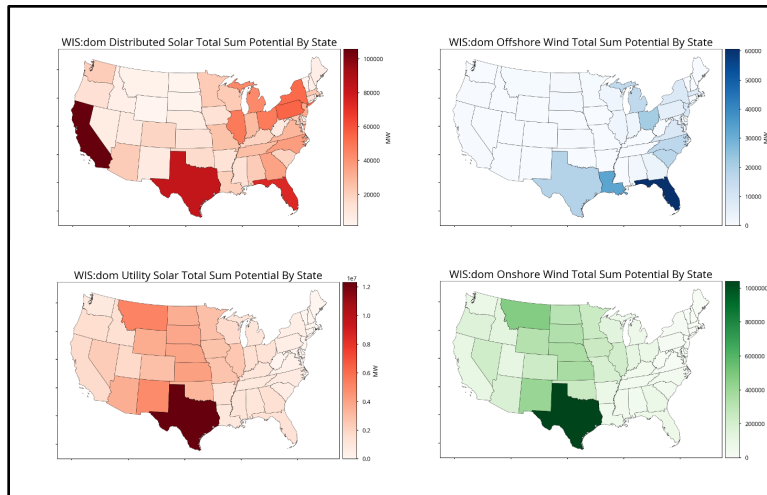


Figure 4.8: WIS:dom Total Sum Potential by state for Rooftop (top left), Offshore Wind (top right), Utility-scale Solar (bottom left) and Onshore Wind (bottom right) in MW for the contiguous US.



4.3 Standard Inputs

There is a standard suite of input data for the WIS:dom-P model that sets the stage for several base assumptions about the energy grid and generator technologies. This includes:

- *Generator cost data (capital, fixed, variable, fuel);*
- *Generator lifetime terms;*
- *Standard generator heat rates;*
- *Transmission/Substation costs;*
- *Legislature in the energy sector:*
 - *Renewable portfolio standards;*
 - *Clean energy mandates;*
 - *GHG emissions requirements;*
 - *Storage and offshore mandates);*
 - *PTC/ITC;*
- *Jobs for various technologies.*

The above list is of the most commonly discussed standard inputs the model uses and are looked at in this document. The above is not exclusive and much more information is ingested by WIS:dom-P to narrow down characteristics of various generation technologies. The list of standard files is constantly growing as the industry evolves. Additional inputs can be easily incorporated into WIS:dom-P.

This is a list of the most commonly discussed standard inputs the model uses and are looked at in this document. The above list is not exclusive and much more information is ingested by WIS:dom-P to narrow down characteristics of various generation technologies. The list of standard files is constantly growing as the industry evolves. Additional inputs can be easily incorporated into WIS:dom-P.

The standard inputs remain constant throughout the scenarios modeled for the study unless specifically requested to change. However, the standard inputs are changing within each scenario throughout each investment period modeled. The overnight capital, fixed O&M and variable O&M costs for each generator technology are predominantly based upon the NREL ATB values. It is noted where this is not the case. The NREL values were chosen to be reputable values; are used by RTOs in their modeling; give high granularity and are updated frequently. The fuel costs come from the EIA Annual Energy Outlook data, another source that is reputable and regularly updated. VCE provides fuel and capital costs multipliers by state to further tune the areal layout of these standard cost inputs. Other standard inputs are a combination of VCE internal research and work with various partners in the industry.

These input assumptions are ingested into WIS:dom-P to provide insight and bounds to the optimization selections for each investment period. It offers the model a picture of what cost options are available to optimize.



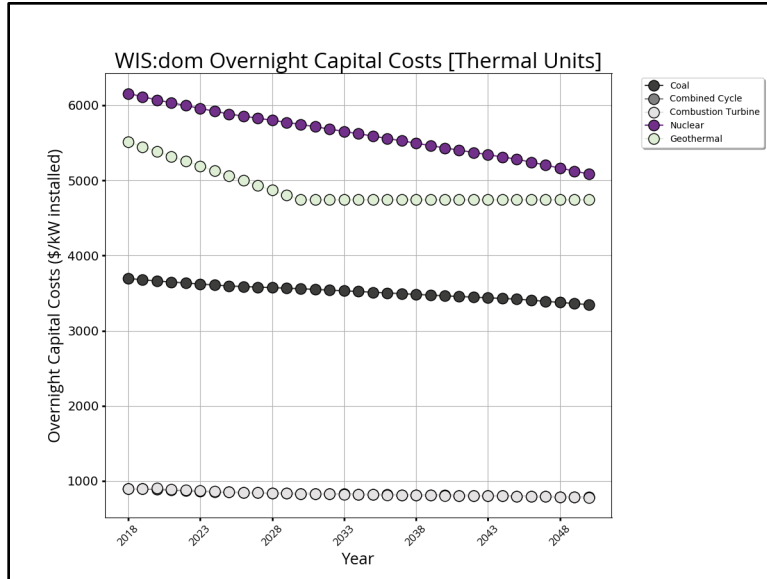


Figure 4.9: The overnight capital costs in real \$/kW-installed for thermal power plants in WIS:dom-P.

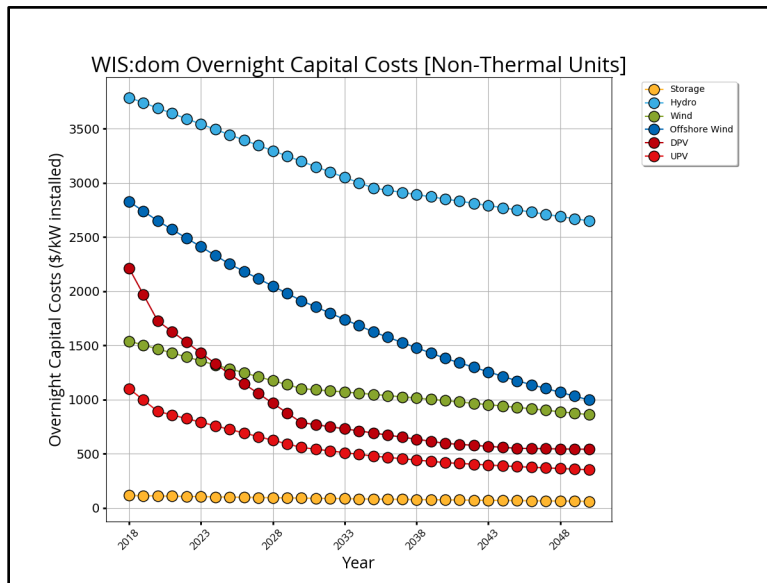


Figure 4.10: The overnight capital costs in real \$/kW-installed for non-thermal power plants in WIS:dom-P. All costs are from NREL ATB 2019, with the exception of storage costs, which were provided by Able Grid, Inc.



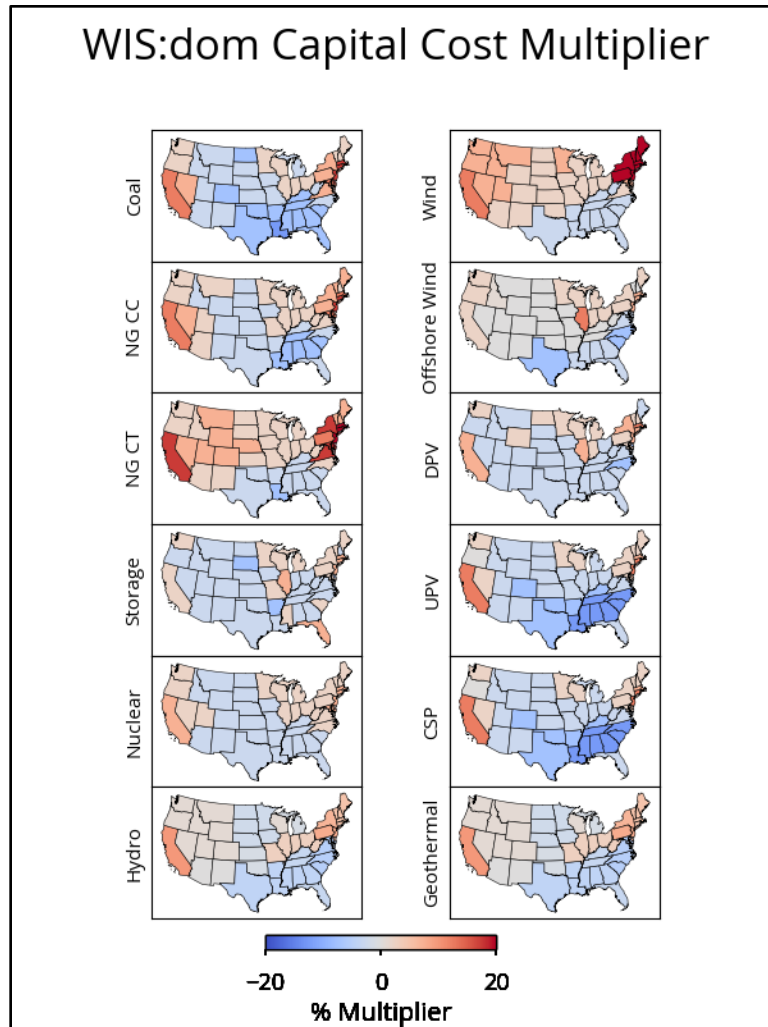


Figure 4.11: The WIS:dom-P Capital Cost Multiplier is shown by state for each technology across the US. Shades of red show where the capital cost is scaled higher by a given percentage. Cool shades show where technology capital costs in the model are scaled down by a given percentage.

Figure 4.11 shows that certain states and regions actually experience lower capital costs when building many technologies from the NREL ATB values. It is shown that Texas and, in general, the Southeast United States, have lower capital costs for all generator technologies. Storage capital cost is the one exception in the Southeast that is more expensive, though not for all southeast states. Certain technologies like Wind and Natural Gas Combustion Turbine technologies are more expensive in the Intermountain West. Wind is especially expensive in the northeast. In general, California and the New England states consistently show higher capital costs multipliers for all generator technologies.



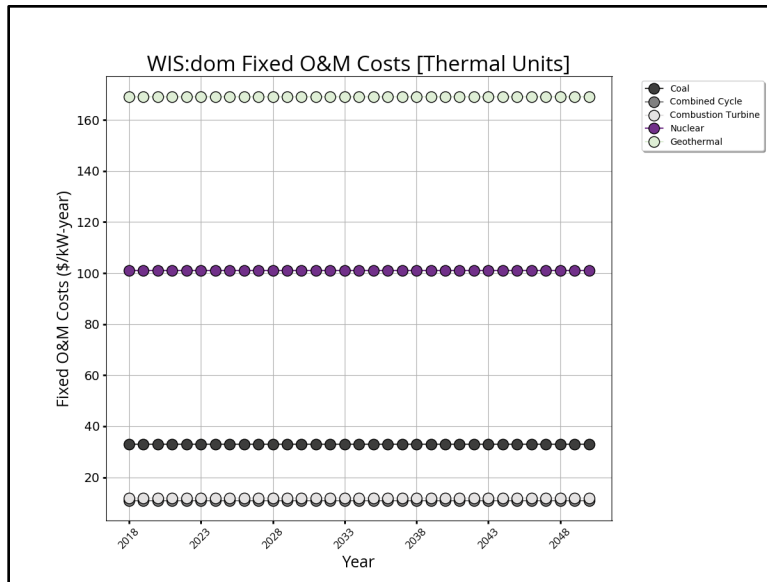


Figure 4.12: The fixed operations and maintenance (O&M) costs in real \$/kW-yr for thermal power plants in WIS:dom-P.

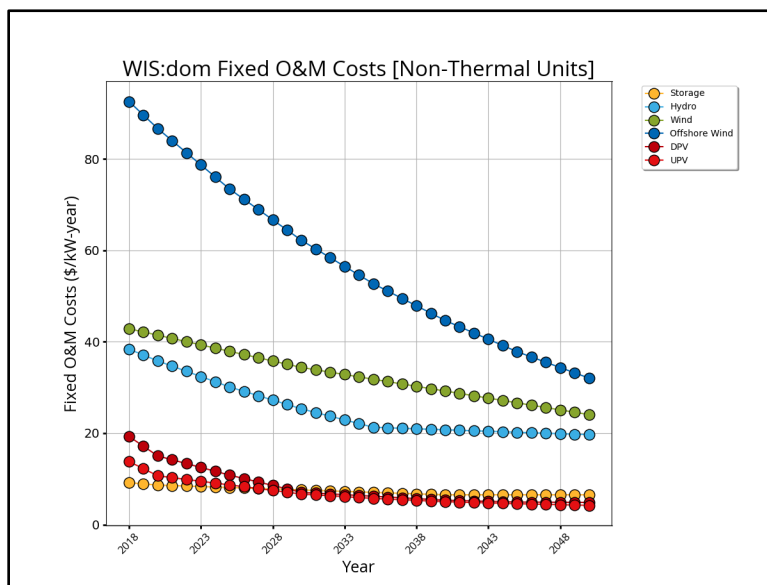


Figure 4.13: The fixed operations and maintenance (O&M) costs in real \$/kW-yr for non-thermal power plants in WIS:dom-P.



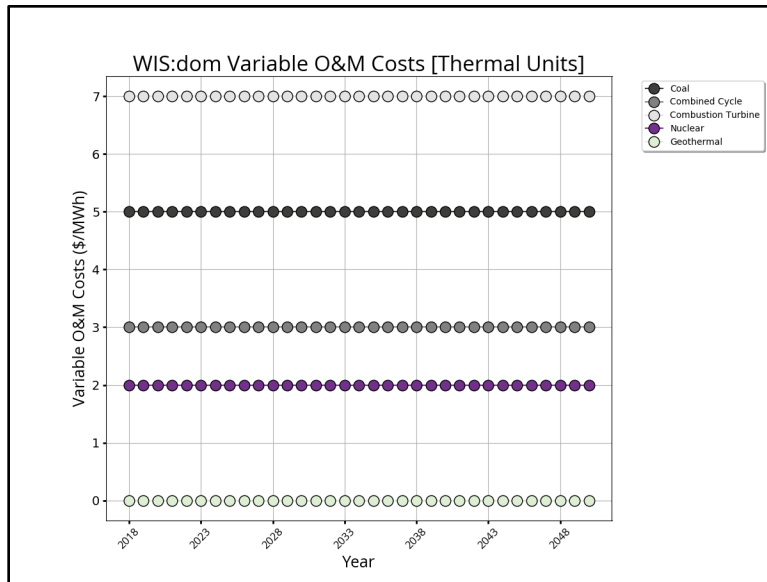


Figure 4.14: The non-fuel variable O&M costs for thermal generators in WIS:dom-P in real \$/MWh. The non-thermal units have zero variable O&M costs as those costs are combined into the fixed O&M costs.

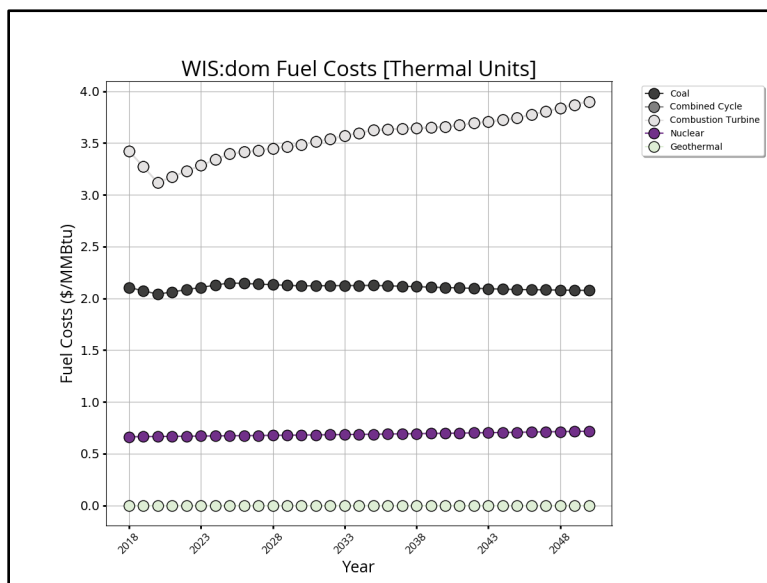


Figure 4.15: The fuel costs for thermal generators in WIS:dom-P in real \$/MMBtu.



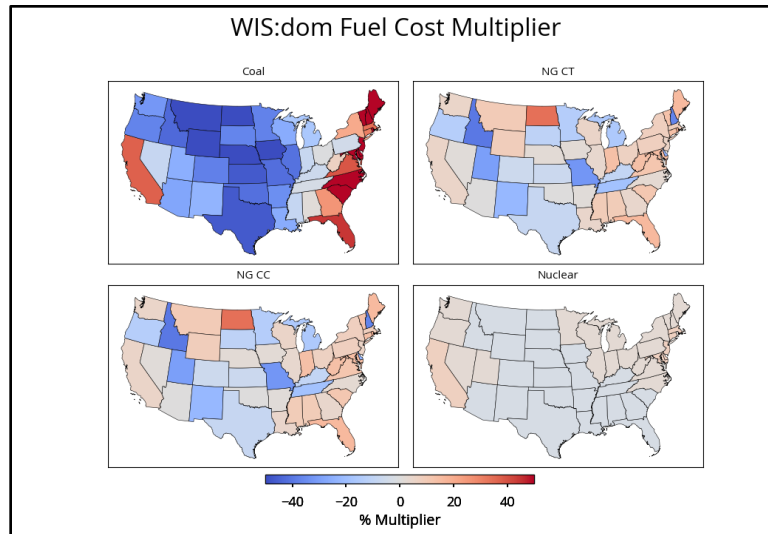


Figure 4.16: The WIS:dom-P Fuel Cost Multiplier is shown by state for each technology across the US. The color scale shows a percentage multiplier applied to standard fuel costs. Shades of red show where the fuel cost is scaled higher by a given percentage. Cool shades show where technology fuel costs in the model are scaled down a given percentage. Renewable fuels are not shown here as those fuel costs are the same no matter where the technology is and those fuel costs are null.

Figure 4.16 shows the spatial variations of fuel costs for thermal units (except geothermal since that cost is zero). California and the New England states show higher fuel costs for most of the technologies. New Hampshire is an exception for natural gas. Fuel costs for coal are much lower in the middle portion of the country. Natural Gas fuel costs are notably lower in Idaho, Utah, New Mexico, Missouri and New Hampshire. There is no fuel cost multiplier applied to renewable fuels (wind, solar, hydro) as those are the same everywhere across the US and they are fuels that have no cost.

Storage is one of the most discussed inputs. Storage can have highly variable cost input values depending on sources. It also is a heavy driver as to how the model handles renewables, transmission and future baseload. The following Fig. 4.17 shows the difference between the 2019 NREL Low ATB costs for storage versus sources from Able Grid, Inc. VCE uses the latter in the modeling for storage because it is more representative of the current market expectations.



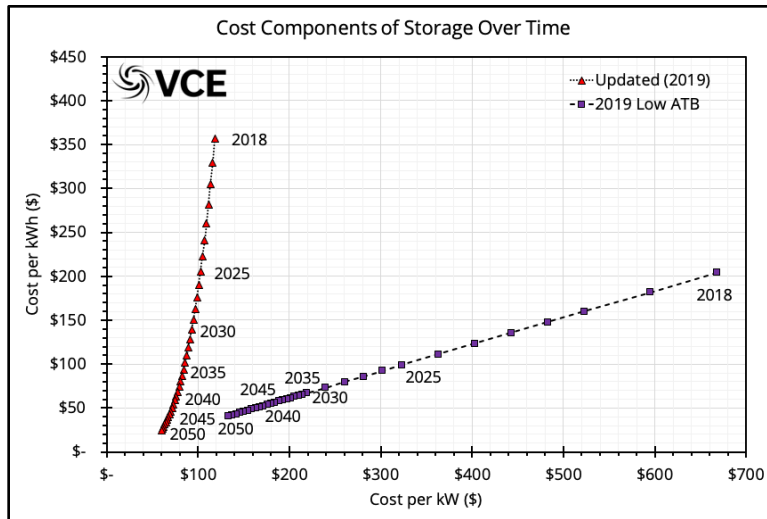


Figure 4.17: The Balance of System Capital Cost (\$/kW) versus the Battery Pack Capital Cost (\$/kWh). This is shown for the 2019 Low NREL ATB values in purple. The same information from Able Grid, Inc is shown in red. The latter is used in the WIS:dom-P model.

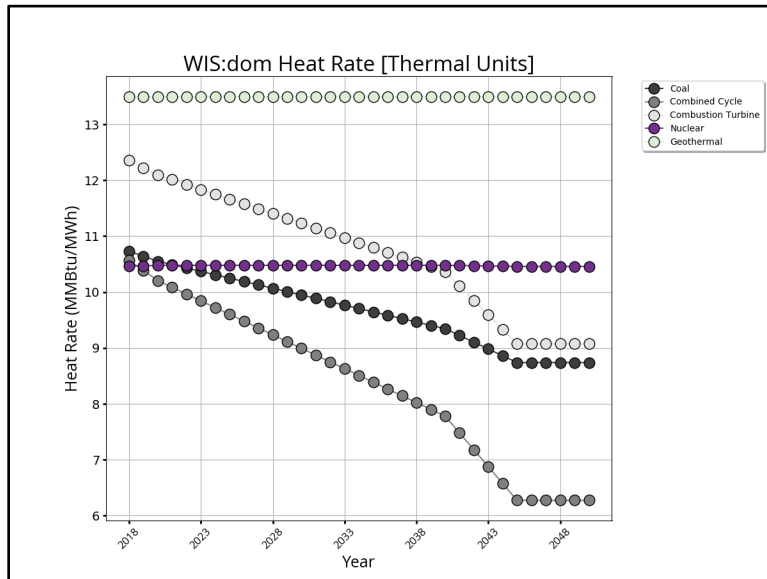


Figure 4.18: The generic heat rate for thermal generators in WIS:dom-P in MMBtu/MWh of electricity generated. Explicit heat rates for currently installed generators come into the model through the Input Generator Datasets and the EIA 860/923 data.

We use the same **real** discount rate for all generator technologies in the WIS:dom-P model. This value is 5.87%, which is applied with the book life of the technologies to provide the model with the amortized capital costs. The lifetime of the various technologies also impacts what/when the model optimally deploys generation as well as when it can retire units. Figure 4.19 shows the standard economic lifetimes for the various technologies used within WIS:dom-P.



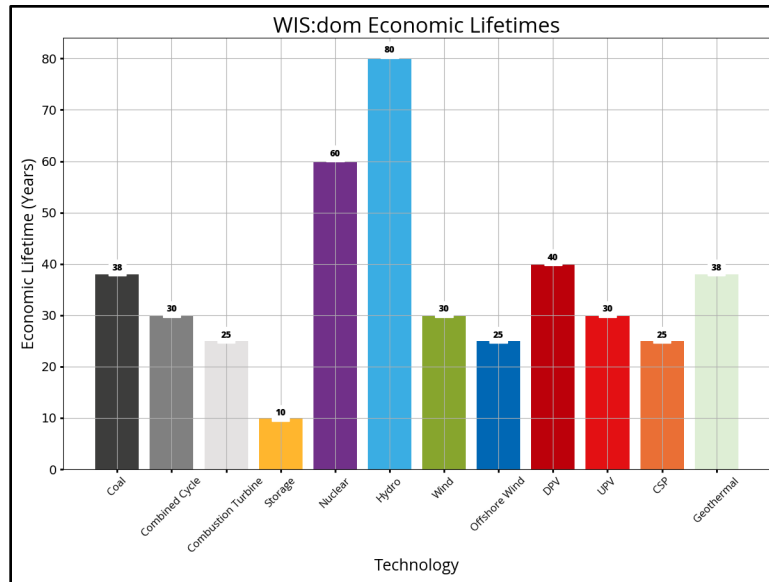


Figure 4.19: The economic lifetime for each generator type within WIS:dom-P in years. The economic lifetime means the time that the debt must be cleared from the units.

Transmission plays a large part in the optimized decisions that the WIS:dom-P model executes. The decision to build renewable technologies can be affected by the standard inputs around transmission aspects.

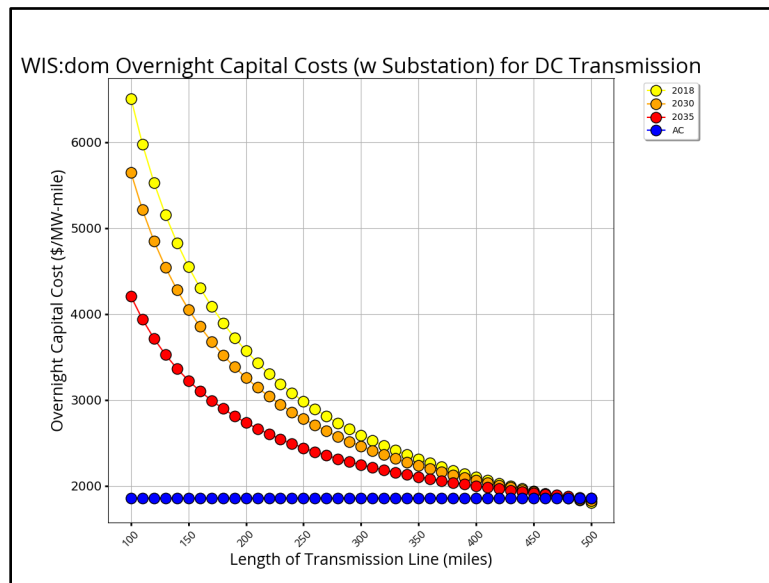


Figure 4.20: Shows the overnight capital cost of DC transmission in WIS:dom-P in real \$/MW-mile installed over various distances. Costs are shown for 2018, 2030 and 2050. The overnight capital cost of AC transmission (including substations) is also shown in blue. This is the same cost no matter the investment period.

The economic lifetime, or rather, length of amortization, of the transmission assets in the model are 60 years for all investment periods.



VCE documents the various state legislature and renewable energy goals by tracking Renewable Portfolio Standards, Clean Energy Mandates, Offshore Wind Mandates, Storage Mandates and GHG Emission Reduction Mandates. This provides the bounds and definitions of what the WIS:dom-P model is required to build as it optimizes systems of the future. Over 30 states have a renewable portfolio standard in place. Just over 10 states currently have a clean energy mandate. The northeast has become increasingly aggressive in setting offshore wind energy targets. Storage mandates have started to show up in the recent years as well. The following figures lay out the legislative goals by 2050. The Production Tax Credit and the Investment Tax Credit for renewables is also discussed. This directly ties into the cost of renewables built in WIS:dom-P.

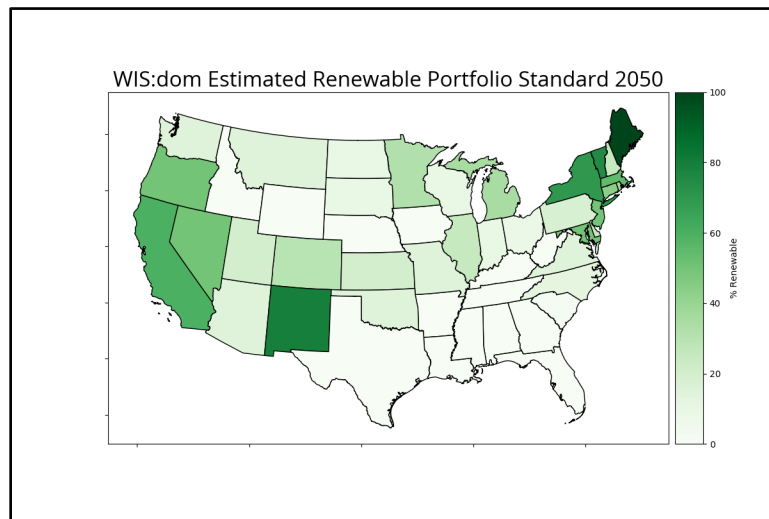


Figure 4.21: The Renewable Portfolio Standards percentage requirement of each state across the US.

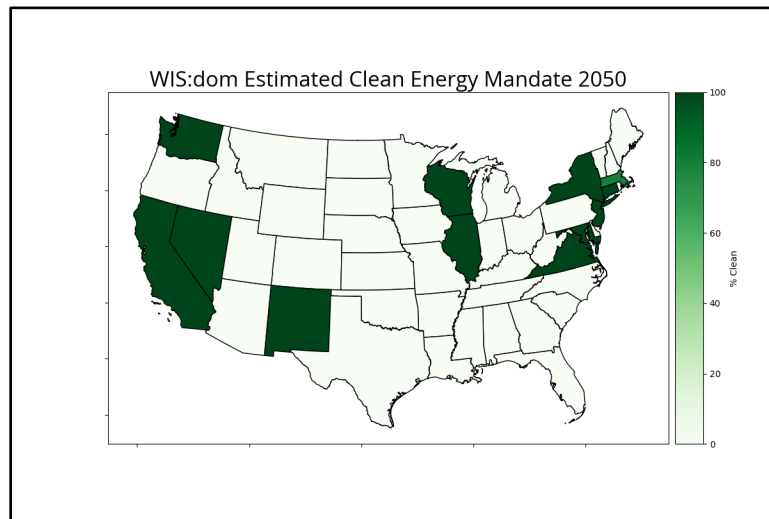


Figure 4.22: The Clean Energy Mandate percentage requirements of each state across the US.



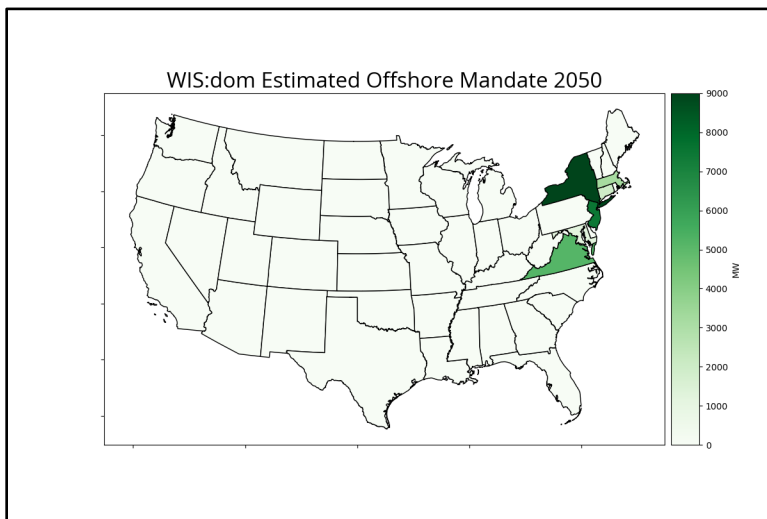


Figure 4.23: The Offshore Wind requirement in MW for each state across the US.

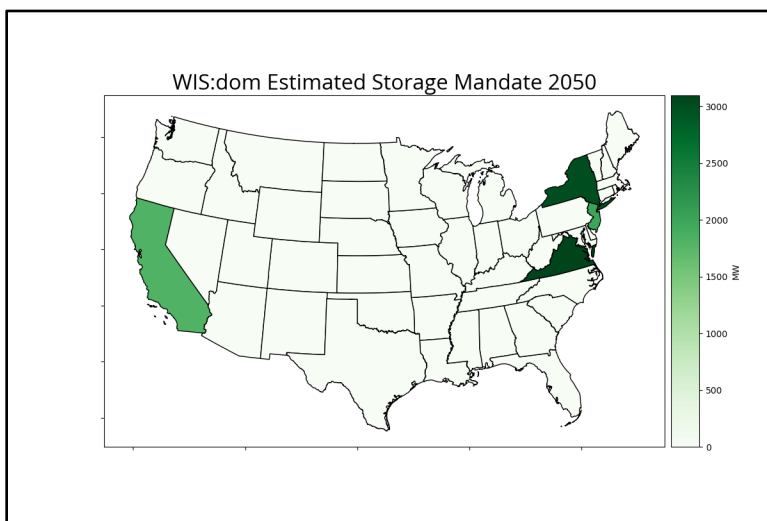


Figure 4.24: The Storage Mandates requirement in MW for each state across the US.



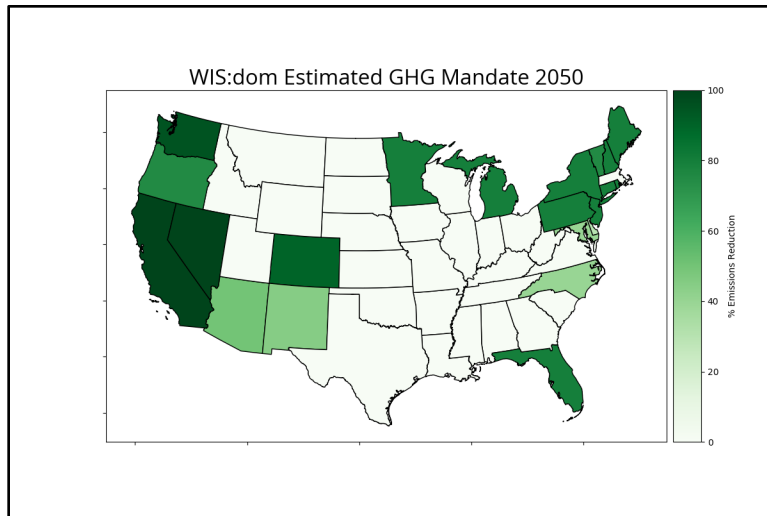


Figure 4.25: The GHG Emissions Reduction percentage requirement of each state across the US.

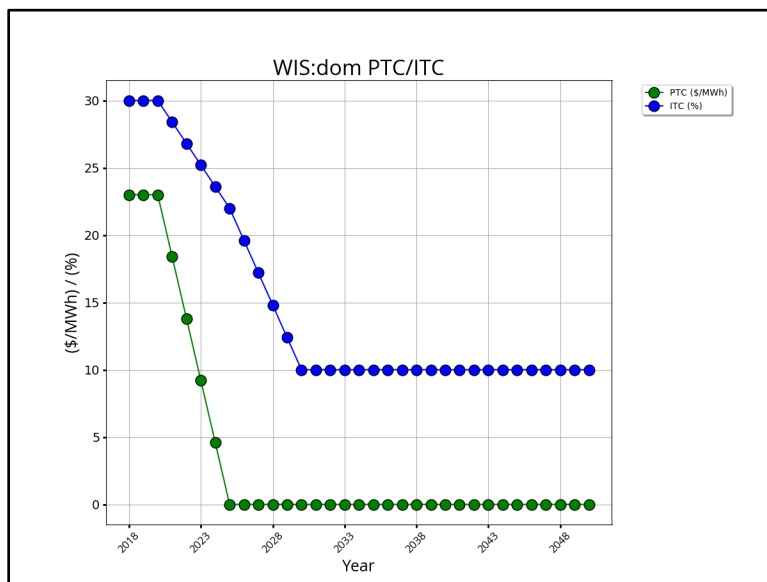


Figure 4.26: The Production Tax Credit subsidiary and the Investment Tax Credit. Note that for 2030 and beyond, the 10% ITC remaining is for utility scale projects only.

VCE also performs work and analysis to represent job numbers that arise from various technologies and transmission across the US. These inputs set the stage for how many jobs become available depending on what is deployed during the various investment periods. This is an important metric for decision makers to know and understand as the energy industry evolves. VCE uses a combination of sources to derive these numbers including IMPLAN, JEDI and US Energy Job reports.



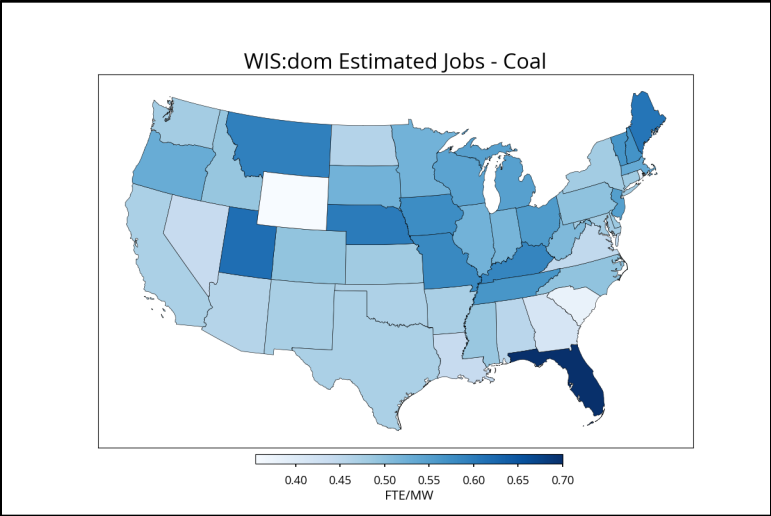


Figure 4.27: Employment per MW available from Coal.

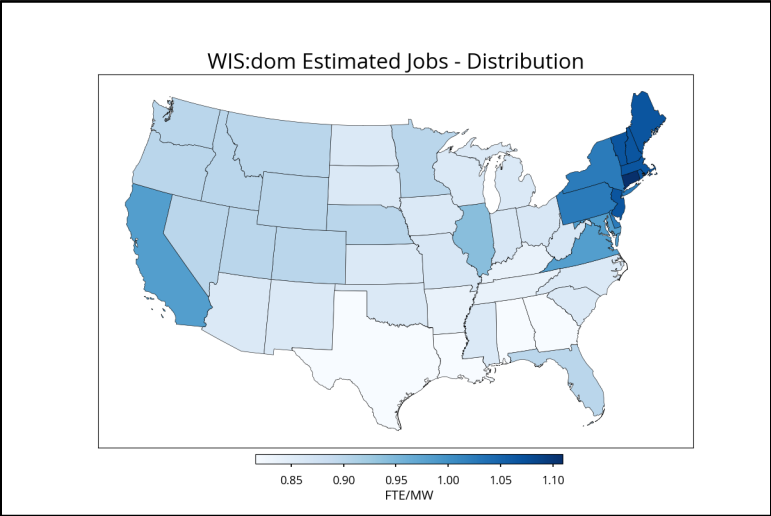


Figure 4.28: Employment per MW available from Distribution.

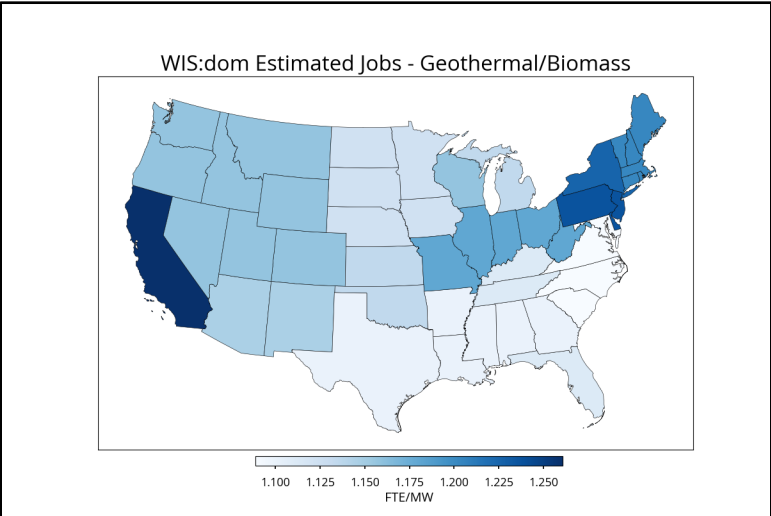


Figure 4.29: Employment per MW available from Geothermal and Biomass.

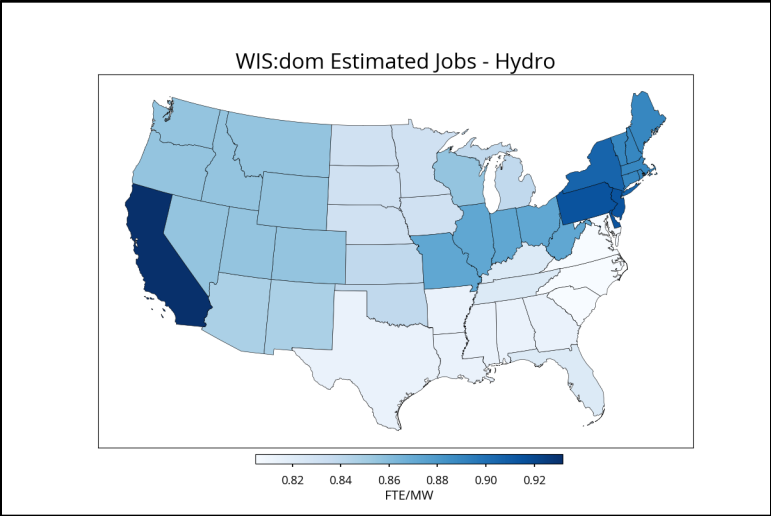


Figure 4.30: Employment per MW available from Hydro.

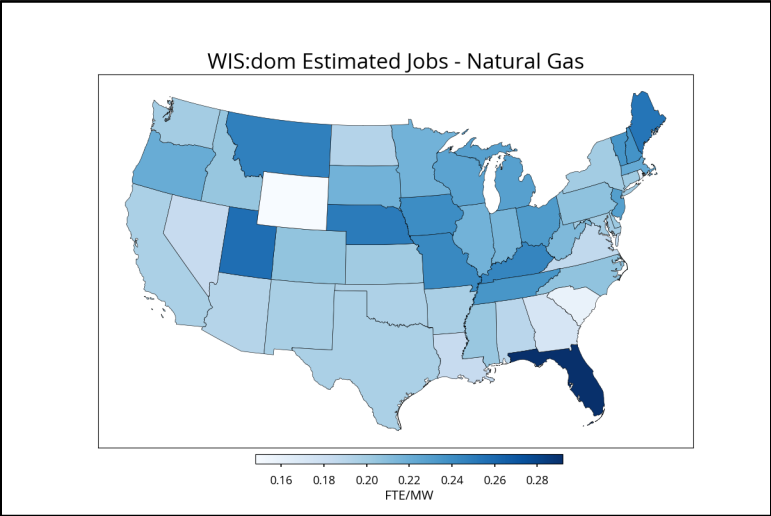


Figure 4.31: Employment per MW available from Natural Gas.

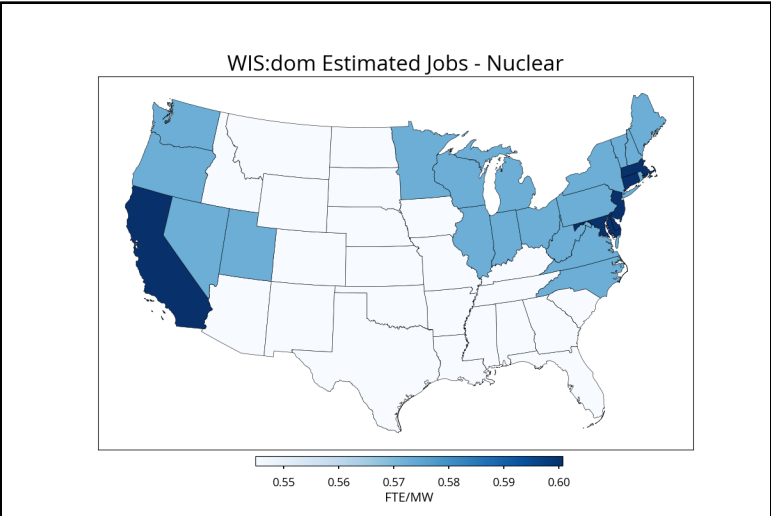


Figure 4.32: Employment per MW available from Nuclear.

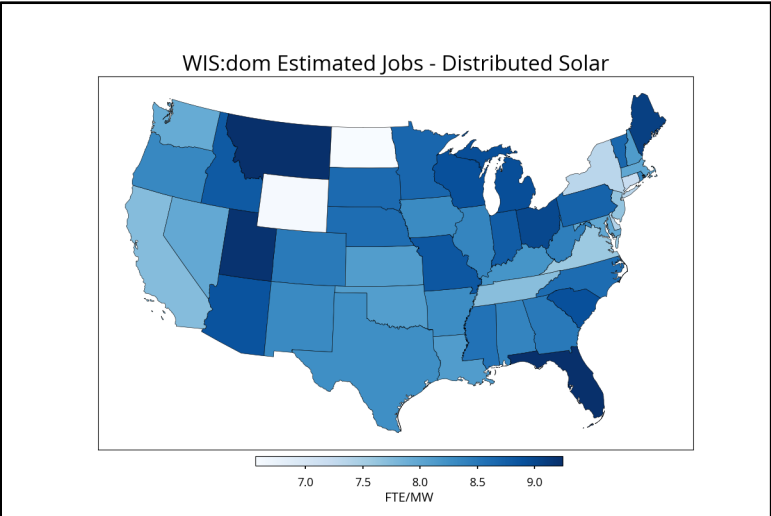


Figure 4.33a: Employment per MW available from Distributed Solar.

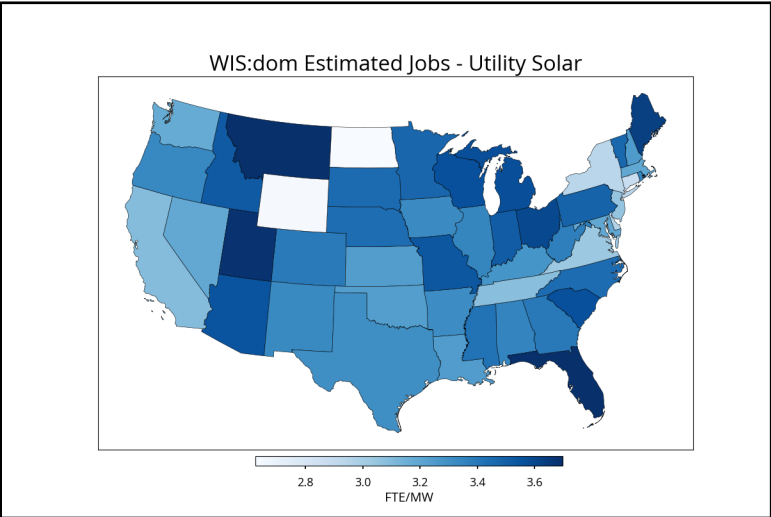


Figure 4.33b: Employment per MW available from Utility Solar.

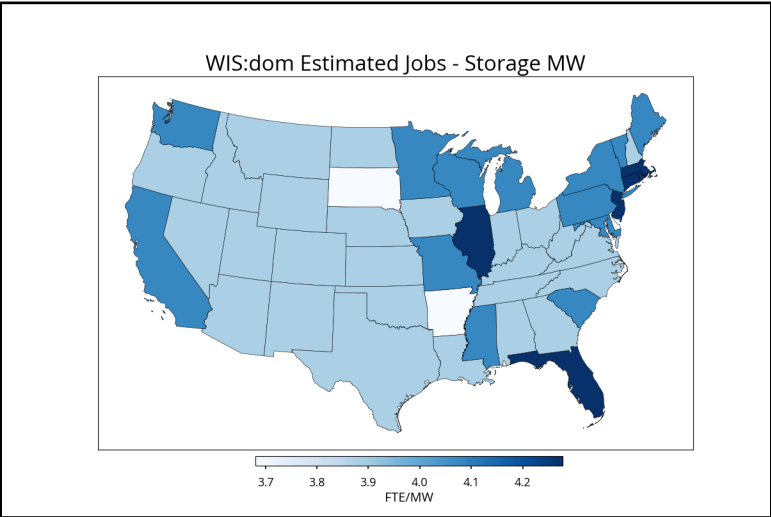


Figure 4.34: Employment per MW available from Storage MW.



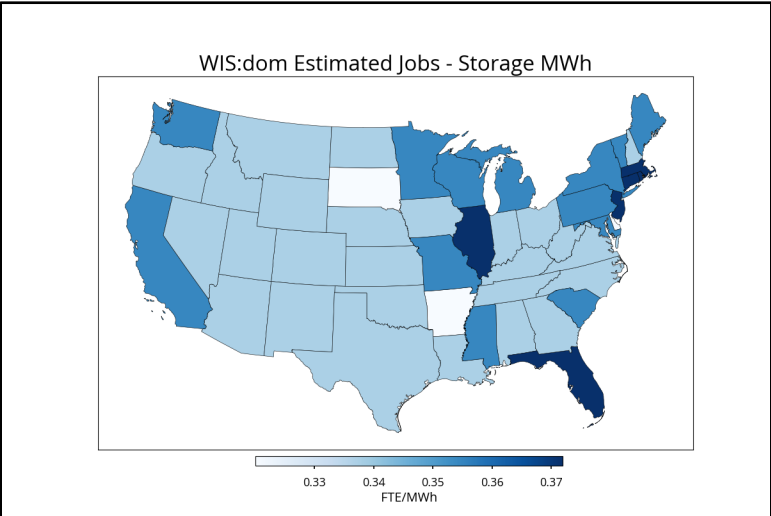


Figure 4.35: Employment per MWh available from Storage.

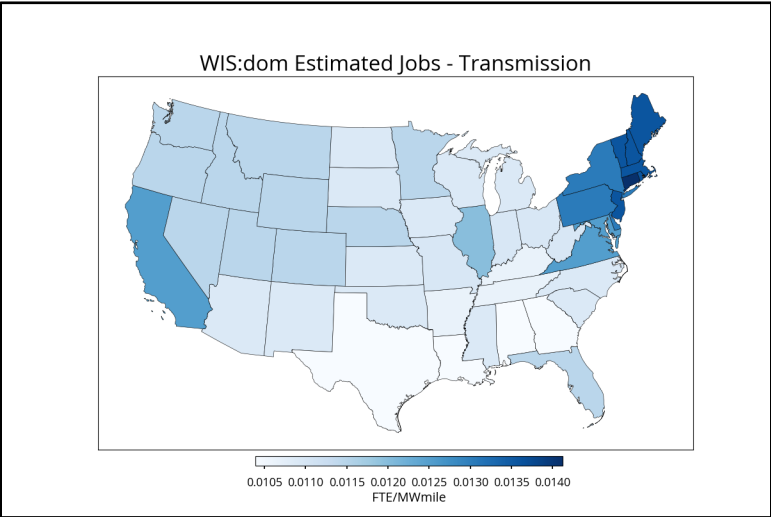


Figure 4.36: Employment per MW available from Transmission.

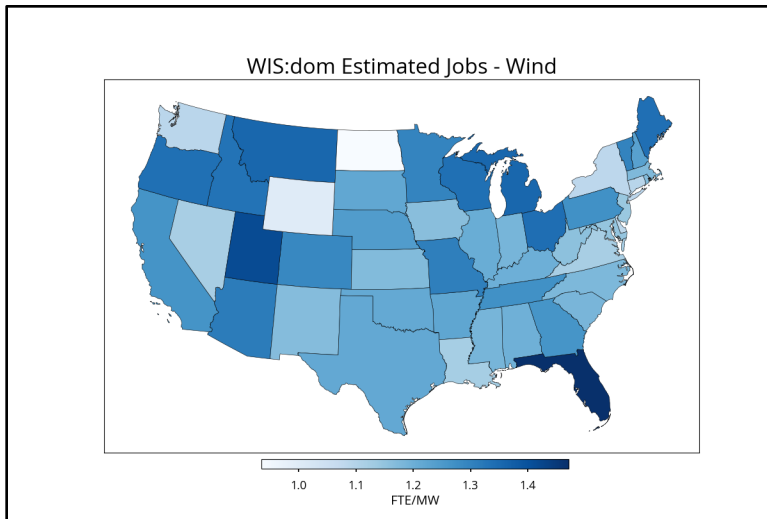


Figure 4.37: Employment per MW available from Wind.



4.4 Weather Analysis

The present section will analyze the weather data available across the contiguous US for this study from 2018. This will provide some insight into how certain renewable sources are selected by the model. Figure 4.38 displays the average wind and solar capacity across this region by hour of the day. The wind is for the 100-meter (above ground) level. The solar technology is single axis tracking pitched to latitude tilt. The load is also displayed for comparison. The series are shown for the average of the entire year and then the summer (June, July, August) and winter (January, February, March) seasons. The weather year for 2018 is used as the basis for this analysis.

Figure 4.38 shows the solar resource is both higher in peak and longer in duration during the summer, reaching around 60% capacity factor in those months for the US. For wind, the reverse occurs where this resource drops during the summer and increases during the winter. The stronger jet stream and weather patterns in winter are apparent. Wind also exhibits a diurnal pattern where stronger resource is observed during the nighttime hours. This is a normal phenomenon for wind when the decoupling of the boundary layer near the surface at night allows for wind speeds to regularly increase due to less friction from the surface. Nighttime hours can see around a 40% capacity factor from the wind resource on average for the whole year. It is easy to see the complementary temporal patterns in the wind and solar resource. The load in the US is much higher in the summer months than in the winter months (driven by air conditioner demand). The shape of the load has a strong correlation to the diurnal solar power patterns.

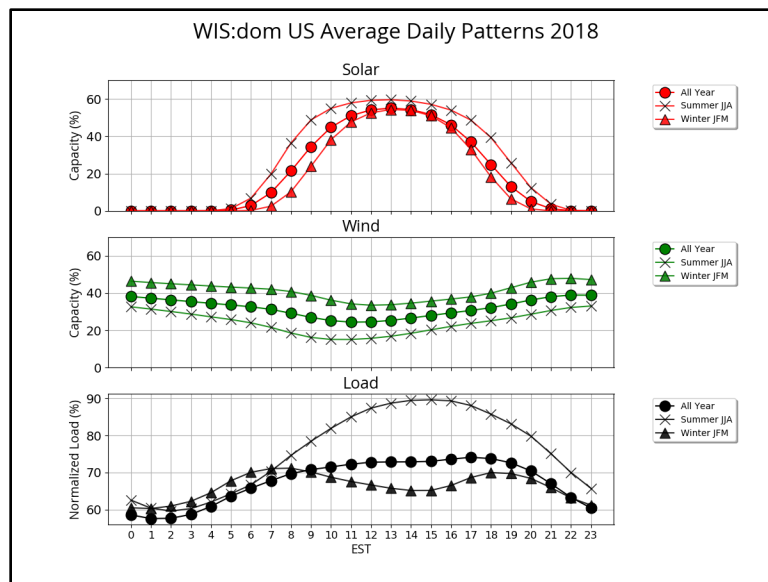


Figure 4.38: The average solar (red) and wind (green) resource shown for the US alongside the corresponding normalized load (black) by hour of the day (EST). The circles show the hourly averages for the entire 2018 year. The other two series look at the summer (JJA) and winter (JFM) months of 2018.

Figure 4.39 is similar to Fig. 4.38; but displaying the three parameters (solar, wind or load) together, to identify how they change against each other for the whole year, summer and winter. In Fig. 4.39, it is clearer that the solar resource peaks near the load peak. In the yearly average, but especially in the summer months, the shapes of these two series show



some correlation, though slightly temporally offset. The peak of the solar tends to occur on average a few hours in advance of the diurnal peak load (leading to large evening ramps, typically described in the “duck curve”). In winter, the shape of the wind resource is more highly correlated with the shape of the load. This observation along with the anti-correlated nature of wind and solar shows the viability of wind.

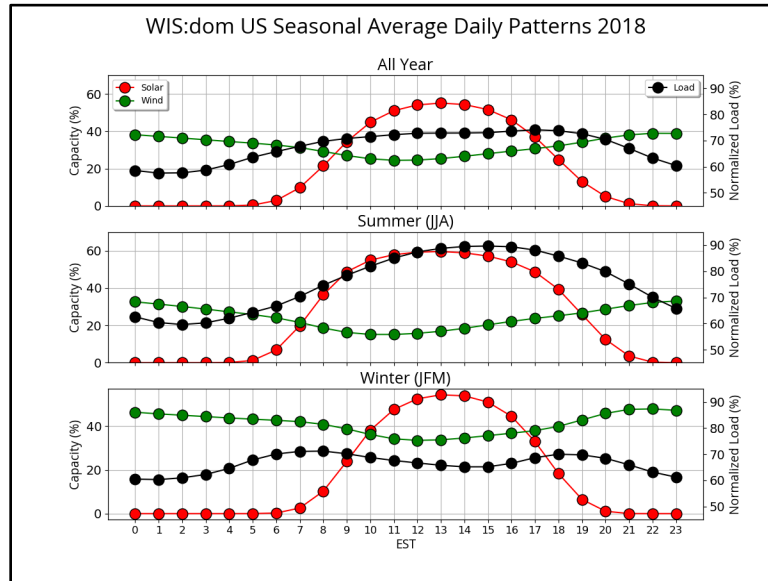


Figure 4.39a: The average solar (red) and wind (green) resource shown for the US alongside the corresponding normalized load (black) by hour of the day (EST). This is shown in seasonal groupings; the entire 2018 year, the summer (JJA) of 2018 and winter (JFM) of 2018.

For this study, VCE investigated the load shapes between a non-electrified and electrified economy in 2050. It is useful to analyze different future load shapes to understand how demand could unfold, in particular, if energy usage patterns change as electrification increases substantially. The diurnal shape of the load in comparison to the solar and wind resources can show when a renewable resource may be relied on more as well. Figure 4.39b below shows the solar and wind resource against normalized load shapes from 2050. The left panel shows the load with economy-wide electrification. The right panel plots the electricity only load from 2050. The same renewable energy resource is used for comparison between both load scenarios. In a standard load scenario, the wind resource in summer in particular is almost anti-correlated with the demand (the right panel of Fig. 4.39b). As wind increases in the nighttime hours, load decreases. In a high electrification scenario, the load is much higher during what is currently considered off-peak hours. Nighttime loads are almost as high as the daily diurnal load peak during the entire year. In winter, the nighttime peak is higher than the daytime peak. The reliance on and importance of wind increases in a high electrification scenario as the shape of the wind resource matches well this new demand shape.



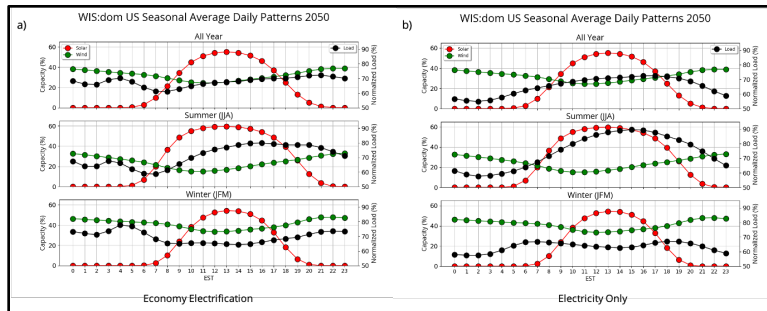


Figure 4.39b: The average solar (red) and wind (green) resource shown for the US alongside the corresponding normalized load (black) by hour of the day (EST). This is shown in seasonal groupings; the entire 2050 year, the summer (JJA) of 2050 and winter (JFM) of 2050. The left panel shows the load for an electrified economy. The right panel shows the load from electricity only.

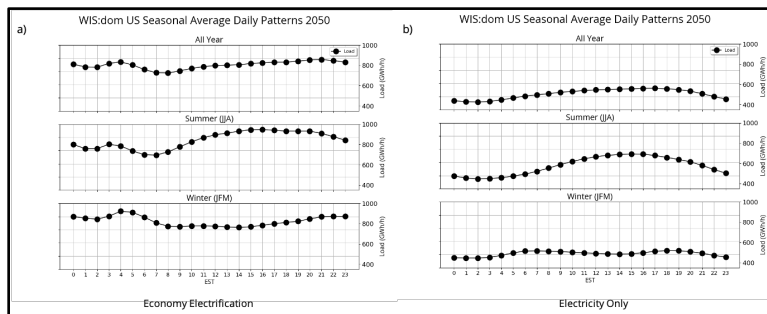


Figure 4.39c: The average load (GWh/h) shown in the US by hour of the day (EST). This is shown in seasonal groupings; the entire 2050 year, the summer (JJA) of 2050 and winter (JFM) of 2050. The left panel shows the load for an electrified economy. The right panel shows the load from electricity only.

The left panel of Fig. 4.39c shows the average hourly load (GWh/h) for an electrified economy. The right panel shows the same from an electricity only standard scenario. It is easy to see the differences in magnitude of demand between the two scenarios and how much more would need to be considered in utility planning. Electrification sees high demand hours during what would now be considered off-peak hours.

VCE investigated the wind and solar resources at different spatial granularities as well for the present analysis. Figure 4.40 and Fig. 4.41 show the average annual solar and wind resources, respectively, throughout the day for each of the contiguous US states. In the solar diurnal series, a few pattern groupings can be observed. In general, the southwest states (California, Arizona, New Mexico, Nevada, Utah and Colorado) have the highest solar resource peak. California along with Oregon, Montana, Idaho and Washington peak later in the day than other states by around 1-2 hours. Wyoming uniquely stands in magnitude between the southwest states and the Pacific Northwest states. The central states peak in solar an hour earlier than the west coast states. States east of the Texas and North Dakota line group together in terms of peak timing around 1200 EST. This is the earliest solar peak across all the states. Of the eastern states, Florida observed the highest solar peaks in 2018. On the lower side are states such as Ohio, Michigan and New York. Oregon and Washington states are where the sun will set the latest and Maine shows the earliest solar resource rise in the morning. The same diurnal plots for wind reveal the central states of the US to have incredible wind resource. Kansas and Nebraska in particular separated from the group in the nighttime hours with high wind resource. Texas observes some big diurnal swings in wind resource capacity as it is among the states with the highest resource in the nighttime



hours, but during the day, drops closer to the capacities observed in the New England coastal states. The Great Lakes region and New England also reveal good wind resource. On the lower end for wind are some of the west coast states. The wind in those states is very localized. For instance, in Washington and Oregon, there is good resource along the Columbia River valley. In 2018, California on average observes the lowest daytime wind lull across all states. The southeast states are also on the lower spectrum for wind, but not as low as some of the state averages along the west coast. Some southeast states such as Florida and the Carolinas are helped by offshore wind resource.

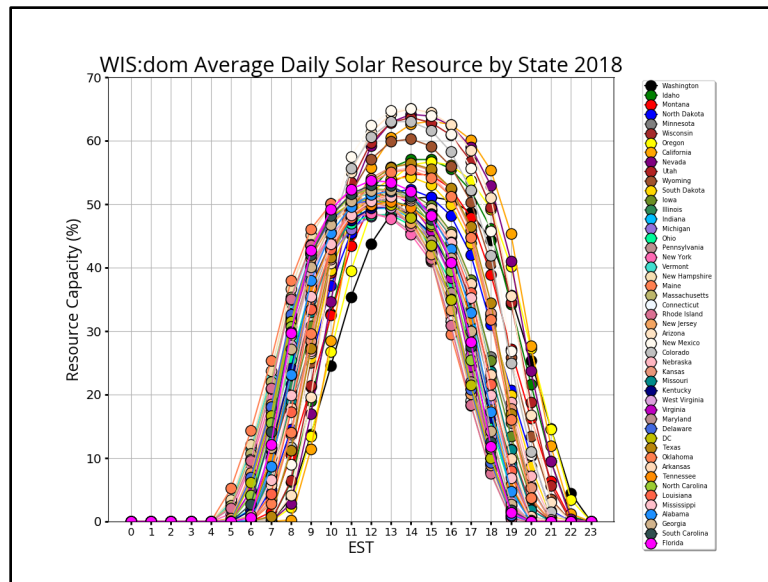


Figure 4.40: The 2018 average hourly solar resource capacity for each state.

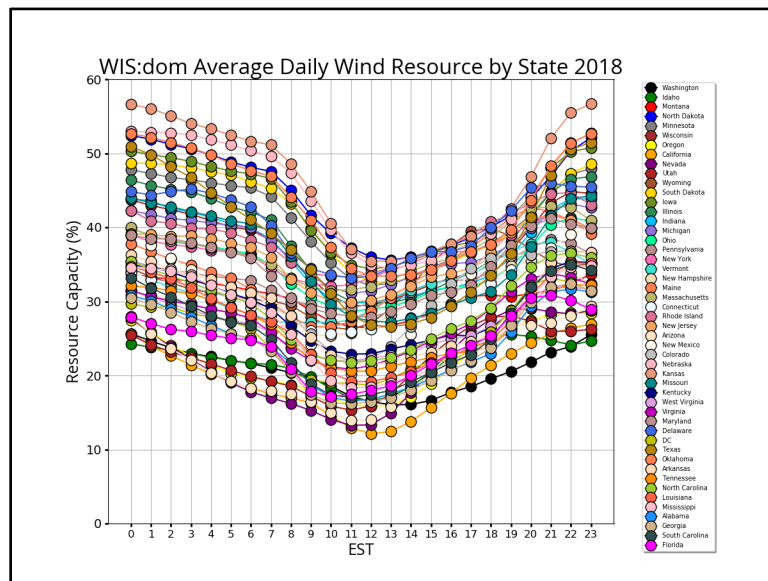


Figure 4.41: The 2018 average hourly wind resource capacity for each state.

Figure 4.42 and Fig. 4.43 shows the average solar and wind resource for the 2018 weather year for each state. For solar, the general trend across the US is that the solar resource



dominates in the southwest. Nevada showed the highest solar resource in 2018. In the east, Florida and other southeast states like South Carolina show decent resource as well. Maine and New Hampshire also reveal good solar resource along the eastern side of the US. For wind in 2018, Kansas held the highest average. The Central, Mid-Atlantic and New England states all show very good wind resource. The Great Lakes and east coast states are helped out by offshore wind resource that is available.

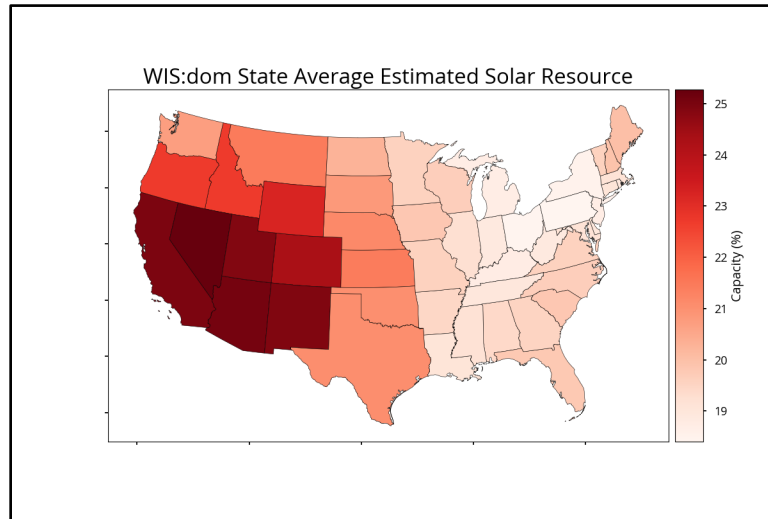


Figure 4.42: The average solar capacity factors (%) for 2018 by state.

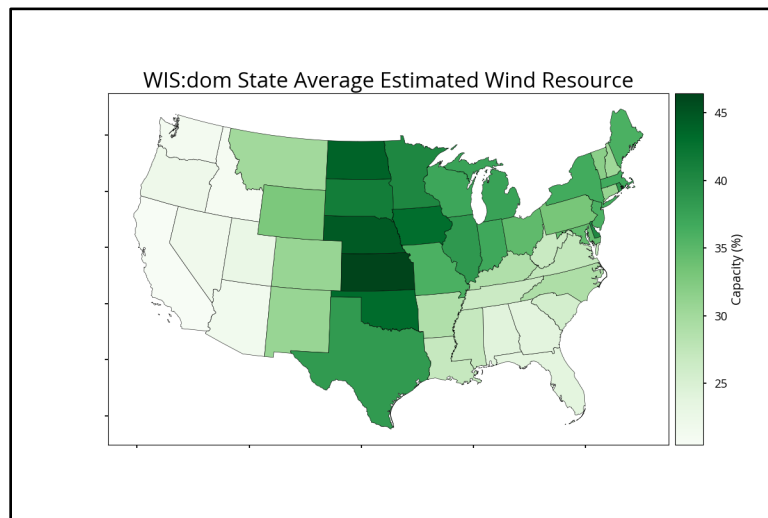


Figure 4.43: The average wind capacity factors (%) for 2018 by state.

VCE utilizes the 3-km NOAA HRRR weather model as the raw inputs for the weather and power datasets. Below is a look at the wind and solar capacity resources at this granularity across the US (Fig. 4.44 and Fig. 4.45 respectively). The high onshore wind resource is observed immediately over the Central Plains on the leeward side of the Rocky Mountains. The high offshore wind resource is also quickly apparent in both the Great Lakes and in the Atlantic. Pockets of high wind resources are seen across the western states. The highest areas of solar resource are observed over the western and, in particular, the southwestern states. Higher pockets of solar resource are seen along the



Appalachian Mountain range in the east. This shows in Maine, Virginia and North Carolina in particular. The southeast, with Florida in particular, also sees generally good solar resource. It is clear from Figs 4.44 and 4.45 that the wind resource is far more heterogenous than the solar resource, but that the US as a whole has very good resource quality in both.

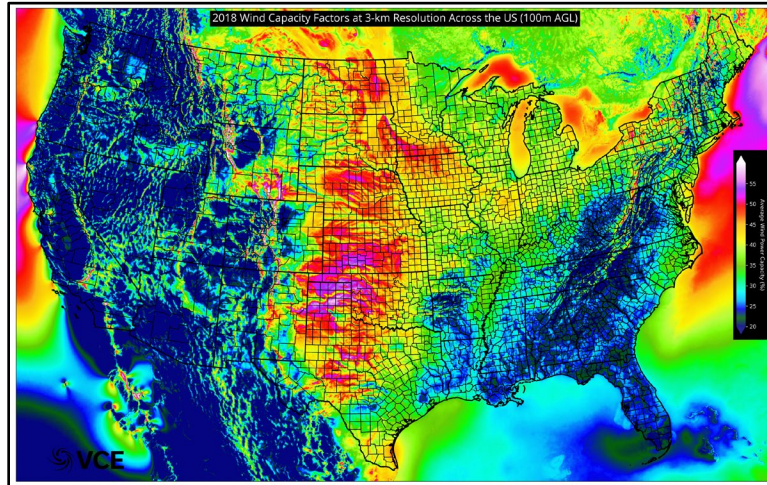


Figure 4.44: The 3-km 100-meter wind capacity resource across the US in 2018.

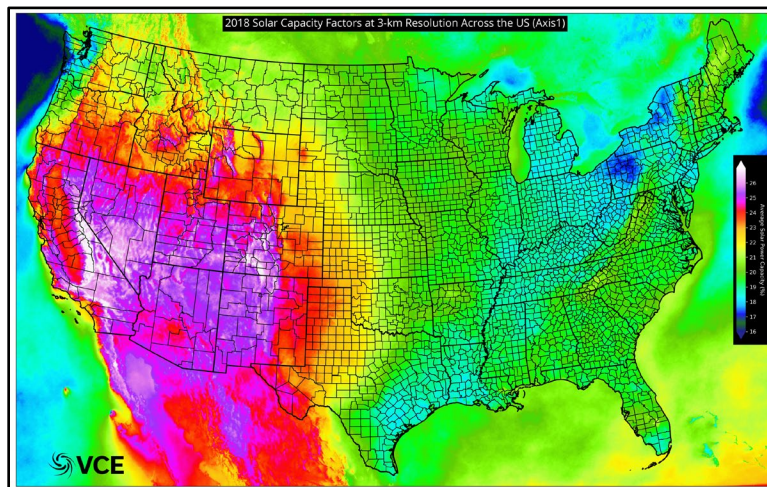


Figure 4.45: The 3-km latitude-tilted solar capacity resource across the US in 2018.

Figure 4.46, reproduced from the NOAA weather archives, shows a surface weather analysis in April 2018. This brought very strong southerly winds over the southeast and south-central plains. Further, winds were strong along the various cold fronts stemming from a storm system developing over eastern Colorado and Kansas. Winds were coming from the north behind these cold fronts as a high pressure airmass pushed south from Canada. Over New England, another storm system was pushing eastward. This was keeping winds over the New England states high. An inverted trough and tighter pressure gradients were also apparent along the west coast. This also brought higher winds. A good portion of the country was experiencing high wind during this event. A time series of wind and solar resource alongside normalized load is also shown below (Fig. 4.47) during this period. Wind capacity factors for the US just about reached 80% during the peak of this event. For a region with this geographic spread, that is an incredibly windy day.



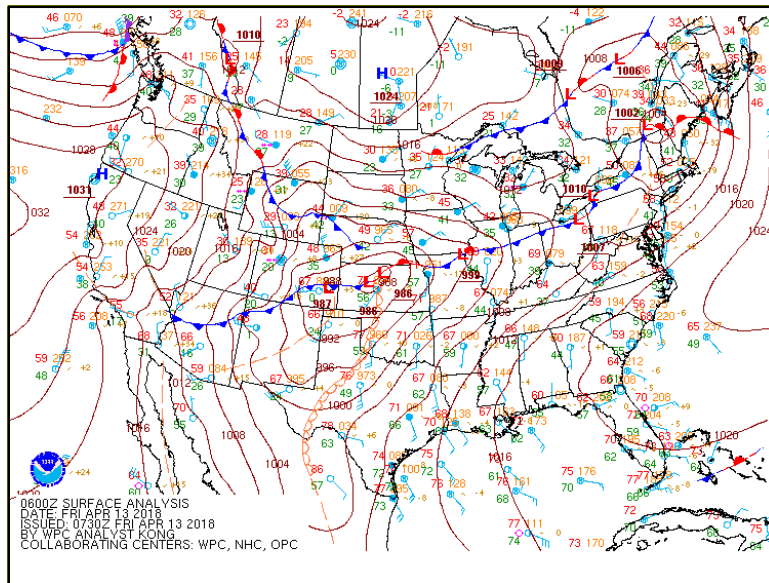


Figure 4.46: Surface Weather Analysis Plot from April 13th, 2018 at 06 UTC. This surface plot is provided from NOAA's Weather Prediction Center Archives (https://www.wpc.ncep.noaa.gov/archives/web_pages/sfc/sfc_archive.php).

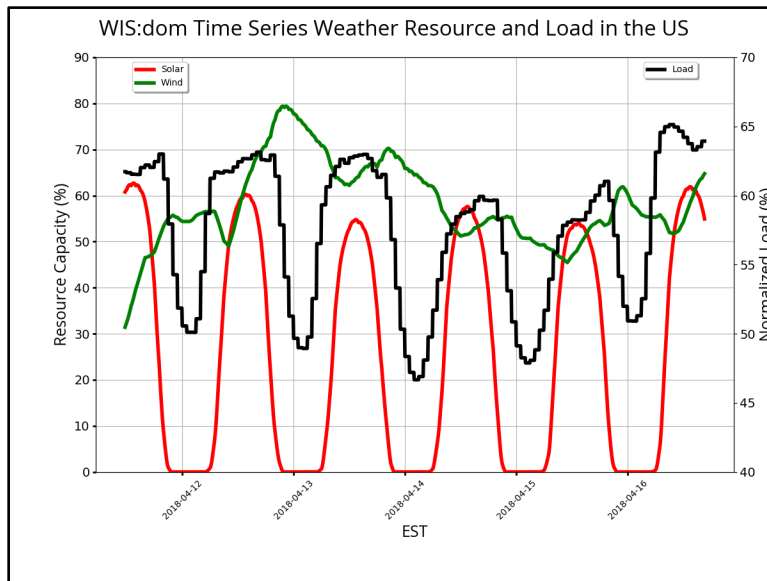


Figure 4.47: A time series of the average solar (red) and wind (green) resources across the US in April 2018. The load (black) is also plotted. This was one of the highest wind periods from 2018.

Figure 4.48 shows an August week that had some of the lowest wind observed in 2018 for the US. The diurnal nighttime increase in wind speed is apparent. The wind resource is not very high during this period, but it consistently reaches 20% capacity every night. This distinctly shows the anti-correlated nature of wind and solar.



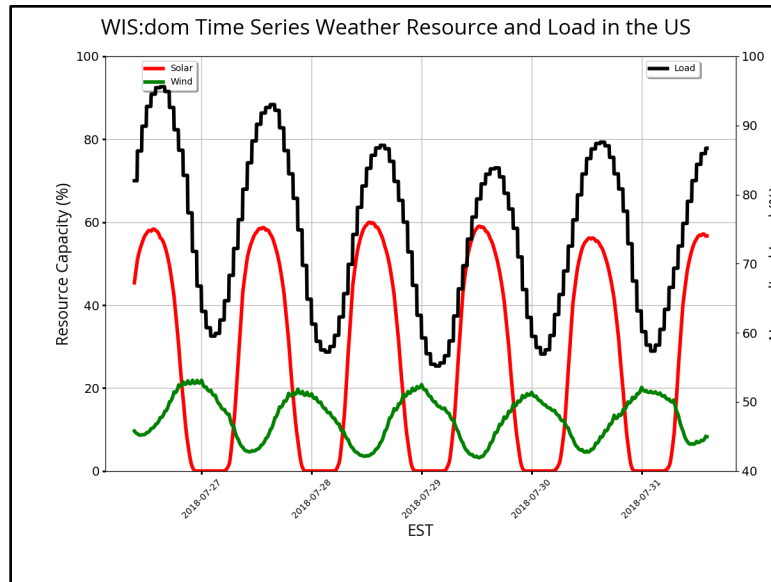


Figure 4.48: A time series of the average solar (red) and wind (green) resources across the US in August 2018. The load (black) is also plotted. This was one of the lowest wind periods from 2018.





Vibrant Clean Energy, LLC
6610 Gunpark Drive
Suite 200
Boulder CO 80301
(720) 287 1150

Vibrantcleanenergy.com
[@VibrantCE](https://www.instagram.com/VibrantCE)